Evaluation of Wet Spinning of Fungal and Shellfish Chitosan for Medical Applications

MSc in Resource Recovery
Industrial Biotechnology

Ghasem Mohammadkhani

Project number (20xx.xx.xx)

Program: Master program in Resource Recovery in major of Industrial Biotechnology

Swedish title: Utvärdering av våt spinning av svamp- och skaldjurschitosan för medicinska tillämpningar

English title: Wet spinning of shellfish and fungal chitosan and their evaluation for medical applications

Year of publication: 2021

Authors: Ghasem Mohammadkhani

Supervisor: Akram Zamani | **Co-supervisor:** Amir Mahboubi Soufiani

Examiner: Dan Åkesson

Key words: Chitosan fiber, Fungal fiber, Wet spinning, Hydrogel, Suture applications

Abstract

The aim of this project was to address the food waste problem, particularly bread waste, to some extent by producing monofilaments obtained from wet spinning of fungal hydrogel through the cultivation of *Rhizopus delemar* on bread waste. The project had two phases. Firstly, the possibility of production of chitosan fiber with wet spinning (using different acids) was evaluated, the process was optimized, and then applied to the production of fungal fiber. Regarding first stage of the project, adipic acid, a non-toxic solvent with two carboxyl groups, was used as acting physical crosslinker between the chitosan chains, resulting in improving properties of the monofilaments. Adipic acid performance was compared with conventional solvents, such as citric, lactic, and acetic acids. By injecting chitosan solutions into a coagulation bath (EtOH or NaOH 1M or EtOH-NaOH or H_2SO_4-EtOH), monofilaments were formed. Scanning electron microscopy showed that uniform chitosan monofilaments with smooth surface were formed using adipic and lactic acids. In general, fibers obtained from adipic acid displayed higher mechanical strength (Young's modulus of 4.45 GPa and tensile strength of 147.9 MPa) than that of monofilaments produced using conventional solvents. Fiber dewatering with EtOH before drying led to greater fiber diameter and lower mechanical strength. As the second stage of this study, *Rhizopus delemar* was cultivated on bread waste in shake flasks and 1.3 M^3 bioreactor. While different combinations of ground bread and K_2HPO_4 was used as the substrate for shake flask cultivations, white bread waste without K_2HPO_4 was utilized for scaling up the process, mostly due to the Glucosamine (GlcN) and N-acetyl-glucosamine (GlcNAc) content in the fungal cell wall. GlcN and GlcNA content obtained from ground bread was remarkably higher than that of obtained from combinations of ground bread and K_2HPO_4 as the substrate. Cultivation in 1.3 M^3 bioreactor resulted in about 36 kg wet biomass with a mean of 14.88% dry weight, indicating 5.95 g biomass/L. The biomass yield of 0.15 g dry biomass/g dry bread was achieved. Alkali insoluble material (AIM) was obtained by alkali treatment of biomass. Fungal hydrogel was prepared by adding adipic and lactic acid to AIM, followed by grinding treatment. While hydrogels treated with lactic acid showed better spinnability and gelling ability, the one from adipic acid was not uniform to be wet spun. Considering hydrogels treated with lactic acid, the optimum grinding cycle for more spinnable hydrogel was 6 negative cycles, contributing to the fibers with the tensile strength of around 82 MPa. Such fibers showed antibacterial property against *Escherichia coli*, making them as a good option for suture applications. However, further *in vitro* and *in vivo* trials are essential to test the fungal fiber for such applications.

Acknowledgement

This thesis was carried out under the financial support of Vinnova as a part of a bigger project "Sustainable Fungal Textiles: A novel approach for reuse of food waste" running at University of Borås. My first, big and endless appreciation goes to Akram Zamani as the ideal supervisor for her ceaseless guiding and support throughout this thesis.

I would also like to acknowledge my examiner Dan Åkesson for his invaluable feedbacks on my analysis. I am heartly thankful to my co-supervisor, Amir Mahboubi for his supports and his valuable feedbacks during the completion of the project. I specially want to thank Kanishka, my inspiring friend and colleague for his generous support and the cherished time spent together in the lab. My deep appreciation goes to Sunil Kumar Lindström Ramamoorthy for his priceless feedback and support on my analysis.

I would like to express my sincere gratitude to Prof. Minna Hakkarainen and Karin Adolfsson form KTH Royal Institute of Technology for their insightful comments and suggestions. Karin was also done Scanning electron microscopy analysis. I would furthermore like to acknowledge Sofie Svensson for her help in measuring GlcN and GlcNAc concentrations and biomass metabolite analysis. Big thank also goes to Jorge Ferreira for his guiding in scaling up the cultivation process in $1.3M^3$ bioreactor. I was lucky to work with Jorge.

I am fortunate to be a part of biotechnology and polymer groups simultaneously. I would like to extend my sincere thanks to lab technicians for their assistance at every stage of this thesis. I would also like to offer my special thanks to PhD students and researchers for their support and friendship in the lab. I am also grateful to Faranak Bazooyar for her continued help in working with polymer's lab equipment.

Most importantly, my immense gratitude goes to my ever loving wife, Sara. None of this could have been accomplished without her help. I am forever thankful for her continuous encouragement and unconditional love.

TABLE OF CONTENTS

List of Figures

List of Tables

1 INTRODUCTION

1.1 Problem description and purpose

Scarcity of cotton supply in the world and adverse environmental impacts of using petrochemical-based textile like releasing of micro-plastics has led to serious environmental concerns. Furthermore, common textiles are difficult to recycle and consequently, renewable fibers, which can undergo biological recycling are highly demanded (Chen and Burns, 2006). One of the promising solutions to respond to such a demand is using natural biopolymers like chitin and chitosan. Chitin as a ubiquitous natural aminopolysaccharide polymer plays structural role in exoskeletons of crustaceans, insects, and fungi cell walls. Chitosan, the most well-known derivative of chitin, can be obtained via enzymatic deacetylation or chemical deacetylation of chitin. From the medical application point of view, metals, ceramics and synthetic polymers have been used as biomaterials over the past decades. However, they have some disadvantages, such as being rejected by the patient's immune system. In addition, synthetic polymers can set the stage for an undesirable immunogenic response, mainly due to the biodegradation products they leave in the body. Therefore, biopolymers can be regarded as a suitable option for medical applications because of their structure, degradability and biocompatibility in comparison to synthetic polymers. Proteins, polynucleotics and polysaccharides (e.g. chitin and chitosan) are the main groups of biopolymers (Rebelo et al., 2017). While Zooplankton cuticles is considered globally as the largest source of chitin, fishing these tiny organisms is not commercially feasible, so shellfish industry wastes including shrimp, crab, and lobster shells with chitin contents of 8–40%, are the main source of industrial chitin. Besides, fungi, particularly filamentous fungi, is suggested as an alternative chitin source. Fungi are gaining more research and commercial attention, in spite of having lower chitin content compared to crustaceans (10–26% as a chitin-β-glucan complex or chitin-chitosan complex). That is because not only is not fungal chitin limited by seasonal and local availability, but also it does not need to undergo aggressive acid treatment, which is necessary for crustacean chitin in order to remove calcium carbonate and other minerals through purification and demineralisation (Jones et al., 2020). Moreover, it is possible to successfully adjust the production yield of products from fungal sources via monitoring of fermentation and processing conditions. Another advantage of using the fungi is that it can grow on low cost substrates such as food waste (Synowiecki and Al-Khateeb, 2003).

From the environmental perspective, food waste contributes to the loss of precious resources like energy, water, land and labor and it also leads to emissions of pollutants. One of the biggest fractions of food wastes is bread waste, and it has the highest environmental footprint of big supermarkets in Sweden. Put differently, the annual bread waste has the largest contribution to the total mass of food waste, the economic costs incurred by the supermarket and the environmental impacts in ozone depletion, freshwater ecotoxicity and resource depletion categories (Brancoli et al., 2017).

As a part of a bigger project (Sustainable Fungal Textiles: A novel approach for reuse of food waste) running at University of Borås, the main purpose of this master thesis is the conversion of bread waste to a monofilament yarn that can be used for medical applications. The thesis includes two stages. Firstly, monofilament yarn has been produced from the pure shellfish chitosan, as a reference material for the fungal chitosan, in order to see the capability of producing continuous monofilament yarn in a simple condition, which is similar to the next stage. For the second part, filamentous fungi (*Rhizopus delemar)* was cultivated on bread

waste and the fungal cell wall containing chitosan has been isolated. For both stages, a wet spinning method was developed for the preparation of the continuous monofilament yarns. Moreover, the antimicrobial properties of the fungal yarns were examined against Gram-negative (e.g. *Escherichia coli*) bacteria. Mechanical properties of the fungal yarn were also tested as well. It should be mentioned that it was already investigated on *Rhizopus delemar*' cultivation using bread waste by Köhnlein (2020) and in the study at hand, the mentioned research was used for the cultivation parts as a reference for the fungal chitosan.

1.2 Social and ethical aspects

In regards to the social aspects of this thesis, several aspects should be pointed out. It is undeniable that a significant amount of human-grade food is being wasted on daily basis. Such remarkable food waste occurs in developing countries as well as wealthier countries (Statista, 2020). However, poor countries are battling against food deficiency. On the other hand, it is speculated that population of the world will reach 9.6 billion by 2050 (Nations, 2021), which means the global food production should increase accordingly. As an alternative, countries can plan to reduce food loss and recover recourse ending in waste. Such a policy, if not implemented, can have a large number of irreparable consequences on the nature as well as mankind life, setting the stage for annihilating of the Earth. To solve the food waste associated issues, a vast variety of parameters including supply chains, supermarkets, restaurants, farms, fluctuation of markets, information strategies, governmental regulations, education programs etc. should be taken into consideration (Statista, 2020). As previously mentioned, the highest environmental footprint of big supermarkets in Sweden can be attributed to bread waste.
In the study at hand, in a "killing two birds with one stone" strategy, not only bread waste handling and management was targeted but also a valuable product was produced from waste. The bread waste (unsold bread), that was used in this project was collected form ICA supermarket in Borås, Sweden. As far as I concerned, production of valuable products for textile and medical application is a very interesting and rational approach to cope with a portion of food waste, resulting in addressing environmental impacts of bread waste to some extent.

1.3 Research questions

The following is a list of questions expected to be answered:

- Is it possible to produce continuous monofilament yarn from commercially available shellfish chitosan and chitosan available in the fungus cell wall by a wet spinning system?
- To what extent are the above-mentioned fibers antimicrobial and biodegradable?
- What is the best solvent and coagulation bath to produce wet-spun chitosan fibers?
- What types of post-treatment procedures can be used to improve the mechanical properties of chitosan fibers and chitosan extracted from the fungus cell wall?
- Is it possible to produce fungal fibers, showing antimicrobial properties to be used for structural applications?

2. Background

2.1 Filamentous fungi

Cellular life is divided into two main domains of prokaryotes and eukaryotes. Prokaryotes consist of two discrete types of organisms, the Bacteria and the Archaea. It is indicated that eukaryotes and Archaea demonstrate sister groups in the tree of life (Eme et al., 2018). Eukaryotes are further divided into the five kingdoms of chromista, protista, plantae, fungi, and animalia. While fungi as heterotroph organisms represent the characteristics of both plants and animals, they are placed in a distinct kingdom. Fungi can be unicellular organisms like yeasts, and multicellular organisms like filamentous fungi and mushrooms (Silvia Hüttner, 2020). Although Chytridiomycota, Zygomycota (the most varied), Ascomycota, and Basidiomycota are four subgroups, phyla, of the fungi kingdom due to their morphological and reproductive traits (Zamani, 2010), the most up-to-date taxonomy of fungi states that fungi are divided into nine major lineages, which are Opisthosporidia, Chytridiomycota, Neocallimastigomycota, Blastocladiomycota, Zoopagomycota, Mucoromycota, Glomeromycota, Ascomycota and Basidiomycota (Naranjo-Ortiz and Gabaldón, 2019). The fungi, *Rhizopus delemar*, which is used in this project, belongs to the Mucoromycota phylum. Over the past years, filamentous fungi have become an excellent biological catalyst being able to produce and refine a wide range of products (e.g. enzymes, pigments, antibiotics, ethanol and lipids) according to their metabolic pathway. As a result, fungal biotechnology plays a key role for many industries, such as food and feed, pharma, pulp and paper, detergent and textile. The European leaders in using filamentous fungi are AB Enzymes, BASF, Bayer, Chr. Hansen, DSM, DuPont, Novozymes companies (Meyer et al., 2016).

In general, fungi grow as either yeast or filamentous fungi. Filamentous fungi (also referred to as mold) grow by apical extension of their filaments named hyphae (miniscule feathery strands). Continued growth of hyphae forms branches, contributing to building an intricate network of hyphae, known as a mycelium (pl. mycelia), which are observable to the naked eye and can grow from centimeter-scale to meter-scale (Powers-Fletcher et al., 2016; Augustina Egbuta et al., 2016). Therefore, if a eukaryotic microorganism exhibits the growth of mycelium as part of their life cycle, it can be considered as filamentous fungi regardless of the taxonomical classification. Figure 1 illustrates the schematic of filamentous fungi.

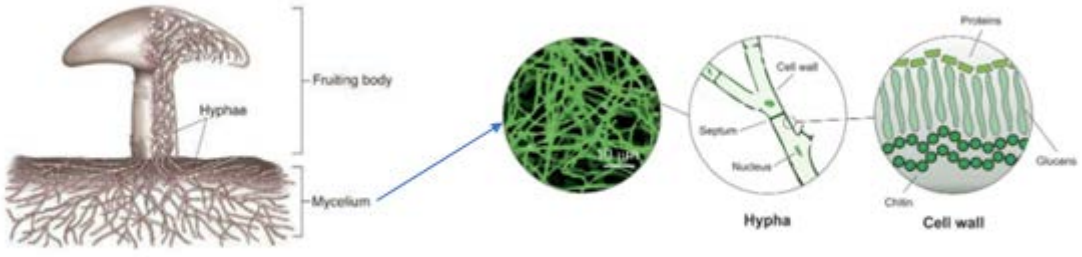

Figure 1. Schematic of filamentous fungi, adopted from Haneef et al. (2017) and Haverford (2017).

The mycelium plays the role of the feeding structure of a fungus. Mycelia's fibrous structure helps them to maximize their contact with the food source. Fungi cannot swim, run and fly to find food. The mycelium has the capability to grow rapidly throughout a food source and address the problems with mobility. Therefore, for the heterotrophic lifestyle of fungi, a mycelium is an efficient structure, which enables the fungus to absorb small organic molecules from its surroundings. The mycelium absorbs nutrients because it penetrates into

surrounding substrate. Fungi secrete enzymes into their surroundings using hyphae, which results in the breakdown of complex macromolecules to simpler nutrients. Such nutrients are then absorbed by mycelium via the cell wall and are used for biosynthesis. Sporangiophores are formed by hyphae growing outside the nutrient medium into regions of air and are used for asexual reproduction via spore propagation (Money, 2016).

As it is shown in figure 2, the fungal cell wall consisting of glucans, chitin, chitosan, and glycosylated proteins plays a significant role in maintaining cellular integrity and viability. The composition of the fungal cell wall depends on the type of the fungi. For example, not all fungi contain chitin and chitosan and if the fungi contain glucan then it does not contain chitosan. Moreover, the only family of fungi containing chitosan in the cell wall is *Zygomycetes* fungi. It should be mentioned that proteins are commonly associated with polysaccharides, which leads to glycoproteins.

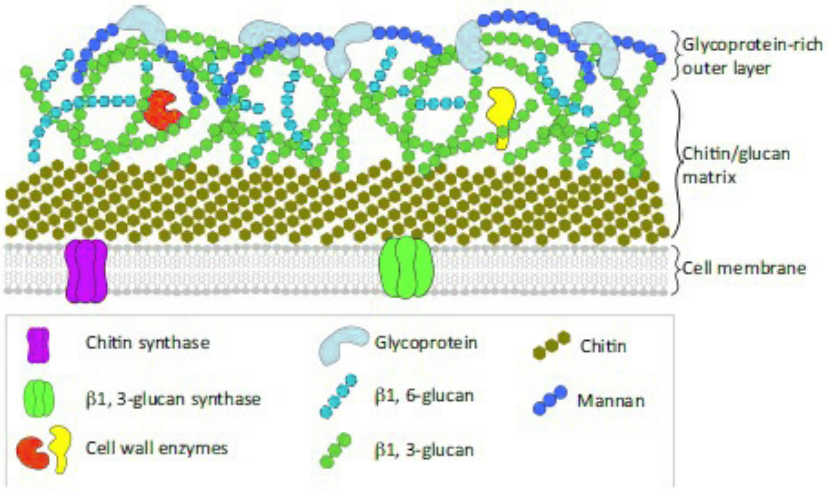

Figure 2. Filamentous fungi cell wall structure, adopted from Geoghegan et al. (2017).

2.2 Source and structure of chitin and chitosan

As the second most abundant polymer in nature, chitin has a similar function to collagen in animals and cellulose in plants. While plants produce cellulose in their cell walls, insects and crustaceans make chitin in their shells. Thus, cellulose and chitin are two polysaccharides, which are related structurally, causing the uniformity of structure and protection to plants and animals. Chitin naturally exists as ordered crystalline microfibrils forming structural components in the exoskeleton of arthropods and in the fungal cell wall to a large extent (Zargar et al., 2015; Afzal et al., 2020). Its natural abundance is equivalent to more than 1000 tons per year and about 70% of this amount comes from marine species, such as shells of shrimp, crab and lobster. Also, it can be found in the exoskeletons of mollusks and insects (Islam et al., 2016). There exists two main polymorphic forms of chitin, α and β, where the most dominant polymorph for both crustacean and fungal chitin is α-chitin. β-chitin can be found only in squid pen, sea tube worms, and some algae (centric diatom) (Jones et al., 2020).

The chitin content of the fungal wall is different based on the morphological phase of the fungus. In yeast cell wall, it is 1–2%; however, in filamentous fungi, it can reach up to 10–20% of the dry weight (Garcia-Rubio et al., 2020). As an example of various fungi that are appropriate for chitin isolation, *Allomyces*, *Aspergillus*, *Penicillium*, *Fusarium*, *Mucor*,

Rhizopus, *Choanephora*, *Tamnidium*, *Zygorrhynchus*, and *Phycomyces* can be pointed out (Synowiecki and Al-Khateeb, 2003).

The chemical structure of chitin and chitosan greatly resembles to the cellulose chemical structure. Cellulose is a homopolymer consisting of glucose units in β-(1→4)-linkage. Natural chitin is a random copolymer of glucosamine (GlcN) and N-acetyl-glucosamine (GlcNAc) in β-(1→4)-linkage. Whereas, chitin is generally defined as a polymer of GlcNA. Although chitosan is also a copolymer of GlcN and GlcNAc units, GlcN is the predominant constituent. Figure 3 shows the chemical structure of cellulose, chitin and chitosan. To clarify further, the hydroxyl group at position C-2 of cellulose is replaced by an acetamide group in chitin, which can be deacetylated to have chitosan (Islam et al., 2016; Schmitz et al., 2019).

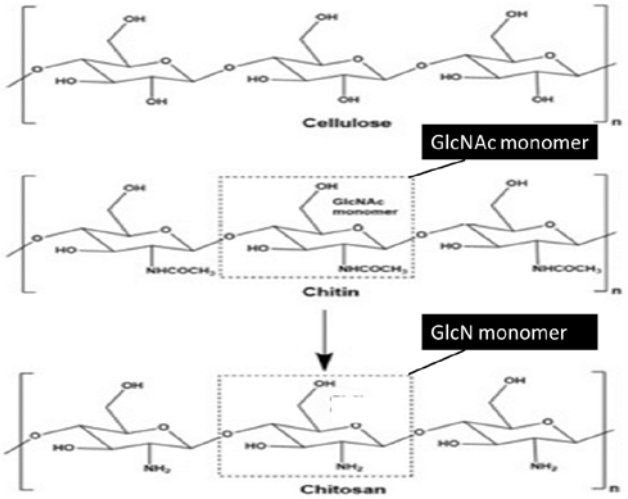

Figure 3. Chemical structures of cellulose, chitin and its fully deacetylated derivative chitosan, adopted from Schmitz et al. (2019).

Chitosan molecules are chitin molecules that are deacetylated to the point where they get soluble in dilute aqueous acidic solution. As complete deacetylation of chitin is extremely difficult to achieve (Knaul et al., 1999), chitosan can be defined by the degree of acetylation (DA), which can be calculated by the following equation (1.1) (Enache, 2018).

$$DA = \frac{nGlcNAc}{nGlcN + nGlcNAc} \times 100$$

$$nGlcNAc - mole\ fraction\ of\ glucopyranose\ acetamido\ unit;$$
$$nGlcN - mole\ fraction\ of\ glucopyranose\ amino\ unit. \quad (1.1)$$

As it is illustrated in figure 4, when the number of GlcNAc units is higher than 50%, the polymer is termed chitin. In contrast, the term chitosan is used if the number of nGlcN units is higher than 50% (Khor and Lim, 2003).

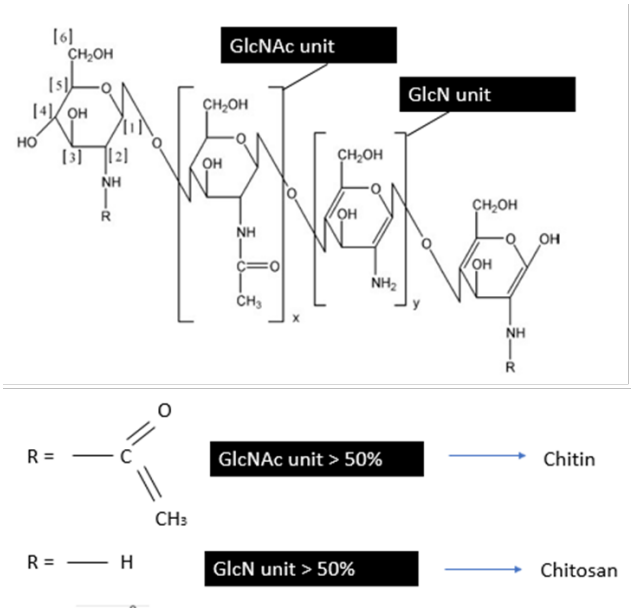

Figure 4. Chitin and chitosan in respect with DA, adopted from Pillai et al. (2009).

Furthermore, chitosan as the most interesting component of fungal cell wall in this project is naturally available in *Zygomycetes* fungi and it is no need for deacetylation of chitin. Table 1 shows chitosan contents of different types of fungi, which were done by Tan et al. (1996) and Pochanavanich and Suntornsuk (2002).

Table 1. Yield of extractable chitosan of Zygomycetes reported by Tan et al. (1996) and Pochanavanich and Suntornsuk (2002).

Fungi	A: Dry weight of mycelia (g)	B: Chitosan(mg)	B/A (%)
Rhizopus oryzae 0602	1.13 ± 0.19	55.70 ± 8.53	4.91
Rhizopus oryzae 0263	0.99 ± 0.03	43.98 ± 3.05	4.43
Rhizopus arrhizus	0.97 ± 0.02	46.80 ± 8.05	4.78
Rhizopus microsporus	0.88 ± 0.04	29.98 ± 1.77	3.40
Rhizopusstolonifer	0.91 ± 0.01	20.48 ± 8.72	2.25
Rhizopus oligosporus	0.93 ± 0.1	29.98 ± 5.81	3.21
Absidia glauca	1.21 ± 0.2	65.24 ± 10.81	5.37
Mucor sp	1.17 ± 0.03	50.4 ± 4.46	4.31
Mucor htemalis	0.89 ± 0.04	51.22 ± 4.63	5.77
Zygorhyncus moelleri	1.15 ± 0.1	47.72 ± 13.09	4.14
Cunninghamella echinulata	1.12 ± 0.02	79.73 ± 6.04	7.14
Gongronella butleri 0489	1.62 ± 0.06	76.63 ± 9.00	4.73
Gongronella butleri 0201	1.63 ± 0.05	93.38 ± 6.69	5.74
Aspergillus niger TISTR3245	1.00	107.00	10.70
Rhizopus oryzae TISTR3189	1.00	138.00	13.80
Lentinus edodes no. 1	1.00	33.00	3.30
Pleurotus sajo-caju no. 2	1.00	12.00	1.20
Zygosaccharomyces rouxii TISTR5058	1.00	36.00	3.60
Candida albicans TISTR5239	1.00	44.00	4.40

Unlike cellulose, chitin and chitosan contain 5–8% nitrogen. In chitin, it is in form of acetylated amine groups and in chitosan, it is in form of primary aliphatic amine groups (at the C-2 position), causing chitin and chitosan to be suitable for general amine reactions.

However, chitosan is chemically more active compared to chitin based on the presence of primary (at the C-6 position) and secondary hydroxyl groups (at the C-3 position) on each repeat unit, and the amine group on each deacetylated unit. These functional groups are easily subject to chemical modification to change mechanical and physical properties (e.g. ameliorating chitosan's solubility at neutral pH range) of chitosan as well as conjugation with special drugs (Islam et al., 2016). On the other hand, the presence of acetyl groups in chitin enhances the inter chain forces and the percentage of crystallization, resulting in a better dry and wet strength in comparison to semi-crystallize chitosan fibers. Moreover, the chitosan fibers represent poor performance in developing a suitable strength, mainly due to having higher moisture regaining property (Roy et al., 2017). The chemical modification of chitosan is an effective technique to control the interaction of the polymer with drugs, increases the load capability, and tailor the release profile of the drug carriers (Pokhrel and Yadav, 2019).

2.3 Processing of chitin and chitosan

From the industrial perspective, chitosan production from chitin available in shellfish exoskeletons is performed through alkali treatment. Firstly, proteins are removed using mild alkali; then strong alkali at high temperature is applied in order to deacetylate chitin (Kumar, 2000). This can happen at various temperature ranges (80 to 140°C for up to 10 h) using sodium or potassium hydroxide solution with concentrations of 30 to 60% (w/v). The concentration of alkali solution, temperature and the time of the process have effects on the degree of deacetylation, molecular weight and molecular weight distribution, as well as the distribution of deacetylated units along with the polysaccharide chain. For instance, moderate concentration of sodium hydroxide, relatively low temperature, and prolonged deacetylation time contributes to a random distribution of deacetylated residues in chitosan molecules. High temperature in chitosan preparation leads to enhancing of the degree of deacetylation; however, diminishing the size of the molecules. As previously mentioned, it is not easy to prepare chitosan with a degree of deacetylation higher than 90% without significant degradation of polysaccharide molecules. An alternative method of chitin processing to obtain completely deacetylated chitosan is comprised of prior incubation of chitin at 4°C in 50% NaOH for 24 h, followed by its separation, mixing with 10% NaOH and heating up to 230°C (Synowiecki and Al-Khateeb, 2003).

From the environmental point of view, such a method (using strong alkali solution at high temperature) can contributes to some problems. Conversely, chitosan production from fungal biomass through enzymatic deacetylation reaction can address the potential environmental issues. To explain further, such a chitosan production does not lead to creation of wastewaters with high chemical oxygen demands as the application of very high concentration of alkaline chemicals is skipped. Besides, the fungi availability does not depend on seasons, meaning that chitosan can be obtained continuously from various waste materials under well-controlled conditions.

Chitosan biosynthesis in *Mucor* species will be elaborated in the following paragraph;
Uridine diphosphate N-acetyl glucosamine (UDP-GLcNAc) acts as a precursor for chitin production in fungal cells. Chitosomes, specific micro vesicles, are responsible for transporting chitin synthase from cytoplasm to the site (apical region of hypha wall) in which chitin can be active. Based on *in vitro* studies, chitin with a highly crystalline structure is not prone to enzymatic deacetylation. That is because chitin deacetylase is not capable of going through the organized structure of chitin. On the other hand, it is shown that having a

digitonin pretreated chitosomal chitin synthase instead of the untreated one leads to a remarkable chitosan production rate due to getting the dissociated subunits of chitin synthase (Karimi and Zamani, 2013). Indeed, such subunits provide more time for growing chains of chitin to be deacetylated through enzymatic deacetylation. Considering *in vivo* conditions for the *Mucor* cells, chitin and chitosan production rate is attributed to the degree of crystallinity of chitin synthase. The associated part of chitin synthase causes to get highly organized chitin while the dissociated subunits of chitin synthase produce chitin chains, which are susceptible to be deacetylated through enzymatic reaction, which means chitosan is produced. In *Mucor* cell wall, the predominant nitrogenous part is chitosan that causes chitin synthase to be dissociated on the cell surface. As the final point for this part, the higher chitosan production rate happens in case of providing conditions for the fungus to experience the maximum growth rate, regardless of the substrate (Karimi and Zamani, 2013).

2.4 Biological property of chitin and chitosan

Chitin and chitosan have a considerable potential to be used in medical and pharmaceutical industry due to their interesting properties such as strong antibacterial effect, biocompatibility, biodegradability, non-toxicity and high humidity absorption. Moreover, other biological properties like analgesic, antitumor, hemostatic, hypocholesterolemic, antimicrobian, and antioxidant properties have also been reported by Islam et al. (2016). The polymer chain length and the distribution of functional groups also can have effects on the biodegradation kinetics of chitin and chitosan. Small oligomeric chitosan compared to the high molecular weight chitosan can easily penetrate the cell membrane of a microorganism, and consequently prevents the growth of the cell by hindering RNA transcription (Islam et al., 2016).

2.4.1 Antimicrobial properties of chitosan

Chitosan displays a broad range of antimicrobial property against both Gram-positive and Gram-negative bacteria and fungi. Several possible explanations have been proposed for antimicrobial activity of chitosan; polycationic chitosan molecule interacting with the lipopolysaccharides and proteins as the predominantly anionic cell wall components of the microorganism. As a consequence, it leads to changes in permeability barrier, resulting in the leakage of intracellular components and the death of the cell or bonding to DNA followed by preventing DNA replication and, subsequently cell death (Sahoo et al., 2009; Yilmaz Atay, 2019). Moreover, chitosan is able to adsorb the electronegative substrate in the cell of microbe and thereby disturb the physiological activities of the microorganism, contributing to the death of cells. A further subtle point is that the degree of deacetylation (DD) of chitosan and its derivatives extremely affect the positive charge density and the higher cationic charge density gives rise to strong electrostatic interaction. For instance, chitosan with a high DD (97.5%) can lead to higher positive charge density providing a stronger antibacterial activity in comparison to the moderate DD (83.7%), mainly based on having more protonated amine groups (Islam et al., 2016). Besides, chitosan antimicrobial activity is indirectly proportional to pH. Additionally, presence of metal ions can set the stage for decreasing antimicrobial activity of chitosan remarkably. However, the choice of solvent does not affect antimicrobial activity of chitosan (Raafat and Sahl, 2009). While antimicrobial activity of chitosan is an undeniable fact, what is to be investigated in that if chitosan antimicrobial activity is affected by the spinning process. More specifically, during the spinning process, chitosan is precipitated in the sodium hydroxide or other solutions. Does that mean the amino groups of chitosan are not protonated anymore?

As a research example, chitosan fibers and chitosan- polyvinyl alcohol (PVA) fibers were prepared using wet spinning system (solvent = acetic acid, coagulation bath = wt. % NaOH solution) (Qu et al., 2014). Chitosan, chitosan-PVA and cotton antimicrobial properties were evaluated against *Escherichia coli* and *Staphylococcus aureus.* A large number of bacterial colonies in the cotton samples were seen; however, it was difficult to find a single bacterial colony in the chitosan samples. Moreover, Chitosan-PVA antimicrobial rate against *Escherichia coli* and *Staphylococcus aureus* was more than 99%. That is because amino groups of chitosan did not experience a remarkable change due to FTIR analysis, which means that they did not crosslink with PVA, implying PVA did not affect the chitosan antimicrobial activity (Qu et al., 2014).

2.5 Chitosan applications

Over the past years, chitosan has been utilized in the food industry as a preservative, a packaging additive, a dietary supplement, and as a nutrient encapsulation system. In addition, in the cosmetic industry, chitosan is used for a vast variety of applications including antioxidant and antibacterial agents in skin protection products, toothpaste and mouthwash, and as a film-forming agent in shampoos and lotions. Moreover, in the agricultural industry, chitosan has been used to defend plants from bacteria, fungi and viruses, and as a fertilizer additive. Considering the wastewater treatment industry, chitosan has also been used to eliminate fats, dyes and heavy metals, mostly due to the fat-binding and chelating properties of chitosan (Schmitz et al., 2019). Besides, chitin and chitosan have been utilized in the textile industry like synthetic fibers production and coatings and textile auxiliaries (Synowiecki and Al-Khateeb, 2003). Figure 5. illustrates the different medical potentials and applications of chitin and chitosan.

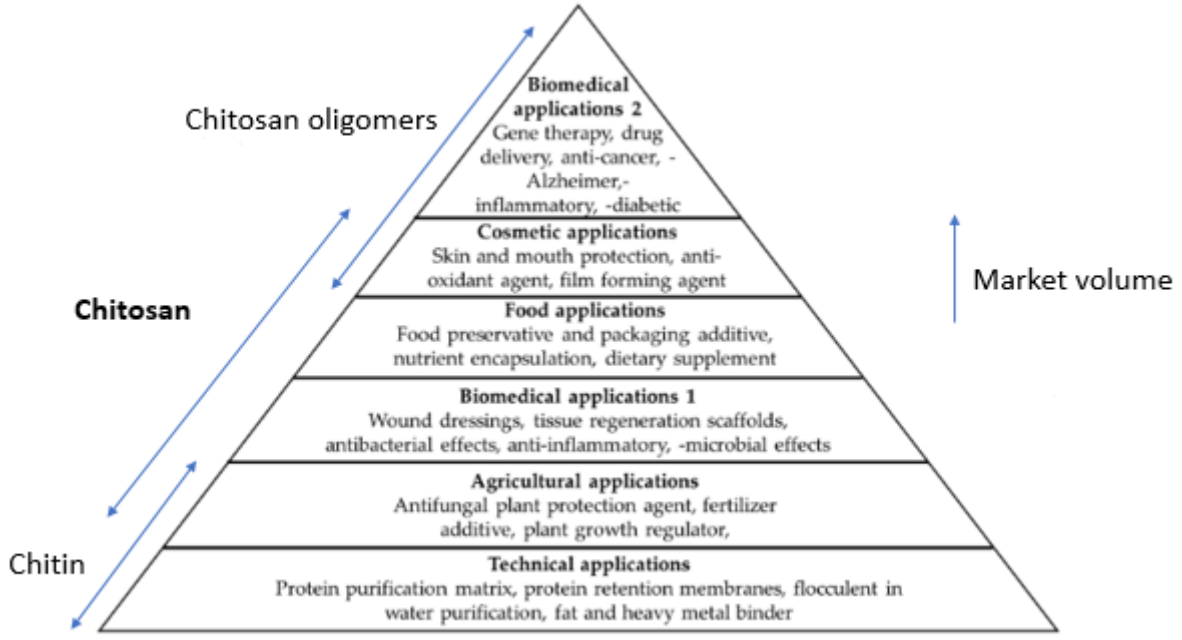

Figure 5. Applications of chitin, chitosan and chitosan oligomers (COS). Biomedical applications are separated into two parts (bulk chitosan and COS), adopted from Schmitz et al. (2019).

2.5.1 Biomedical applications

Chitosan is a biocompatible, biodegradable and non-toxic biopolymer. Promising properties like antimicrobial and anti-inflammatory features has been made chitosan as an excellent option for medical applications like tissue engineering, controlled drug delivery and artificial kidney membrane. To explain further, chitosan has a high mechanical strength as well as having permeability to urea and creatinine, making it suitable as an artificial kidney membrane. Furthermore, these membranes are impermeable to serum proteins. A vast variety of chitosan membranes have been proposed for reverse osmosis, ion exchange, metal ion uptake, diffusion of dyes and separation of water-alcohol mixture systems based on film-forming properties of chitosan (Islam et al., 2016). On the other hand, one of the major impediments of using chitosan for biomedical application is its low solubility at physiological pH; however, chitosan oligomers (COS) are more soluble. Thus, COS are more suitable for medical applications. Besides, COS have bioactive properties, which are insufficient in the longer chitosan polymer since these small molecules are able to penetrate cell membranes, allowing them to affect gene expression and biological processes like apoptosis (Schmitz et al., 2019).

Over the years, a large number of researches have been conducted to study the application of chitin and chitosan as an accelerator of wound healing. Chitin and its derivatives can be used safely for animals and humans (Islam et al., 2016). Wound healing as a complicated biological process consists of four stages: hemostasis, inflammation, proliferation, and remodeling. Such a mechanism performs well enough to repair the injured skin rapidly (Jones et al., 2020). Su et al. (1997) used chitin with fungal mycelia from the fungus *Ganoderma tsugaue* to produce wound healing sacchachitin membranes. Two different materials were examined. The improvement in the wound healing process by covering with Sacchachitin membrane was quite significant in comparison to cotton gauge (or Beschitin). The comparative effectiveness of Sacchachitin membrane with respect to Beschitin in wound healing process can be attributed to N-acetylglucosamine as the main structural monomer of chitin (Su et al., 1997). In another study, the British Textile Technology Group (BTTG) used micro-fungal *mycelia*, which grew in a nutrition solution. Then it was washed and the treatment was done using NaOH to remove protein and then chitin/chitosan were remained as alkali insoluble material (AIM). After that, they used paper-making equipment for the preparation of the dispersion of fibers and finally they did filtration and wet-laid matt preparation. Micro-fungal fibers as their final medical product have highly branched and irregular structures. Moreover, they are unmanageably brittle in case they are allowed to dry and a plasticizer has to be associated with the whole process and a wet-laid matt is used as the basic product (Kumar, 2000).

2.5.1.1 Suture

Surgical sutures are filaments representing one of the main categories of biomaterials for holding body tissue together and wound closure in human and veterinary medicine. Also, they have the capability of drug loading to improve their performance via drug direct administration. Suture probably has the largest market share of material implants, which are used in the human body with a total turnover exceeding $1.3 billion annually (Pillai et al., 2009). An ideal suture providing a secure wound healing process should be biologically inert, flexible, sterilized and handled easily. Also, a suitable suture does not contribute to complications like supporting bacterial growth, causing tissue reaction and allergic reaction. Besides, it has uniform high tensile strength, uniform diameter and size, and at the same time

is capable of dissolving in body fluids in proportion to the rate of tissue strengthening. On the other hand, firstly, different tissues need different ranges of time to be effective. Secondly, each tissue will be healed at different rate because of infection, debility, respiratory problems, obesity, collagen disorders and etc. Based on United States Pharmacopeia (USP), a non-governmental agency for suture materials' standardization, sutures have three classes, which are collagen, synthetic absorbable (e.g. Polyglycolic Acid sutures, Polyglactin 910, Catgut, Poliglecaprone 25 and Polydioxanone sutures.), and nonabsorbable (e.g. Polypropylene sutures, Nylon (polyamide), Polyester, PVDF, silk and stainless-steel sutures.) as follows:
Type I – Twisted or braided and monofilament silk or synthetic fibers.
Type II – Cotton or linen fibers or coated natural or synthetic fibers in which the coating contributes to suture thickness without adding strength.
Type III – Metal suture of monofilament or multifilament construction.
The diameter of the suture is denoted by zeros and indicates the size of the suture. The suture diameter reduces as the zeros expressing the suture size increase (e.g. 6-0 is less than 2-0). Various suture diameters are suitable for different operations since larger diameter contributes to higher tensile strength (Pillai and Sharma, 2010).

As previously mentioned, an ideal suture should have a proper knot safety, which demonstrates the capacity of suture to keep the strength and firmness of the knot without loosening in the course of time. Knop safety increases by reducing the thickness of suture. In contrast, knot safety is proportional to the suture's quality and functional result. Moreover, multifilament and natural sutures can be handled easily in comparison to the synthetic monofilament sutures, meaning that synthetic monofilament needs a greater number of throws to each knot to have a secure knot. Also, monofilament sutures are more susceptible to be loosened after being tied due to their low coefficient of friction (Qin, 2016).
The actual diameter of thread for a given U.S.P. size differs depending on the suture material class as it is illustrated in the Table 2.

Table 2. Suture sizes and knot security based on USP designation for different type of sutures Golnit (2017) and Wikipedia (2020).

USP designation	Collagen Sutures			Synthetic (Absorbable & Non-absorbable)		
	Metric size	Diameter Range (mm)	Average Knot. Pull Tensile (N) (USP)	Metric size	Diameter Range (mm)	Average Knot. Pull Tensile (N) (USP)
# 10-0		0.02		0.2	0.02 – 0.029	024*
# 9-0	0. 4	0.04 – 0.049		0.3	0.03 – 0.039	049*
# 8-0	0.5	0.05 – 0.069	0.44	0.4	0.04 – 0.049	069
# 7-0	0.7	0.07 – 0.099	0.69	0.5	0.05 – 0.069	1.37
# 6-0	1	0.1 – 0.149	1.76	0.7	0.07 – 0.099	2.45
# 5-0	1.5	0.15 – 0.199	3.73	1	0.1 – 0.149	6.67
# 4-0	2	0.2 – 0.249	7.55	1.5	0.15 – 0.199	9.32
# 3-0	3	0.3 – 0.339	12.2	2	0.2 – 0.249	17.5
# 2-0	3.5	0.35 – 0.399	19.6	3	0.3- 0.339	26.3

# 0	4	0.4 – 0.499	27.3	3.5 0.399	0.35 –	38.2
# 1	5	0.5 – 0.599	37.3	4 0.499	0.4 –	49.8
# 2	6	0.6 – 0.699	44.3	5 0.599	0.5 –	62.3
# 3	7	0.7 – 0.799	58.7	6 0.699	0.6 –	71.5
# 4	8	0.8 – 0.899	68.6	6 0.699	0.6 –	
# 5					0.7	

* The tensile strength of the indicated USP size is measured by straight pull.

Table 3 demonstrates the mechanical properties of some commercially available sutures, which are synthetic absorbable monofilament sutures for the indicated size.

Table 3. Tensile properties of 2/0 size sutures available commercially Pillai and Sharma (2010).

Suture	Failure load (Kg): Straight	Failure load (Kg): Knotted	Elongation at break (%)	Work of rupture (kg cm)	Tensile strength (kg/cm^2)
PDO II	4.4±0.2	–	5.7	18.07	–
Maxon	7.09	4.41	4.39	15.92	6056.5
Monocryl	7.26	3.67	39		91,100
Novafil[b]	4.35	2.57	2.94	6.29	4749.4
Gore-Tex (CV-4)[a]	1.78	1.75	1.42	1.55	1558.8
Biosyn[a]	3.7	2.4	44	2.76[b]	55.3[c]

[a]3/0 size. [b]0–10% in kg mm. [c]kg/mm²

Few studies have been conducted on the use of chitosan for suture application. This is probably due to the difficulty of obtaining chitosan filaments with a suitable tensile strength. In order to increase the tensile strength, it is possible to produce biocomposite fibers comprising chitosan reinforced with chitin nanofibrils. Such strong fibers with a good antimicrobial activity can be used for different medical applications (Yudin et al., 2014). In addition, the mechanical properties and absorption resistance of fibers can be improved by adding crosslinking agents through chemical treatment (Singh and Ray, 2000).

In their research, Fan et al. (2007) used wet spinning process to produce chitosan and konjac glucomannan (KGM) blend fibers. The coagulation bath was an aqueous solution of NaOH and ethanol, and 2% acetic acid was used as the solvent. The fibers that were treated by alcoholic solution of acetic acid showed suitable antibacterial activity against *Staphylococcus aureus*. Such a fiber may be a good option for using as sutures.

Besides so many excellent properties of chitosan mentioned previously, chitosan can be degraded *in vivo* by several enzymes e.g. lysozyme. da Silva et al. (2019) conducted a research on the production of absorbable surgical suture, using wet spinning system, from chitosan incorporated with N-acetyl-D-Glucosamine (GlcNAc). They could produce chitosan and Chitosan/GlcNAc filaments with a diameter of 145 μ and 148 μ, respectively. The mechanical resistance of the chitosan filaments diminished with the incorporation of the GlcNAc drug. Inversely, the biodegradation rate of the chitosan filaments was improved by the addition of GlcNAc.

2.6 Wet spinning

There are several spinning techniques to manufacture fibers: melt spinning, electrospinning, wet spinning, dry-jet wet spinning, reaction spinning and gel spinning (Qin, 2015). Wet spinning, dry-jet wet spinning and electrospinning are the main technologies to obtain chitosan fibers. In fiber spinning, firstly, the desired amount of polymer is dissolved in a suitable solvent and directly extruded into a coagulation bath containing a liquid, which is miscible with the spinning solvent; however, a non-solvent of the polymer. Therefore, the solvent will be removed from the polymer, contributing to a precipitated solid fiber in the solution. Wet spinning is usually subdivided into three major steps according to different spinning strategies; 1. Phase separation: rapid formation of the fiber structure happens due to the polymer solution exposure with the coagulation bath. When the polymer fluid is injected into the nonsolvent, the solvent is removed from the polymer solution. It causes the polymer to be precipitated in the bath to form a semi-solid fiber. Further solidification into a coagulation bath brings adequate cohesion and strength for the fiber in order to be collected continuously. 2. Gel separation: The polymer is coagulated based on intermolecular bonds like ionic cross-linking using a salt or another reacting agent. 3. Liquid crystal spinning: a solid crystalline phase for fibers will be formed since lyotropic crystalline solution provides enough alignment and cohesiveness (Foroughi et al., 2018).

Another aspect to point out is that a comprehensive wet spinning system has two more baths. After coagulating in the first bath, washing of the filaments occurs in the second bath in order to remove the coagulation agent, which is followed by drying of the filament in the third bath to remove the remained fluid. Drying can be done through different methods such as using methanol bath, ethanol bath, isopropanol bath and etc. as well as air drying. Stretching of fibers in different baths, draw ratio of each step and the composition of each bath determine the properties of final fibers. Figure 6 represents a schematic of wet spinning setup. ν is the linear extrusion rate at the end of the spinneret, ν_1 is the speed of the stretching rollers at the end of the coagulation bath, ν_2 is the speed of the stretching rollers at the end of the washing bath, and ν_3 is the winding speed (Desorme et al., 2018). In this study, various coagulation baths, washing bath (Milli-Q water) and ethanol bath as dewatering bath have been used; however, they are not connected to each other by rollers and the fibers were taken to different bath manually. Moreover, the injection system should have some pneumatic purge valves in order to eliminate the air bubbles. Such valves, if not considered, can set the stage for the breaking of the fiber in the coagulation bath (David et al., 2018). In this project, the chitosan solution was centrifuged to remove air bubbles and an adjustable syringe pump was used for the dope injection.

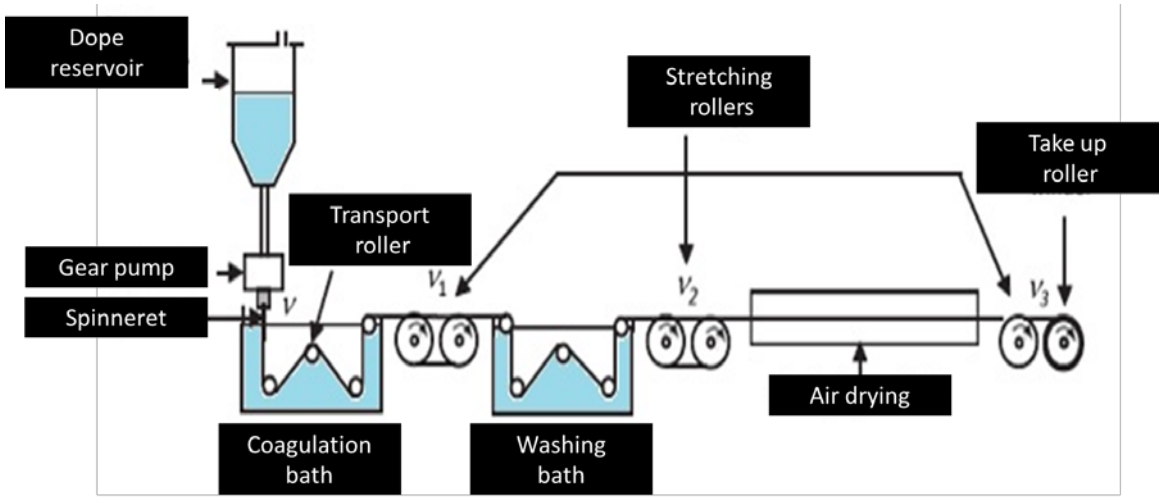

Figure 6. Schematic of a chitosan wet spinning system, adopted from Desorme et al. (2018)

2.6.1 Dissolution and coagulation

Chitosan is not soluble in water due to its hydrogen bonds and hydrophobic interactions between the chain segments (hydroxyl, amino, acetamido, ether and carbon skeleton). In an aqueous medium (except sulfuric acid), which is acidic to a small degree, the protonation of the amine groups supplies adequate electrostatic (repulsive) energy to destroy these intra- and interchain interactions, contributing to solvation of the chains (Enache, 2018). According to Knaul and Creber (1999), it has two steps as follows:

Step 1: $GlcN\text{-}NH_{2(s)} + CH_3COOH_{(aq)} \rightarrow GlcN\text{-}NH^{+}_{3\,(aq)} + CH_3COOH^{-}_{(aq)}$

Step 2: $GlcN\text{-}NH^{+}_{3\,(aq)} + CH_3COOH^{-}_{(aq)} + NaOH_{(aq)} \rightarrow GlcN\text{-}NH_{2(s)} + CH_3COONa_{(aq)} + H_2O$

For instance, the dissolution of chitosan can happen in 1–10% acetic acid (important to provide a stoichiometric amount of acetic acid to protonate the amino groups of the chitosan) below pH 6 to get a viscous dope (Roy et al., 2017).

There are four different categories of solvent used for chitosan. Category 2 (10% oxalic acid and 2M dichloroacetic) represents solutions with pseudo-plastic behavior. Solvents of category 3 (0.0252 M sulfanilic acid, 0.36 M salicylic acid and 0.041 M benzoic acid) are able to dissolve very small amounts of chitosan, and chitosan is insoluble in solvents of category 4 (dimethylformamide, ethylamine, nitrilotriacetic acid, trichloracetic acid, pyridine and etc.). Eventually, the most suitable solvent for chitosan is category 1 (acetic acid, citric acid, lactic acid, malic acid and etc.). However, it has been reported that the chitosan can be dissolved in an alkali medium as well (Enache, 2018). In this study, acetic acid, citric acid, lactic acid and adipic acid were used as the solvent to prepare the chitosan solution and find the optimum solvent for the second stage of the thesis.
Adipic acid as the novel solvent is an abundant, nontoxic, and biocompatible compound. It is also the most important industrial dicarboxylic acid. Commercial adipic acid is mainly obtained from benzene (Polen et al., 2013) and is extensively used for the production of nylon 66 and polyurethane (Falamarzpour et al., 2017). Recently, Niu et al. (Niu et al., 2020) reported the first example of direct biosynthesis of adipic acid using the lignin-derived compound. Besides, the possibility of preparing chitosan hydrogels for e.g. food texturing

agents, nutraceutics and controlled drug delivery by utilizing different acids including adipic acid has been studied (Hamdine et al., 2005).

A large number of coagulations systems were studied by different researchers. Various coagulating agents that were used in the researches on chitosan along with wet spinning before 1990 are shown in Table 4 (Enache, 2018).

Table 4. Various solvents and coagulation baths for chitosan before 1990 Enache (2018).

Solvent	Coagulation bath
1.2% acetic acid aqueous solution	4.6% sodium acetate 2% sodium hydroxide 0.2% sodium dodecyl sulfate
0.5% acetic acid aqueous solution 2 parts of zinc acetate, 4 parts of glycerin and 0.5 parts of alcohol	100 parts water 2 to 2.5 parts NaOH, 15 parts glycerin X parts of sodium sulfate
0.5% acetic acid aqueous	solution 5% NaOH aqueous solution
1% acetic acid aqueous solution	2% dodecyl sulfate de sodium aqueous solution
dichloroacetic acid aqueous solution	CuCO3-NH4OH aqueous solution
dichloroacetic acid aqueous solution	5 to 20% sodium hydroxide aqueous solution + NaOH/methanol
2-4% acetic acid aqueous solution	1) 2M CuSO4: NH4OH (1: 1 v/v) 2) mixture 5% NaOH: 70:30 v / v ethanol 3) 2M CuSO4: 1M H2SO4 + other treatments: 1) and 3) 50% ethanol aqueous solution + 0.2M EDTA • 4Na 2) 50% ethanol aqueous

Here, other new coagulation agents, solvents and researches on wet-spun chitosan fibers are represented. Even though shellfish chitosan has been wet spun in several studies, to the best of our knowledge fungal chitosan has not been wet spun and this is the focus of current thesis.

East and Qin (1993) produced wet-spun chitosan fibers, which were then acetylated in order to get chitin fibers. To prepare the dope, 50 g chitosan (DD = 84%) was dissolved in 950 mL of 2% (v/v) acetic acid solution. A candle filter system was used to filter the solution, then it was added to the reservoir of the spinning equipment, where it was deaerated under vacuum. The metering pump (1 cm^3/rev) and a spinneret (20 holes, 80 mm diameter) were used. Plus, a dilute NaOH bath was considered for the coagulation bath. Fibers that were prepared in this study can have up to 0.24 N/tex tenacity.

Knaul et al. (1998) examined various methods to improve the drying process (forced air, heat, acetone bath, methanol bath and isopropanol bath) for wet-Spun chitosan fibers. Their dope consisted of 6% by weight chitosan (DD = 97.3%) dissolved in 3% by volume acetic acid solution. The linear extrusion rate of the chitosan solution was kept at 2.47 m/min. The coagulation bath was a 1M NaOH solution with an immersion path of 2 meters in length. It was expected to have complete coagulation for the residence time of 48.6 s due to the extrusion rate and length of the bath. The temperature was considered 24 $\pm$ 1°C. The optimum take-up velocity at the end of the coagulation bath was 2.50 m/min. For the extrusion, a variable speed infusion pump was used along with a stainless steel 20-hole spinneret (each hole 100 mm in diameter & the capillary length of 200 mm), resulting in a chitosan yarn of 16–20 filaments. Furthermore, a 40 mm stainless steel filter was mounted behind the spinneret and solutions were degassed using vacuum for 24 h. They concluded that the optimum drying bath was methanol, contributing to having filaments with low moisture content. Moreover, methanol drying led to chitosan fibers with smaller diameter, superior surface smoothness and superior mechanical properties (elongation at break 18.5 % and tenacity 1.05 g/denier) in comparison to other drying methods (Knaul et al., 1998b).

As reported earlier by Tamura et al. (2004), calcium chloride or calcium acetate saturated water-methanol (1:1 v/v) was better coagulation solvent to prepare chitosan filament compared to conventional coagulation baths. Also, ethanol performed effectively as a coagulation agent of chitosan filament instead of methanol, causing ethanol to be the better option from the biomedical safety point of view. Chitosan powder (DA = 6.5%) was dissolved in 100 ml of 10% aqueous acetic acid solution under severe agitation. Subsequently, it was filtered and kept overnight to de-bubble. The dope was extruded under the pressure of 0.6–0.8 kg/cm, which was applied on a stainless-steel nozzle (3 cm of diameter) with 0.1 mm $\emptyset \times 50$ holes as the spinneret. The first coagulation bath prepared by suspending 100 g of calcium chloride or calcium acetate in water-methanol (or ethanol) of 1:1(v/v) mixture, which was followed by 1 h refluxing. The second coagulation bath consisted of 50% aqueous methanol or ethanol according to the composition of the first bath (Tamura et al., 2004).

Researchers produced well-defined chitosan macrofibres, which were processed into a textile structure (3D nonwoven structures, stable knitted and woven textile fabrics) in order to use as textile scaffolds in regenerative medicine such as cartilage and bone tissue (Toskas et al., 2013). In this study, an industrial scale custom-made wet spinning machine was used. Chitosan by 8.5% (wt.) was dissolved in an acetic acid buffer solution (pH = 4.5). A candle filter system then was used for the filtration and the solution was stirred for 5–10 hours. Subsequently, it was deaerated under vacuum. A solution of 0.5 M NaOH/10% EtOH at temperature of 30 - 45 °C was used to coagulate the chitosan. For the washing stage, water bath at 30 – 50 °C was used, which was followed by an air-drying unit. Chitosan fibers with tenacities up to 24.9 cN/Tex could be achieved.

Yudin et al. (2014) reported their progress in biocompatible and bioresorbable composite production using chitosan fibers filled with anisotropic chitin nanofibrils. The degree of deacetylation of chitosan was 83% with the Mw of 215 kDa. The solvent was acetic acid solution (2%) and the coagulation bath was 1:1 mixture of 10% solutions of NaOH and C_2H_5OH. To explain further, the aquods solution of chitin nanofibrils was homogenized using ultrasonic mixer. Then a suitable amount of chitosan was added to chitin nanofibril solution until getting 4 wt% solution. The concentration of the chitin nanofibrils' depended on dry chitosan and were altered between 0.05 - 20 wt.%. Afterwards, the solution was stirred at

ambient temperature for 30 minutes, which was followed by adding the 2% aqueous acetic acid solution into the mixture. Chitosan with the chitin nanofibrils was stirred at ambient temperature for 90 minutes. Degassing was done for 24 h at 0.1 atm pressure. The solution was extruded via the hole with a diameter of 0.6 mm. Extrusion rate was 5.5 mm/s and the residence time of precipitation was 150 s. Washing was done using the distilled water and then dried at 50 °C for 10 minutes. Adding 0.1 - 0.3 wt% in the chitosan matrix results in improving the mechanical properties of the composite like the strength and Young modulus.

In another study, chitin nanocrystals were used to improve the mechanical properties of wet-spun chitosan fibers. Chitosan by 3 wt% concentration was dissolved in 3 wt% acetic acid solution under agitation (stirring at 30 ˚C). Chitin nanocrystal (powder) was added into in deionized water and homogenized by ultrasonication. After that it is mixed with chitosan solution. Mass ratio of chitin nanocrystal to chitosan was controlled (0, 2.5, 5, and 10 wt.%). The coagulation bath for the solution of chitosan and chitin nanocrystal was NaOH–Na_2SO_4. The mechanical properties of the composite improved due to uniform distribution of chitin nanocrystal in chitosan, which can be attributed to the hydrogen bonds formed between chitin and chitosan. The optimum mass ratio was 5 wt.%, contributing to the modulus of 145.6 cN/dtex (Yan et al., 2014).

Mirabedini et al. (2017) used rotary wet-spun chitosan fibers to obtain a torsional artificial muscle. Chitosan solution comprised 3% by weight chitosan (DD = 80% and M_W = 4.5 x 10^5 Da) dissolved in 2.5% by volume aqueous acetic acid solution. In order to get a homogenous solution, it was stirred at 50˚C overnight. The coagulation bath was 1 M sodium hydroxide (Ethanol/H_2O: 1/4). The coiled fibers that were produced with this method demonstrated remarkable torsional actuation. Two especially constructed rotors with adjustable distance rotating in opposite direction were used to make coiled fibers. Wet fibers were hanged between two stiff supports, which were fixed at both ends and kept the fibers straight during the twisting process. As the rotors start spinning in opposite directions, a symmetric twist was put into the fiber, contributing to shortening the length.

Wet-spun chitosan fibers (monofilament and multifilament) were examined for possible use as sutures by Costa Da Silva et al. (2020). Four percent (w/v) chitosan (DD = 88% and MW = 270 KDa) was dissolved in 2% (v/v) lactic acid aqueous solution and homogenized overnight under constant mechanical stirring at 600 rpm. The extrusion rate was considered 45 mL/h using a syringe of 20 mL with the spinneret of 1 mm. The coagulation bath was 1 M NaOH and the residence time was 24 hours at room temperature. This was followed by firstly washing the fibers with distilled water and secondly drying with methanol at 60°C for 2 h. By twisting two of 150 mm long monofilament fibers together, the multifilament fibers were manufactured. Finally, it was concluded that multifilament wires represented higher tensile strength. Also, the multifilament wires are larger than monofilament wires in terms of diameter. From the mechanical properties point of view, chitosan wires are compatible with the U.S. Pharmacopeia specifications for surgical sutures, causing such filaments to be a suitable option for use as surgical sutures. (Costa Da Silva et al., 2020).

2.6.2 Production of fungal fiber and cellulose-based nanofibers

Structure and composition of cell wall of zygomycetes was explained in sections 2.1 and 2.2. As the final section of this chapter, some important studies regarding the production of fungal fiber and fibers obtained from chitin will be mentioned.

Methylcellulose/cellulose nanocrystal (MC/CNC) nanocomposite fibers with suitable ductility and high toughness modulus were prepared using a simple wet spinning system. For the fiber spinning of MC/CNC hydrogel, a high-pressure pump, a sample, an extrusion capillary tube with L=1.50 m and ∅=0.5 mm was used. The MC/CNC hydrogel was centrifuged (1-5 min at 3000 rpm) to debubble. The coagulation bath was 96.1% (v/v) ethanol. The extrusion rate was fixed at 1.0 mL/min. Furthermore, the fibers resided in the ethanol bath for 10 min before being cut and were dried at room temperature (hung and fixed at both ends for at least 20 h). Besides, it was illustrated that continuous spinning process could be done. The extrusion flow rate was reduced to 0.06 mL/min in order to be harmonized with the take-up winder rate and to maximize the residence time within the coagulation bath, which was altered to isopropanol to facilitate coagulation (Hynninen et al., 2019).

Berglund et al. (2016) studied the production potential of cellulose nanofibers from industrial residues, which were carrot (the juice industry waste) and a byproduct of the brewing industry, brewer's spent grain (BSG). They purified carrot residue and BSG thereafter carrot bleached pulps and BSG were ground using a grinder (MKCA6-3, Masuko Sangyo, Japan) which is similar to the grinder that was utilized in this thesis. Briefly put, after dispersing the both suspension with a shear mixer, grinding treatment was performed for around 20 min (gap size of -70 μ, rotation speed of 1500 rpm). They reported that carrot residue is an excellent option for the industrial production of cellulose nanofibers, which is mainly because the dried carrot nanofiber network had strength and Young's modulus of 210 MPa and 12.9 GPa, respectively. Furthermore, the carrot residue showed a 10% higher yield compared to the BSG. Moreover, carrot residue was better than BSG considering raw material cost and processing efficiency.

Ifuku et al. (2009) prepared chitin nanofibers from dried crab shells using a grinding treatment in wet-state. The obtained nanofibers had an even width of 10 to 20 nm. They showed that the N-acetyl group and the α-chitin crystal structure were not removed during the extraction of nanofibers from the crab shell. For the fibrillation part, after making a suspension of purified wet chitin from dry crab shells and water at 1 wt%, the suspension pH value was adjusted to 3 using acetic acid to facilitate the fibrillation. Afterwards, the 1 wt% suspension was passed through the grinder (MKCA6-3, Masuko Sangyo, Japan). The gap size and the rotation speed were set to 0.15 mm and 1500 rpm, respectively. Such a simple but powerful method provides the chance of achieving homogeneous chitin nanofibers in their original state from waste crab shell in large scales.

Das et al. (2012) produced hydrogels containing surface-deacetylated chitin nanofibrils (micrometer length, around 9 nm diameter and 1.35 wt%), which could be used as a spinning solution at room temperature to obtain macrofibers using a coagulation bath of ethanol (30 min). To prepare the hydrogel, partial deacetylated chitin was prepared by dispersing commercial chitin powder in 20 wt% sodium hydroxide solution. The deacetylated chitin was then collected with centrifugation thereafter washed using distilled water. After preparing a suspension (1.35%) of wet sample and water, acetic acid was used for pH adjustment to 4.

Subsequently, the suspension experienced grinding treatment using a grinder (MKCA6−3, Masuko Sangyo, Japan). The clearance gauge and the speed of rotation were 1.5 and 1500 rpm, respectively. The obtained biofibers showed interesting mechanical properties with a large plastic region of about 12% in strain, in which frictional sliding of nanofibrils contribute to dissipation of fracture energy, resulting in a high work-of-fracture of near 10 MJ/m^3.

Svensson et al. (2021) could produce monofilaments from the cell wall of a zygomycetes fungus, *Rhizopus delemar*, using wet spinning procedure. In brief, *Rhizopus delemar* was cultivated on bread waste. The obtained biomass was treated chemically (alkali treatment), contributing to 36% and 23% glucosamine and N-acetyl glucosamine as chitosan and chitin in the cell wall, respectively. For the mechanical treatment, the AIM was dispersed in distilled water (100 ml/g dry AIM) followed by 1 min kitchen blender processing. Further treatment was homogenizing (IKA T25 Ultra-Turrax homogenizer) in distilled water (200 ml/g dry AIM). After centrifugation (5 min, 5000×g), lactic acid or acetic acid was added to prepare the hydrogel. Afterwards, hydrogel material was used for wet spinning in the coagulation bath of ethanol. The obtained fibers displayed a tensile strength and Young's modulus of 69.5 MPa and 4.97 GPa, respectively.

3 MATERIALS AND METHODS

3.1 Materials

Chitosan (commercial medium Mw, DD 85%, viscosity 120 mPaS, and ash content less than 1%) was obtained from BioLog (Germany). Chitosan was used without further purification. The solvents including acetic acid glacial and citric acid anhydrous were purchased from Scharlau (Spain). Adipic acid and lactic acid with purity of 90% and water content of 10% were acquired from Sigma-Aldrich (Japan and USA, respectively). Sulfuric acid and sodium hydroxide pellets, pure GlcN, agar, tryptone, sodium chloride and K_2HPO_4 were obtained from Sigma-Aldrich. Calcium carbonate and ethanol absolute were purchased from VWR. Yeast extract was obtained from Scharlau.

3.2 Production of chitosan fiber

3.2.1 Preparation of chitosan solutions and coagulation baths

In order to prepare chitosan solution (4% w/w), chitosan powder was dissolved in an aqueous solution of lactic acid and acetic acid. It should be noted that a stoichiometric amount of acids (0.239 mol/L) was provided to protonate amino groups of chitosan. Adipic acid is a divalent acid, which means that it has two carboxyl groups. Therefore, $\frac{0.239}{2}$ mol/L of adipic acid was enough to dissolve chitosan. As citric acid is a trivalent acid, it has three carboxyl groups, meaning that $\frac{0.239}{3}$ mol/L of citric acid could be enough to dissolve polymer. However, chitosan was not dissolved in $\frac{0.239}{3}$ mol/L of citric acid probably due to the fact that this acid is not strong enough. Eventually, 0.239 mol/L of citric acid was needed to prepare chitosan solution. Since the calculation of needed amount of acid to prepare chitosan solution was not that straightforward, the calculation for adipic acid samples, as an example, is provided here. Considering equation (1.1) and DD of chitosan which is 85%, mol fraction of glucopyranose amino unit (nGlcN) is 0.85 and mol fraction of glucopyranose acetamido unit (nGlcNAc) would be 0.15. Mw of GlcN and GlcNAc is 179.17 g/mol and 221.21 g/mol, respectively. on

the other hand, when polymerization reaction is happening, 1 molecule of for example glucosamine is reacted from two sides, from one side one OH group is removed and from other side one H group is taken out and instead two covalent bonds are formed. As a consequence, we removed Mw of one molecule of water to calculate the molecular weight of glucosamine repeating unit in the chitosan chain. Moreover, 1 mol chitosan-amine group (NH_2) needs 0.5 mol adipic acid for protonation because adipic acid has two carboxyl groups.

$$1\ mol\ chitosan = 0.85 \times (179.17 - 18) + 0.1 \times (221.21 - 18) = 167.3\ g$$

$$4\%\ chitosan\ by\ weight: \frac{40\ g}{1\ l} \times \frac{1\ mol}{167.3\ g} = 0.239\ \frac{mol}{l}$$

$$Mw\ of\ aipic\ acid\ is\ 146.14\ \frac{g}{mol};\ 0.239\ \frac{mol}{l} \times \frac{146.14}{2}\ \frac{g}{mol} = 17.46 \frac{g}{l}\ adipic\ acid$$

The chitosan solutions were maintained under mechanical stirring (600 rpm, ambient temperature) for 2 h. Afterwards, the solutions were centrifuged (5000×g) for 10 min to remove the trapped air bubbles and kept at room temperature. Three different coagulation baths were used, which were 1:1 mixture of 10% solution of NaOH and EtOH (Yudin et al., 2014), 1M NaOH (East and Qin, 1993) and 1:1 mixture of 2% solution of H_2SO_4, and EtOH.

3.2.2 Viscosity and pH measurement

Viscosity measurement of solutions were performed at room temperature using a Sinewave vibro-viscometer (SV-10, A&D, Tokyo, Japan). Similarly, the measurement of solutions' pH values was done at room temperature using a pH meter (METTLER TOLEDO, USA).

3.2.3 Wet spinning method

The chitosan solutions were injected into the coagulation bath using a 10 ml syringe and a syringe pump (WPI, Germany) at a fixed feed rate of 1 mL/min to form the chitosan fibers. The length and diameter of syringe needle was 40 mm and 0.8 mm diameter, respectively. The needle was submerged directly into the bath through a hole in the coagulation bath's wall (Figure 7). Monofilaments were remained in the first bath for around 2 minutes. Subsequently, the filaments were transferred to the second bath, which is the washing bath (distilled water). Afterwards, ethanol bath was used for dewatering. To evaluate the effect of ethanol bath on the monofilament's properties, samples that were not treated using an ethanol bath were evaluated as well. Finally, the fibers were collected from the last bath (water bath or ethanol bath) and fixed between two points on a whiteboard at room temperature to dry.

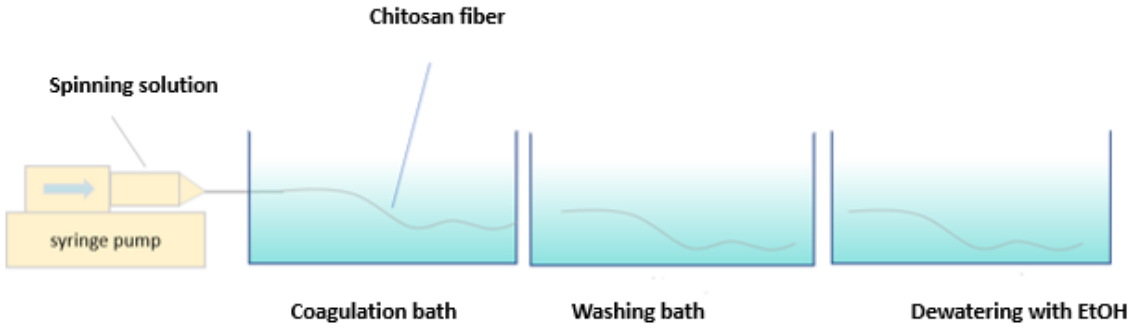

Figure 7. Schematic steps of the wet spinning procedure.

3.2.4 Chitosan monofilaments characterization

3.2.4.1 Scanning Electron Microscopy (SEM)

Scanning electron microscopy was used to analyze the morphology of the chitosan fibers. The images were obtained by ultrahigh-resolution FE-SEM (Hitachi S4800). To coat the samples a 2 nm Pd/Pt layer was used and 3 kV acceleration voltage was applied.

3.2.4.2 Mechanical properties

Tensile testing was used to characterize the mechanical properties of the chitosan fibers. Tensile tests were performed on a Testing Machine (Tinius Olsen Ltd, England) equipped with pneumatic grips and a load cell of 100 N at room temperature. The test speed and the gauge length were 20 mm/min and 20 mm, respectively. The average diameters of monofilaments were 0.165 - 0.293 mm, which was determined by axiosStar microscope Nikon SMZ800 (Germany). Samples were preconditioned 24 h at 20 °C and 65% relative humidity before tensile testing (Fan et al., 2007). The slope of stress-strain curves between 0.1-0.5% strain was considered to calculate Young's modulus.

3.2.4.3 Fourier Transform Infrared Spectroscopy (FTIR)

FTIR was used to evaluate the molecular structures of commercial chitosan powder and wet-spun chitosan monofilaments using a Nicolet iS10 FTIR spectrometer (Thermo Scientific, USA) in transmittance mode over a wavenumber range of 600 to 4000 cm^{-1}. The resolution was 4 cm^{-1} through the accumulation of 32 scans for all spectra. Samples were kept in a desiccator for 3 h prior to the analysis.

3.2.4.4 Differential Scanning Calorimetry (DSC)

DSC-Q2000 apparatus (TA Instruments, USA) was used to examine thermal behavior of fibers. Each specimen (5-10 mg) was put in a covered aluminum sample holder. As the reference for all measurements, an empty aluminum holder and its lid was used. The sample and reference cell were heated at the same time from -30 °C to 230 °C under nitrogen atmosphere. The heating rate was 10 °C/min and the flow rate of nitrogen gas was fixed at 50 mL/min.

3.2.4.5 Water retention test of chitosan fibers

For all of adipic acid samples and sample with highest tensile strength, which were obtained from acetic acid and lactic acid, water retention test was performed. This test was carried out according to ASTM D2402 – 07. Briefly, each chitosan monofilament was immersed in a determined beaker of distilled water at room temperature for 5 min. Samples were centrifuged (9800 m/s^2) and wet samples were weighed. The wet sample then was dried at 110℃ for about 1.5 hour and reweighed. The water retention of monofilaments was calculated as equation (2.1):

$$R = 100\ (\frac{M-D}{D-T})$$

Where R is water retention (%), M is the mass of wet sample with its tare mass (g), D demonstrates the mass of dried specimen with its tare mass (g), T is the mass of the tare (g).

3.3 Production of fungal fiber

The following sections are focused on the cultivation of the *Rhizopus delemar* on bread waste. Bucuricova (2019) found the optimum condition for *Rhizopus delemar* cultivation on bread waste including concentration of bread particle in suspension, the medium pH and time of cultivation. In the study at hand, the cultivation was firstly done in lab scale (shake flasks) to find out the best condition contributing to obtaining the better gel-like material for wet spinning. For instance, different amount of K_2HPO_4 were added to the cultures to examine the effect of K_2HPO_4 on the growth yield as well as chitosan amount of biomass. Moreover, it was evaluated whether the mentioned phosphate compound contributed to better spinnable gel or not. Those experiment are explained in details in the following sections. Afterwards, cultivation was scaled up to acquire the possible maximum amount of fungal biomass, which were needed for remaining experiments including preparation of AIM, AIM treatment with lactic and adipic acids and evaluating the obtained hydrogels for fungal fiber production using wet spinning.

3.3.1 Shake flasks cultivation

3.3.1.1 Substrate preparation

Ground bread using grinder

The bread waste (yesterday bread) was collected from ICA supermarkets near the University of Borås, Borås, Sweden. The bread was diverse including bread loafs, buns, puff pastries etc. While the bread outer surface might have imperfections, no visible signs of mold were seen. The bread was cut into roughly palms sized pieces. To have a homogenized substrate, 1:2 (w/w) mixture of bread and water was passed for four cycles through a disc mill grinder (MKCA6-5, Masuko Sangyo, Kawaguchi, Japan) using the MKE #46 grindstone with a rotation speed of 1500 rpm and a clearance gauge of 0.2, 0, 0, and -0.2, respectively. To clarify further, the clearance gauge or gap size illustrates the shift from a zero position, where the grinder stones have zero distance from each other. A positive clearance gauge demonstrates an open gap. Conversely, a negative clearance gauge shows that discs of grinder are being pressed onto each other. Therefore, a clearance gauge of -1 corresponds to a 0.1 mm shift from the zero position. When the grinding was applied in the contact mode (negative clearance gauge), immediately after suspension feeding, the gap size was set and the clearance gauge was changed to positive mode as soon as there was no suspension between the

grindstone. In order to remove the residue of bread-water suspension, the grinder was cleaned using tap water. The washing slurry was added to the suspension.
The dry weight of bread solution was calculated by weighing triplet specimens of bread in aluminum cups using a digital balance (AEJ 200-4CM, Kern, Balin-gen, Germany). The samples of 5 g were then kept in an oven (Termaks, Sweden) at 70°C over night. The dry weight was obtained from the average of dry weight of three samples using the equation (2.2) (Köhnlein, 2020):

$$\mathrm{Db} = \frac{M2}{M1} * 100\%$$

Where Db is concentration of dry bread, *M1* is mass of bread solution before drying and *M2* is mass of bread solution after drying.

Bread powder and inner parts of bread
Two more substrates were also used to optimize the substrate of scaling up process based on the spinnability of hydrogels obtained from them.
- Dried-milled bread previously prepared by (Köhnlein, 2020) was sieved by very fine sieve (0.5 mm pore size) to obtain flour-like material. Two mediums 1- 4% bread solution and 2- 4% bread solution with 1 g/LK_2HPO_4 were prepared using the bread powder.

- Another substrate was 4% bread solution using inner part of white and brown roll baguette.

3.3.1.2 Cultivation on ground bread

The following experiments were performed in sterile conditions. Agar medium (17 g/Lagar, 20 g/Lglucose, 4 g/Lpeptone, pH 5.5) was prepared for the inoculation of *Rhizopus delemar*. The medium was then autoclaved (VX-95, Systec, Linden, Germany) at 121°C for 20 minutes. When the temperature reached around 60°C, the medium was transferred to agar plates. Agar plates were kept at room temperature overnight to see whether they got contaminated or not. Ten milliliter of sterile ultrapure water (MiliQ, Sigma-aldrich) was added to fungi spore and the fungal spores were suspended in water using a sterile loop, subsequently 100 ul of spore suspension was added to each agar plate in sterile conditions and spread out on the surface of plates using sterile cell spreader. Afterwards, agar plates were kept in an incubator at 30°C for 3.5 to 4 days. However, the ideal temperature for the growth of *Rhizopus delemar* is 35°C. Eventually, plates were sealed using parafilm and kept in refrigerator a at +4°C until used for inoculation of Erlenmeyer flasks. For shake flask cultivations, five different substrates as listed in Table 5 were examined. To prepare shake flasks, 200 ml solution of each substrate (triplet samples) was added to 500 ml cotton-plugged Erlenmeyer flask and the pH was adjusted to 5.5. Erlenmeyer flasks then were autoclaved at 121°C for 20 minutes and kept in cold room at +4°C until inoculation. For the inoculation, 20 ml of sterile ultrapure water was added to three agar plates under the sterile conditions. Spores were suspended in water using sterile cell spreader, subsequently 4 ml of spore suspension was added to each shake flask, contributing a 2% spore concentration. All 15 shake flasks were put in water bath shaker (Grant Instruments (Cambridge) Ltd, UK) at 35°C, 100 rpm for 48 h.

Table 5. Different mediums from ground bread used in shake flasks cultivations.

Sample name	Substrate
0-GB_1	4% ground bread solution
0-GB_2	4% ground bread solution

0-GB_3	4% ground bread solution
0.5-GB_1	4% ground bread solution and 0.5 g/LK_2HPo_4
0.5-GB_2	4% ground bread solution and 0.5 g/LK_2HPo_4
0.5-GB_3	4% ground bread solution and 0.5 g/LK_2HPo_4
1-GB_1	4% ground bread solution and 1 g/LK_2HPo_4
1-GB_2	4% ground bread solution and 1 g/LK_2HPo_4
1-GB_3	4% ground bread solution and 1 g/LK_2HPo_4
2.5-GB_1	4% ground bread solution and 2.5 g/LK_2HPo_4
2.5-GB_2	4% ground bread solution and 2.5 g/LK_2HPo_4
2.5GB_3	4% ground bread solution and 2.5 g/LK_2HPo_4
5-GB_1	4% ground bread solution and 5 g/LK_2HPo_4
5-GB_2	4% ground bread solution and 5 g/LK_2HPo_4
5-GB_3	4% ground bread solution and 5 g/LK_2HPo_4

The calculation for preparing 4% ground bread solution and 1 g/LK_2HPO_4 is provided here; Since 200 ml solution of each substrate was needed, 8 g dry ground bread was needed to get 4% bread solution. Dry weight of ground bread was 24.2%.

$$\frac{100\ g\ solution\ of\ ground\ bread}{25\ g\ dry\ bread} \times 8 g\ dry\ bread = 33.31\ g\ solution\ of\ ground\ \text{bread}$$

Thirty-two grams of that solution comprised 8 g dry bread and 25.31 g water, meaning that it was allowed to add

$$200 - 25.31 = 174.69\ g\ water$$

Therefore, to prepare the solution: 32 g solution of ground bread and 0.2 g K_2HPO_4 were added to 176 g water. Biomass harvesting was done after 48 h. Biomass was collected using a very fine sieve and 1.5 ml of solution was taken for analysis of biomass metabolites.

3.3.1.3 Alkali treatment

Alkali treatment is considered as a common treatment to separate fungal biomass from the cell wall skeleton, resulting in removing protein fractions and other alkali soluble materials. Since chitin and chitosan as the main part of the cell wall material are alkali insoluble, chitinous fractions of biomass can be separated readily using alkali treatment.(Svensson et al., 2021; Köhnlein, 2020). Considering shake flasks cultivations, AIM was needed for two main reasons: 1- evaluating the chitin and chitosan content of the AIM. 2- examining the spinnability of gels obtained from AIM using different concentrations of phosphate.

3.3.1.3.1 AIM preparation to determine of GlcN and GlcNAc content

The following experiment was performed in duplicate in order to obtain the yield of the AIM (g AIM/g dry biomass) as well as determination of GlcN and GlcNAc content. Fungal biomass was mixed for each phosphate concentration and then 0.5 g dry of each concentration was taken. Afterwards, 50 ml of 0.1M sodium hydroxide was added to each of them, which means alkali treatment was done using 100 ml of 0.1 M NaOH/g dry biomass. In order to disperse the biomass in the alkali solution, kitchen blender was used for 1 minutes, followed by autoclaving the solution at 121 °C for 20 min. After the temperature reached room temperature, samples were centrifuged for 10 min (5000 g force) and the supernatant was discarded. The insoluble material was AIM. The rest of the centrifuge tubes were filled with

water and the solutions were mixed manually and the centrifugation was repeated. This washing process was repeated several times until the pH of the supernatant became neutral (using pH paper indicator). Washing process was carried out carefully to avoid losing target solids. This solid material is the fungal cell wall. Finally, the AIM was freeze dried for GlcN and GlcNAc analysis as well as measurement of the AIM yield.

3.3.1.4 Spinnable hydrogel preparation

Gelling ability of AIM which were obtained from different phosphate concentrations was examined in this section. To prepare AIM, the rest of the dried biomass for each phosphate concentration was mixed manually and 100 ml of NaOH 0.1 M/g of biomass was then added to each sample. The experiment was followed by autoclaving all the solutions at 121 °C for 20 min. The AIM was collected after cooling using a very fine sieve. Afterwards, the AIM was washed with water and the sieving was repeated until neutral pH using pH paper indicator. Thereafter, 0.5 g of wet AIM was kept in the oven at 70°C over night to measure the AIM dry weight. This dry weight was later used for the calculation of the needed amount of acid in the next step of the experiment, which is adding adipic acid or lactic acid to the washed AIM to get 5% AIM with pH 4 and evaluating visually if we get a proper spinnable gel. The AIM which was treated by each acid was then treated mechanically using mechanical agitation (IKA T25, DIGITAL ULTRA TURRAX, Germany) to get microfibers, which were to be used for wet spinning.

3.3.1.5 Cultivation on other substrates

Cultivation was performed on two other substrates; the bread powder (dried-milled bread) and inner part of white and brown roll baguette. Regarding the former, two mediums (1- 4% bread solution and 2- 4% bread solution containing 1 g/LK_2HPO_4) were prepared using the bread powder (dried-milled bread). For each medium, triplet samples were prepared. Considering white and brown roll baguette, only one medium of 4% bread solution was prepared (duplicate). Table 6 shows the labelling of different samples used in this section. 0-DB represents the medium with no K_2HPO_4 addition and the bread solution from dried-milled bread. 0-IB shows that the bread solution was prepared by inner parts of bread and there was no K_2HPO_4 in the medium. The process from agar plate preparation to hydrogel formation has been done similar to what was presented in section 3.3.1.2.

Table 6. Different mediums from bread powder and bread inner parts used in shake flasks cultivations.

Sample name	Substrate
0-DB_1	4% ground bread solution
0-DB_2	4% ground bread solution
0-DB_3	4% ground bread solution
1-DB_1	4% ground bread solution and 1 g/LK_2HPo_4
1-DB_2	4% ground bread solution and 1 g/LK_2HPo_4
1-DB_3	4% ground bread solution and 1 g/LK_2HPo_4
0-IB_1	4% ground bread solution and 2.5 g/LK_2HPo_4
0-IB_2	4% ground bread solution and 2.5 g/LK_2HPo_4

3.3.2 Scaling up the process in 1.3 M^3 bioreactor

3.3.2.1 Substrate preparation for 1.3 M^3 bioreactor cultivation

Bread was collected over 10 days from ICA supermarkets near the university of Borås, Sweden. It should be noted that only white bread was used for this purpose. The bread waste comprised of bread loafs, buns, puff pastries and etc. The bread surface looked mold-free. Sweet pastries and similar bread containing large amounts of fruits or custard were eliminated as their presence could prolong the drying process, cause clogging difficulties during grinding and leaving residuals in the final gel. Residual particles may get stuck in the syringe, causing syringe and needle narrowing or clogging during the injection of spinning hydrogels. Before drying, the bread was manually cut into roughly palm sized pieces, then spread out on tablecloth for drying at room temperature for 3 days. A cutting mill (SM 100, Retsch, Haan, Germany) was used to grind the dry bread to a particle size of around 3 mm. The bread was used in the same day as the substrate of all steps (three cultivations). This is further explained in the following paragraphs of this section. Figure 8 illustrates bread preparation for the cultivation in 1.3 m^3 bioreactor.

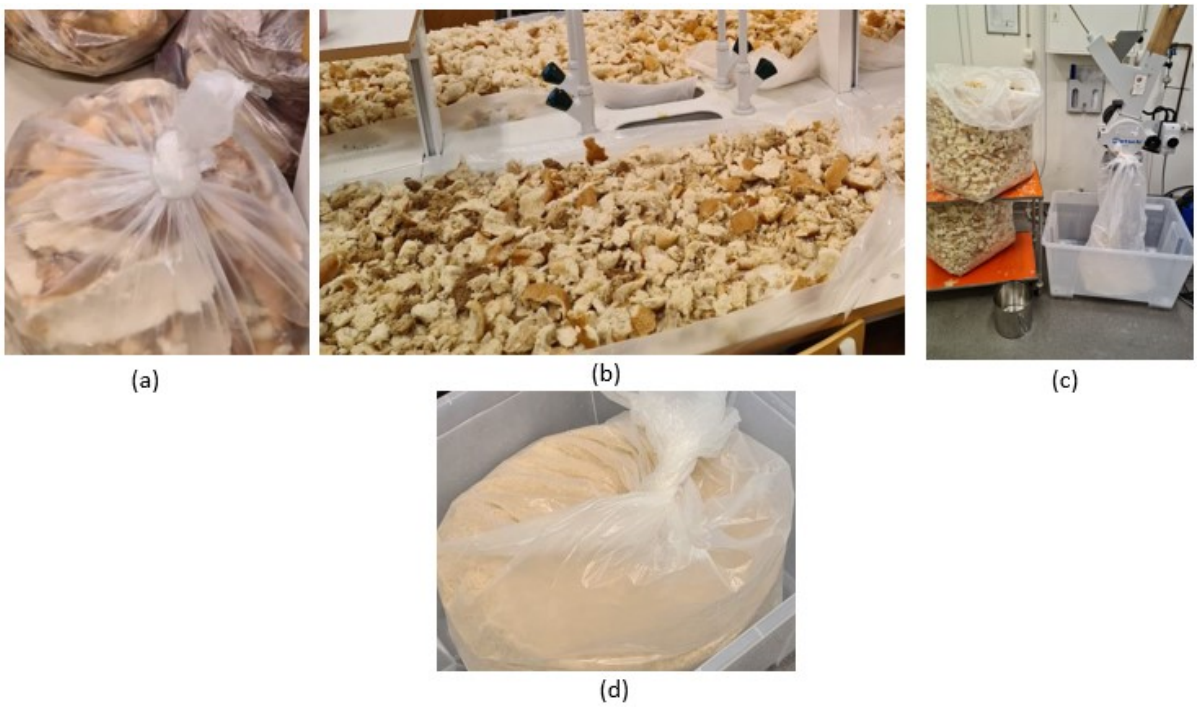

Figure 8. Substrate preparation. (a) yesterday bread, (b) drying process, (c) milling, (d) dried and milled substrate

3.3.2.2 Cultivation in 1.3 m^3 bio-reactor

Rhizopus delemar batch cultivation in 1.3 m^3 bioreactor had three main steps as shown in Figure 9. Firstly, agar plates were prepared as it was explained in section 3.3.1.2 followed by shake flasks cultivation. To prepare shake flasks, 100 ml solution of 4% bread (triplet samples) was added to 250 ml cotton-plugged Erlenmeyer flask. The pH was adjusted to 5.5 and then solutions were autoclaved at 121°C for 20 minutes. Flask inoculation was performed as presented in previous sections. Erlenmeyer flasks were incubated in water bath shaker at 35°C, 100 rpm for 24 hours.

The second step was cultivation in a 26-litre bubble column airlift reactor (Bioengineering, Wald, Switzer-land). To clarify further, in a bubble column reactor, air is used to have a continuous oxygen exchange as well as agitation. Air is provided from the bottom of the vessel and move through the continuous liquid phase (Ferreira et al., 2017). For the inoculation of the 26-litre reactor, 300 ml pre-culture, which was prepared in the previous step was used. The substrate (4% bread solution) was prepared using 20 L ultrapure water and 800 g ground bread. which were serialized separately and mixed immediately before the inoculation. The substrate was then added to the 26-liter reactor without pH adjustment. The cultivation was done at 35°C for 24 hours with the aeration of 1 vvm (volume of air per volume of liquid per minute).
As the final step of scaling up, a 1.3 m^3 airlift bioreactor (Knislinge Mekaniska Verkstad AB, Kristianstad, Sweden) was used. To explain further, an airlift reactor is manufactured with a second internal tube/riser. Providing air at the bottom of the reactor contributes to creating a circular motion of the liquid phase, causing the liquid to move upward inside the inner tube and downward between the inner tube and the reactor shell side (Ferreira et al., 2017). The reactor vessel was filled by ca. 900 l of tap water, then the bread particles (39.75 kg, dry weight 91%) were added manually through a funnel inlet at the top of the reactor. The mixture of bread and water was sterilized inside the reactor (80°C, 1 hour). Harvesting of 26-litre reactor after 24h resulted in 20 L of biomass, which were transferred into the 1.3 m^3 bioreactor as the inoculation.

Eventually, the fungal cultivation was carried out at 35°C for 48 hours with the aeration of 1vvm. The pH was continuously adjusted with a pH meter (METTLER TOLEDO, USA) using 1M and 10M NaOH since it decreased continuously after inoculation. To check the cultivation progress, samples were taken at 0, 5, 24, 31 and 48 hours after initiation for high-performance liquid chromatography (HPLC) analysis. As it is shown in Figure 9, biomass harvesting was done after 48 hours using manual sieving as well as using a compact sieve (Russell Finex, India) to separate biomass from liquid (the sieve pore size, 1 mm). Afterwards the biomass was rinsed three times using tap water and pressed using a pillow cloth by hand to remove excess water. Finally, the biomass was kept in plastic bags of ca. 1 kg and stored at -18°C until use.

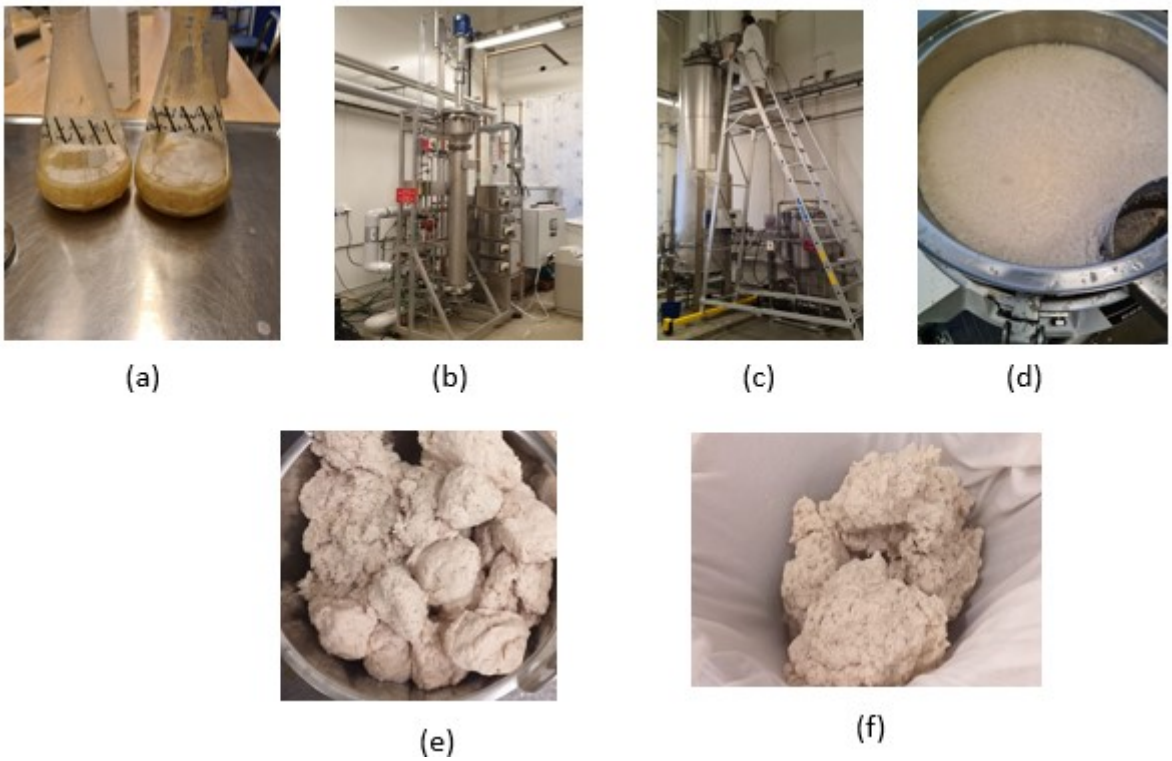

Figure 9. Scaling up *Rhizopus delemar* cultivation. (a) pre-inoculum for the 26 L reactor, (b) cultivation in 26 L reactor, (c) cultivation in 1.3 m3 bioreactor, (d) compact sieving of biomass-water suspension, (e) collected biomass, (f) washed biomass

3.3.2.3 Alkali treatment and AIM preparation.

Pilot scale cultivation in 1.3 m^3 bioreactor resulted in 6.7 kg wet biomass. Triplet specimens of 10 g biomass were taken to measure the dry weight. While 100 ml of 0.1M NaOH/g dry biomass was used for the chemical treatment in previous experiments, 30 ml of 0.3M NaOH/g dry biomass was considered in this section, which is mainly because the dry biomass was around 990 g, meaning that around 90 L 0.1M NaOH was needed. Biomass homogenization before alkali treatment was done using the grinder (1 cycle, gap size of +50 µ) as described in section 3.3.1.1. The following calculations are related to adding 30 ml of 0.3M NaOH/g dry biomass.

$$6.7\ kg\ wet\ biomass\ (14.88\%\ dry\ weight)\ included\ 996.9\ g\ dry\ biomass\ and\ 5.703\ L\ water.$$

$$Mw\ of\ NaOH = 40\ g, 0.3M\ NaOH = 12\frac{g}{l} NaOH, 30\ ml\ of\ \frac{0.3M\ NaOH}{g\ dry\ biomass}\ was\ used$$

$$996.9\ g\ dry\ biomass \times\ 30\ ml\ of\ \frac{0.3M\ NaOH}{g\ dry\ biomass} = 29.907\ L\ NaOH\ 0.3M$$

$$29.907 -\ 5.703 = 24.204\ L\ water\ allowed\ to\ add$$

$$To\ make\ the\ solution\ preparation\ easier, it\ was\ done\ in\ three\ same\ batchs;$$
$$For\ each\ batch: \frac{6.7\ kg\ wet\ biomass}{3}, \frac{24.204\ L\ water}{3}\ and\ \frac{29.907\ L\ NaOH\ 0.3\ M}{3}\ were\ used$$

Considering the amount of water allowed to be used for each batch, 3 and 4.068 L water were used to make water-biomass suspension and remove the biomass residue remained in the grinder, respectively. The water used for the washing was also added to the final biomass suspension. one liter of water was used to make 0.3M NaOH solution which was then added to the biomass-water suspension. The final solution was autoclaved at 121°C for 20 minutes using 5 L glass beakers, which were filled to ca. 4 L with the solution. The AIM was collected by removing the liquid fraction using a very fine sieve. Thereafter, the AIM was washed with tap water and sieved with compact sieve (Russell Finex, India) several times until neutral pH was reached.
To measure the dry weight of AIM, triplet samples of 20 g wet AIM were placed in an oven at 70°C over night. The acquired dry weight (2.6%**)** was further used for the calculation of the amount of acids needed.

3.3.2.4 Spinnable hydrogel preparation

Based on the results of chitosan fibers' production, pH values of 4.8 and 4.5 contributed to fibers with high mechanical strength from adipic acid (AD) and lactic acid (LA) using commercial chitosan solutions, respectively. Therefore, hydrogels were prepared by adjusting pH to the mentioned values using AD and LA (0.239 mol/L). As the first trial of this section, 1 L AIM (initial pH 10.2) was diluted using tap water to attain a concentration of 2%. In order to adjust the pH to 4.5, a small volume (50 g) of AIM was used to find out how much lactic acid was needed. Afterwards, the AIM-water suspension went through repeated grinding cycles using the same grinder used for substrate preparation with a rotation speed of 1500 rpm. The MKE #46 grinding disc set was used as the grinder stone. AIM-water suspension was added to the grinder once setting a clearance gauge of + 0.5 (a gap size of +50 µ). Subsequently, the gap size was set to -70 µ and the suspension was passed through the grinder 6 times in total. Samples were taken after 1P (1 cycle, open gap), 1N (1cycle, negative gap) 3N (3 cycle, negative gap) and 6N (6 cycle, negative gap). To label the samples, name of acid, type of grindstone, number of cycles and grinder mode were mentioned, respectively. For instance, [LA]-[MKE]-[6N] is the abbreviation for samples treated with lactic acid, passed 6 times through the grinder with a negative clearance gauge using MKE #46 grindstone. All ground AIM samples without any further treatment were used for fiber production using wet spinning.

Since some amount of the AIM suspension remained in the grinder, a new experiment was designed to acquire more diluted suspension through the grinder. In this regard a 1.35% AIM solution (initial pH, 9.3) (Das et al., 2012) was prepared. After adjusting the pH to 4.5, grinding was operated. Clearance gauge was set to +0.5 and -0.1 (-100 µ gap size) for the positive and negative gap size, respectively. Apart from gap size, all parameters were similar to the pervious grinding treatment. Sample of 6N was taken for the hydrogel preparation. In order to achieve more homogenized hydrogel, samples were centrifuged (30 min, 5000×g) and the new concentration was calculated. Centrifugation was repeated three times to obtain the hydrogel with the highest possible concentration. However, it was not possible to get that concentrated hydrogel using centrifugation.
To get AIM with the concentration of around 5% or higher, a vacuum filtration funnel was used. The maximum volume of the cylindrical funnel was 1 L, which was attached to a circular PVDF-coated support screen with a support holder. A removable filter (nylon mesh)

with the pore size of 30 μ was placed on the screen. Immediately after adding the suspension, vacuum should be applied. By switching on the pump, the bottom vessel becomes vacuum and since there is pressure in the top vessel, water will travel from the top vessel to the bottom through the filter. The dry weight was measured after the filtration. AIM- water suspension (1.35%) was fed through the funnel to be filtered and attain concentrated AIM. However, it was not that effective. Therefore, AIM suspension was diluted more with tap water (1:4 ratio of AIM suspension and tap water) before pouring into the funnel, resulting in around 5% AIM hydrogel after 20 minutes. It was possible to get more concentrated hydrogel in case the filtration was continued.
There are several reports on the effect of pH on the quality of produced chitin nanofibers. Ifuku et al. (2011) showed passing chitin extracted from mushroom through the grinder at pH 3 can facilitate nanofabrication. Moreover, Das et al. (2012) reported that adjusting pH value to 4 can ease obtaining nanofibrils. Therefore, it was decided to examine the effect of pH on quality of fibers in this work. LA was used to prepare AIM with pH values of 2.5, 3, 3.5 and 4 from filtered AIM (5%) which already had pH value of 4.5. After pH adjustment, all samples were sonicated (BRANSONIC ULTRASONIC, USA) for 60 min at room temperature. Subsequently, spinnability of 5% hydrogel with different pH were evaluated with wet sinning system.

In regards to hydrogel preparation with AD, 1 L AIM (2.6%, initial pH 9.5) was diluted to obtain 1.35% AIM suspension. For this trial, rotary evaporator (Heidolph instruments, Germany) was used for better mixing after adding adipic acid (2 h, 100 rpm). The grinding treatment was carried out with a gap size of +50μ and -100μ for the positive and negative clearance gauge, respectively (rotation speed, 1500 rpm). Regarding grinding stone, MKE #46 grinding disc set was utilized. The suspension was passed through the grinder once and 10 times for the positive and negative gap size, respectively. Specimens of 1P, 1N, 3N, 6N and 10N (10 cycle, negative gap) were obtained through this approach. 10N sample was centrifuged (30 min, 5000×g or 20 min, 9000×g) to evaluate the spinnability of obtained hydrogel. Since the output was not homogeneous and uniform, spinning was not performed. Afterwards, the suspension was subjected to vacuum funnel filtration for 20 minutes. Unlike preparation of lactic acid hydrogel, there was no need to dilute the suspension before pouring into the funnel. The schematic of the process from AIM to hydrogel is shown in Figure 10.

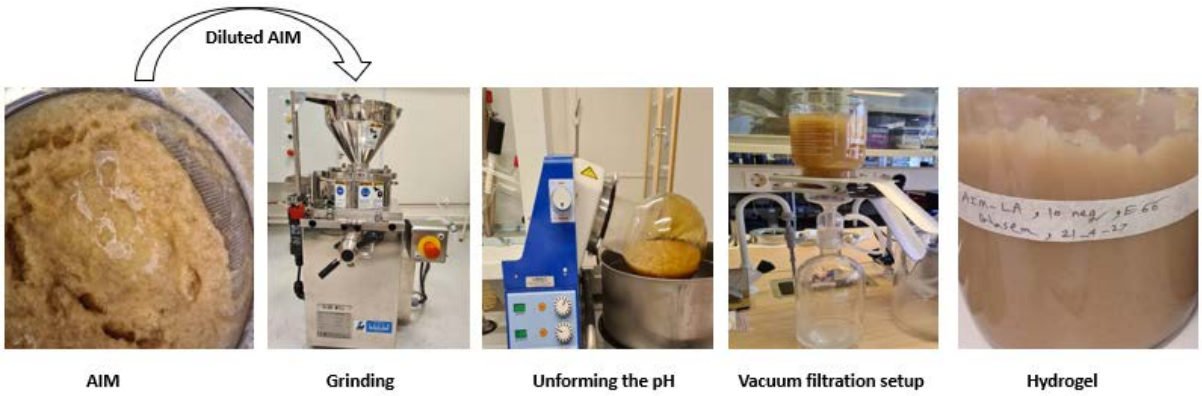

Figure 10. The schematic of the process from AIM to hydrogel

In order to evaluate lactic acid treatment for 10N samples, another new grinding process was conducted, where, MKG-A #80 grinding disk set was used as well as MKE #46 grindstone. MKE #46 (fine grinding, Sic+Al_2O_3) is standard grindstone for soft material. However,

MKG-A #80 (ultrafine grinding, Al_2O_3) is used for pulverizing and emulsifying fibrous material (Figure 11). Briefly put, 3.8 L AIM (2.6%, initial pH 9.1) was diluted to obtain 1.35% AIM suspension. Rotary evaporator (Heidolph instruments, Germany) was utilized (room temperature and 100 rpm) to achieve a suspension with uniform pH (final pH, 3.8). The grinding treatment with MKE #46 grindstone was performed as explained in previous experiment (preparation of adipic acid hydrogel). New experiment was operated utilizing the MKG-A #80 as the grindstone with the same conditions in terms of number of cycles, sampling, rotation speed, and etc. The dry weight of all samples were measured followed vacuum funnel filtration was applied for 10N samples, subsequently the dry wight of 10N sample after filtration was measured.

Figure 11. Different set of grindstones (left) MKE #46 grindstone, (right) MKG-A #80 grindstone

3.3.3 Analysis of the obtained biomass from shake flasks cultivations

3.3.3.1 Biomass metabolites analysis

Biomass metabolites were analyzed using high-performance liquid chromatography. Analysis was performed to determine contents of ethanol, acetic acid, glucose, glycerol, lactic acid and other sugars. To prepare samples, 1.5 ml of filtrate was centrifuged (14000 rpm, 6 min) using a microcentrifuge (Thermo Fisher Scientific, Waltham, MA, USA). The 1 ml supernatant was syringe filtered into HPLC vials. HPLC analysis was operated by a hydrogen-ion based ion-exchange column (Aminex HPX-87H, Bio-Rad, Hercules, CA, USA), performing at 60°C and using 0.6 ml/min of 0.005M sulfuric acid (mobile phase) with a refractive index (RI) detector.

3.3.3.2 Biomass yield

After collecting biomass using the very fine sieve, biomass was washed with water two times to remove unwanted bread particles, which might set the stage for problems during the wet spinning. Biomass was kept in freezer overnight in order to be freeze dried next day using a freeze dryer (FreeZone 2.5L, Labconco, Kansas City, USA). Samples were freeze dried for 36 hours and the dry weight of fungal biomass was measured.

3.3.4 Analysis of the prepared AIM and hydrogels

3.3.4.1 AIM yield

The AIM was freeze dried and the yield of the AIM (g AIM/g dry biomass) was calculated.

3.3.4.2 Viscosity and pH measurement

The measurements of viscosities and pH values of ground AIM were performed at room temperature, using a sinewave vibro-viscometer (SV-10, A&D, Tokyo, Japan) and a pH meter (METTLER TOLEDO, USA), respectively.

3.3.4.3 Glucosamine and N-Acetyl glucosamine analysis

The composition of the cell wall was studied by determining the glucosamine (GlcN) and N-Acetyl glucosamine (GlcNAc) content in the freeze-dried AIM using the method developed by Mohammadi et al. (2012). AIM samples were pulverized with a pulverizing machine (FRITSCH, Germany) with the speed of 6000 rpm. 2,5-anhydromannose concentration represents the total GlcN and GlcNAc residues. To convert chitin and chitosan contents of AIM to 2,5-anhydromannose, following steps were performed.10 mg of AIM was placed in a 13 ml screw cap tube, followed by adding 0.3 ml of sulfuric acid (72% v/v). The solution was mixed every 15 minute for 1.5 hour at ambient temperature. Subsequently, 8.4 ml of water was added and the suspension was then autoclaved at 121 °C for 60 minutes. After that, a 0.5 ml sample was taken immediately by reaching the temperature around 100 °C. when the temperature went down to room temperature, 0.5 ml of sodium nitrite ($NaNO_2$, 1M) was added to the sample under the fume hood. Afterward, the lid was closed tightly and the solution was again mixed, and kept for 6 hours at room temperature. Thereafter the cap was removed and the solution kept overnight under a laminar air flow hood.
To this stage chitin and chitosan contents of AIM has been converted to 2,5-anhydromannose. Eventually, ammonium sulfamate (0.5 ml, 12 wt%) was added to neutralize the surplus nitrous acid, subsequently the sample was mixed for 4 min, which was followed by centrifugation (10 min, 4000g). Moreover, different solutions of pure GlcN (0, 0.125, 0.25, 0.5, and 1 g/L) were prepared using in 2.48% (v/v) sulfuric acid and subjected to the mentioned steps (from taking hot samples to the end of the process). Furthermore, after autoclave step described above, 1.5 ml of samples were also taken when the samples temperature went down to the room temperature. These samples were used to determine acetic acid concentration. HPLC with an ion exchange Aminex column was used to determine the concentration of 2,5-anhydromannose at 60 °C with 0.6 mL/min of 0.005M sulfuric acid (mobile phase) with an RI detector. In order to determine the GlcNAc, acetic acid concentration in cold sulfuric acid hydrolysates was determined simultaneously using HPLC. Moles of acetic acid in each sample is equal to GlcNAc moles. Therefore, the GlcN concentration can be calculated using 2,5-anhydromannose and GlcNAc concentration.

3.3.4.4 FluidScope™ scanning technology (oCelloScope)

The automated time lapse microscopy pictures captured with the FluidScope™ scanning technology using the oCelloScope (BioSense Solutions ApS, Farum, Denmark) was utilized to examine the size of the fungal fibers in the AIM and the hydrogels (ground AIM treated with acids) in the wet state. Lactic acid hydrogel (1.35%) and adipic acid hydrogel (1.35%) were diluted 50 times with the aqueous solution of lactic acid (pH ~ 4.5) or adipic acid (pH ~ 4.8). The AIM sample (2.6%, without any acid and grinding treatment) were diluted 100

times using ultrapure water to acquire suitable fiber dispersions to be able to observe individual fibers in the images. Default settings of a 24-wells plate (Sigma-Aldrich) were set for the picture acquisition, which are illumination time of 2 ms, 4.9 µ imagine distance and scan arear length of 855 µ). Images number for each sample was fixed to 20.

3.3.4.5 Scanning Electron Microscopy (SEM)

To analyze the morphology of AIM and ground AIM treated with lactic acid and adipic acid, materials were diluted (water solution, 0.1 wt%) and the suspension was freeze-dried thereafter the material were placed on an aluminum surface (Salehinik et al., 2021). After extra solvent evaporation, AIM and ground AIM were coated with Pt/Pd of 3.5 nm and observed via FE-SEM using 3kV acceleration voltage.

3.3.5 Wet spinning

All wet spinning trials done in the stage 2 of the project was performed similar to the section 3.1.4. However, coagulation bath was ethanol and there was no need for any further bath. Residence time and the injection speed were 2 minutes and 0.6 ml/min, respectively. The needle diameter was 1.2 mm with the length of 50 mm (Svensson et al., 2021). Coagulated monofilaments were collected from the ethanol bath and fixed between two points on a whiteboard at room temperature for drying.

3.3.6 Fungal fiber characterization

3.3.6.1 Scanning Electron Microscopy (SEM)

Scanning electron microscopy was utilized to investigate the morphology of the fungal fibers as explained in section 3.2.4.1.

3.3.6.2 Mechanical properties of fungal fibers

Tensile testing was conducted with the same equipment utilized in the section 3.2.4.2. The average diameter of fibers was 110 to 240 µ, measured by simple micrometer (Mitutoyo Crop., Japan). The crosshead speed was set to 1 mm/min and pre-load of 0.01 N. Each fungal fiber was sandwiched between two pieces of paper on either side of it using glue to secure the attachment to grips of the instrument. Samples were preconditioned 24 h at 23 °C and 50% relative humidity before operating the test (Svensson et al., 2021). To calculate Young's modulus, the slope of elastic area of stress-strain curve (between 0.1-0.5% strain) was considered.

3.3.6.3 Antibacterial properties of fungal monofilaments

Antibacterial properties of the obtained fugal monofilament were evaluated against Gram-negative (*Escherichia coli*) bacteria. A new agar plate of *E. coli* was prepared and single colony of the bacterium was transferred into 20 ml of fresh sterile medium containing tryptone (1%), yeast extract (0.5%) and NaCl (1%). The pH was adjusted to 7 with NaOH 1M. Subsequently, it was incubated overnight at 37°C. Fibers were cut in length of 1 cm and 5 mg of fibers was placed in small flasks. Then, flasks were closed and autoclaved with fibers to be sterilized. Afterward, 50 µl of the obtained bacterial suspension was added to each flask, which contained 5 mg fibers in a way that the fibers become wet with bacterial suspension followed by the incubation of flasks for 24 h (37°C). Then, 10 ml of fresh liquid medium was

added to each flask and 0.2 ml of liquid was taken from each flask and placed in a well (in 96 well plates). Flasks and 96 well plates were kept in incubator at 37°C. In order to observe the fibers behavior, at times, 0, 2, 4, and 6, and 24 hours, 96 well plate was taken out from the incubator and the images were taken by oCelloScope. A blank sample (three flasks with no fiber) was used as control.

4 Results and discussion

4.1 Production of chitosan fiber

4.1.1 Fibers formation

Chitosan was dissolved in lactic acid (LA), acetic acid (AC), citric acid (CI) or adipic acid (AD) in order to investigate the effect of different spinning solvents on the monofilament characteristics. To protonate the amino groups of chitosan, a stoichiometric amount of the acids was used. Table 7 represents the viscosity and pH values of chitosan solutions in different acids. If pH values are between 3.7 to 5.6, aggregation of the chitosan does not occur (Toskas et al., 2013).

Table 7. pH value and viscosity of different spinning solutions.

Type of solvent	Solvents' ID	pH	Viscosity (Pa.s)
Lactic acid	LA	4.5	3.0
Adipic acid	AD	4.8	3.3
Citric acid	CI	4.2	2.4
Acetic acid	AC	5.5	3.3

Chitosan solutions were extruded into the different coagulation baths as listed in Table 8. All monofilaments were washed with distilled water after coagulating process. By entering different chitosan solution into the different coagulation bath, the monofilaments formed immediately which were collected manually. Stable good quality chitosan monofilaments were obtained from the adipic acid solution as an acid that has not been used previously for production of wet-spun chitosan fiber. The preliminary experiments displayed that using only H_2SO_4 as a coagulation bath contributed to the formation of unstable fibers which were impossible to collect from the bath. Whereas, a mixture of H_2SO_4 and EtOH as the coagulation bath remarkably improved the fiber formation. Considering all chitosan solutions, monofilaments coagulated in NaOH and NaOH-EtOH were collected easily. In contrast, it was much harder to collect and place the monofilaments coagulated in H_2SO_4–EtOH on whiteboard. That is because the fibers obtained from the bath containing H_2SO_4 absorbed more water compared to the other monofilaments, causing them to be less stable. Another point to be mentioned is that fibers, which experienced NaOH and NaOH-EtOH bath could be stretched easily before fixing on the whiteboard. However, most of the fibers obtained from H_2SO_4-EtOH coagulation bath broke upon stretching. Considering all acids tested, lactic acid led to fibers with higher stretchability in the wet form. Monofilaments were obtained from adipic acid solutions displayed good spinnability and stretchability in the wet form, meaning that it was easy to handle them in coagulation bath and collecting process.

Table 8. Monofilament production in different conditions

Solvent	Samples' ID	Coagulation bath	Dewatering

			(EtOH)
Lactic acid	[LA]-[NaOH]-[N]	NaOH 1 M	No
Lactic acid	[LA]-[NaOH]-[Y]	NaOH 1 M	Yes
Lactic acid	[LA]-[NaOH-EtOH]-[N]	(1:1) 10% solution of NaOH and EtOH	No
Lactic acid	[LA]-[NaOH-EtOH]-[Y]	(1:1) 10% solution of NaOH and EtOH	Yes
Lactic acid	[LA]-[H_2SO4 -EtOH]-[N]	(1:1) 2% solution of H_2SO4 and EtOH	No
Lactic acid	[LA]-[H_2SO4 -EtOH]-[Y]	(1:1) 2% solution of H_2SO4 and EtOH	Yes
Adipic acid	[AD]-[NaOH]-[N]	NaOH 1 M	No
Adipic acid	[AD]-[NaOH]-[Y]	NaOH 1 M	Yes
Adipic acid	[AD]-[NaOH-EtOH]-[N]	(1:1) 10% solution of NaOH and EtOH	No
Adipic acid	[AD]-[NaOH-EtOH]-[Y]	(1:1) 10% solution of NaOH and EtOH	Yes
Adipic acid	[AD]-[H_2SO4 -EtOH]-[N]	(1:1) 2% solution of H_2SO4 and EtOH	No
Adipic acid	[AD]-[H_2SO4 -EtOH]-[Y]	(1:1) 2% solution of H_2SO4 and EtOH	Yes
Citric acid	[CI]-[NaOH]-[N]	NaOH 1 M	No
Citric acid	[CI]-[NaOH]-[Y]	NaOH 1 M	Yes
Citric acid	[CI]-[NaOH-EtOH]-[N]	(1:1) 10% solution of NaOH and EtOH	No
Citric acid	[CI]-[NaOH-EtOH]-[Y]	(1:1) 10% solution of NaOH and EtOH	Yes
Citric acid	[CI]-[H_2SO4 -EtOH]-[N]	(1:1) 2% solution of H2SO4 and EtOH	No
Citric acid	[CI]-[H_2SO4 -EtOH]-[Y]	(1:1) 2% solution of H2SO4 and EtOH	Yes
Acetic acid	[AC]-[NaOH]-[N]	NaOH 1 M	No
Acetic acid	[AC]-[NaOH]-[Y]	NaOH 1 M	Yes
Acetic acid	[AC]-[NaOH-EtOH]-[N]	(1:1) 10% solution of NaOH and EtOH	No
Acetic acid	[AC]-[NaOH-EtOH]-[Y]	(1:1) 10% solution of NaOH and EtOH	Yes
Acetic acid	[AC]-[H_2SO4 -EtOH]-[N]	(1:1) 2% solution of H_2SO4 and EtOH	No
Acetic acid	[AC]-[H_2SO4 -EtOH]-[Y]	(1:1) 2% solution of H_2SO4 and EtOH	Yes

4.1.2 Chitosan monofilaments morphology

The SEM images of the obtained monofilaments are shown in Figure 12. Fibers with round cross-sections were obtained in all cases. Figure 12a represents the monofilaments from adipic acid applying different conditions (c.f. Table 8). Monofilaments coagulated in NaOH as without experiencing EtOH bath for dewatering displayed a very uniform and even surface morphology as well as smaller diameters than the other adipic acid fibers. Conversely, dewatering by EtOH had negative impacts on the surface of monofilaments surfaces (e.g. [AD]-[NaOH-EtOH]-[Y] sample). Knaul et al. (1998b) also described a similar effect of the drying process on the surface of chitosan fiber. Surface irregularities could stem from the rapid dehydration using ethanol, creating porous regions. The presence of EtOH in the coagulation bath also led to a similar effect on the monofilaments (e.g. [AD]-[NaOH-EtOH]-[N]). Whereas, less irregularities were seen compared to a bath containing only EtOH probably because of the lower concentration of EtOH. Moreover, the monofilaments made in H_2SO_4-EtOH without dewatering showed a rather even surface. This can be rooted in the higher affinity of the fibers to absorb water in the presence of H_2SO_4. The protonated amino groups of chitosan can create an ionic complex of chitosan-sulfate immediately after contact with sulfuric acid. Although, it is not soluble in aqueous solutions anymore (Akram and Mohammad, 2010), it had a higher interaction with water in comparison to the non-protonated amino groups of chitosan, which were precipitated in the presence of NaOH. Furthermore, the non-protonated part of chitosan in NaOH bath resulted in the formation of stronger interactions along the chitosan chains and led to acquiring monofilaments with smaller diameters as well as higher stability in the wet form than the fibers coagulated in H_2SO_4-EtOH bath (Cui et al., 2008).

Figure 12b represents the fibers made in H_2SO_4-EtOH bath using lactic acid, citric acid, and acetic acid as solvents, respectively. The images showed that H_2SO_4 could be used as a part of an effective coagulation bath, resulting in monofilaments with an even and uniform surface.

As Cruz et al. (2016) described earlier, the presence of small white particles, which can be seen on some monofilaments (e.g. [LA]-[H_2SO_4-EtOH]-[N]) might be attributed to NaOH contamination from the coagulation bath, which was not eliminated in the washing process. The obtained monofilaments with the highest tensile strength from lactic acid, citric acid, and acetic acid are shown in Figure 12c (c.f. Figure 13a). It should be noted that all of these monofilaments with uniform and smooth surface were made in NaOH-EtOH.

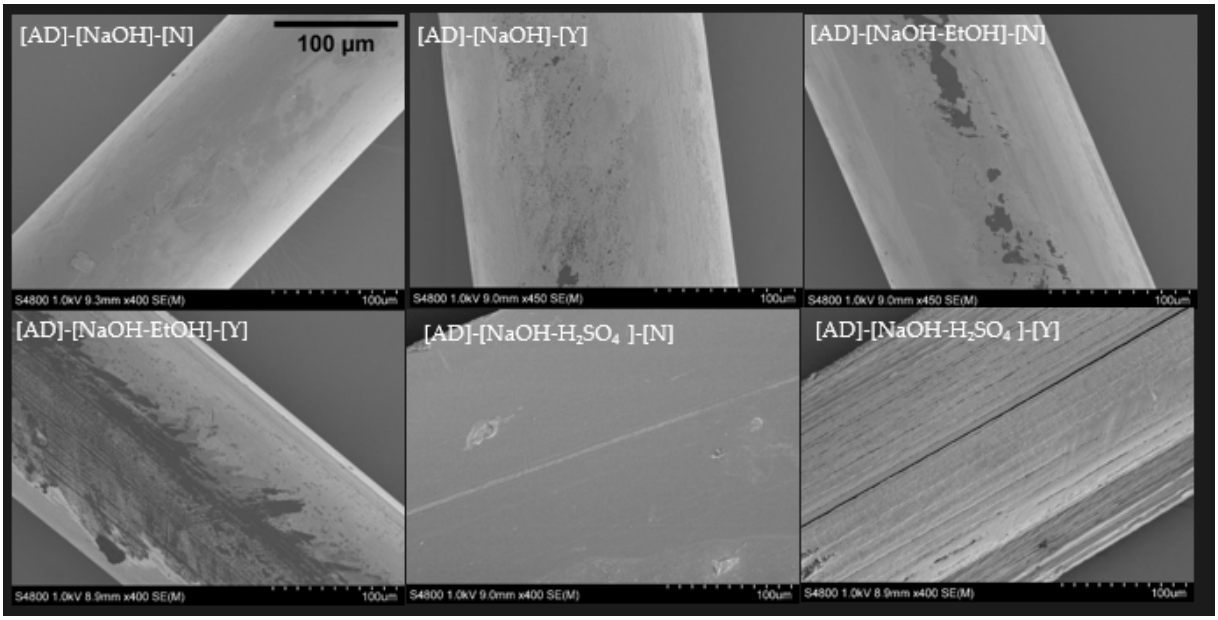

(**a**)

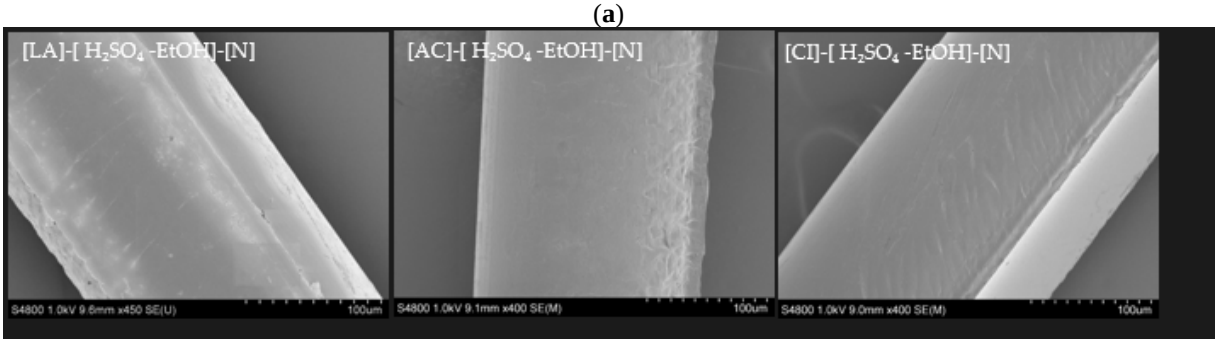

(**b**)

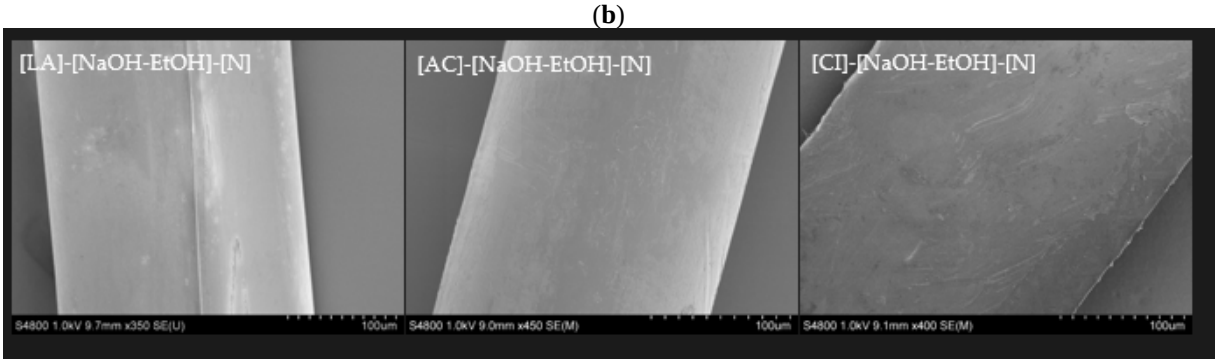

(**c**)

Figure 12. SEM images of chitosan monofilaments. Fibers produced using (a) adipic acid as a solvent in different coagulation baths with and without dewatering, (b) lactic acid, citric acid or acetic acid as solvents made in H_2SO4-EtOH bath without dewatering, (c) lactic acid, citric acid or acetic acid as solvents made in NaOH-EtOH bath without dewatering.

4.1.3 Monofilament mechanical properties

Mechanical properties of the fibers which were obtained using the different fabrication processes were examined through tensile testing. All the measurements were conducted at room temperature. For the samples' preconditioning, they were kept at 20 °C, and 65 % relative humidity for 24 hours. As illustrated in Figure 13, generally monofilaments made from the new solvent, adipic acid, exhibited higher mechanical strength compared to the fibers made by utilizing other conventional solvents. The exception were fibers prepared in NaOH-EtOH as the coagulation bath without dewatering. Monofilaments obtained under these conditions using lactic acid, acetic acid and adipic acid showed similar tensile strength properties of 151.7 (± 8.7) MPa, 150.1 (± 9.8) MPa and 147.9 (±6.9) MPa, respectively; however, clearly lower tensile strength was obtained for the monofilaments made from citric acid (110.7 MPa) (Figure 13a).

As it is presented in Figure 13b, samples dewatered AD and non-dewatered AD exhibited the highest Young's modulus of 4.5 GPa and 4.1 GPa, respectively. This demonstrates that the preferable solvent and coagulation bath, from a strength and modulus point of view, were adipic acid and NaOH-EtOH, respectively. The highest elongation at break was 9.5 % related to using lactic acid as the solvent and NaOH-EtOH as the coagulation bath (Figure 13c). But, the elongation at break of wet-spun monofilament made using adipic acid was at the same level (8 %). Another interesting point is that while sulfuric acid-derived fibers were less stable in the wet form, they displayed promising tensile strength (141.7 MPa) as dried, which is comparable with the highest tensile strength value for adipic acid monofilaments.

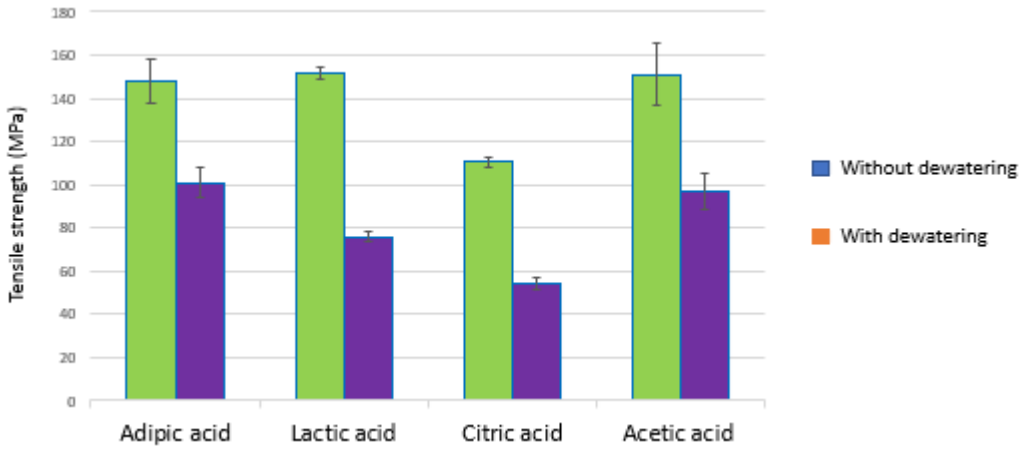

(**a**)

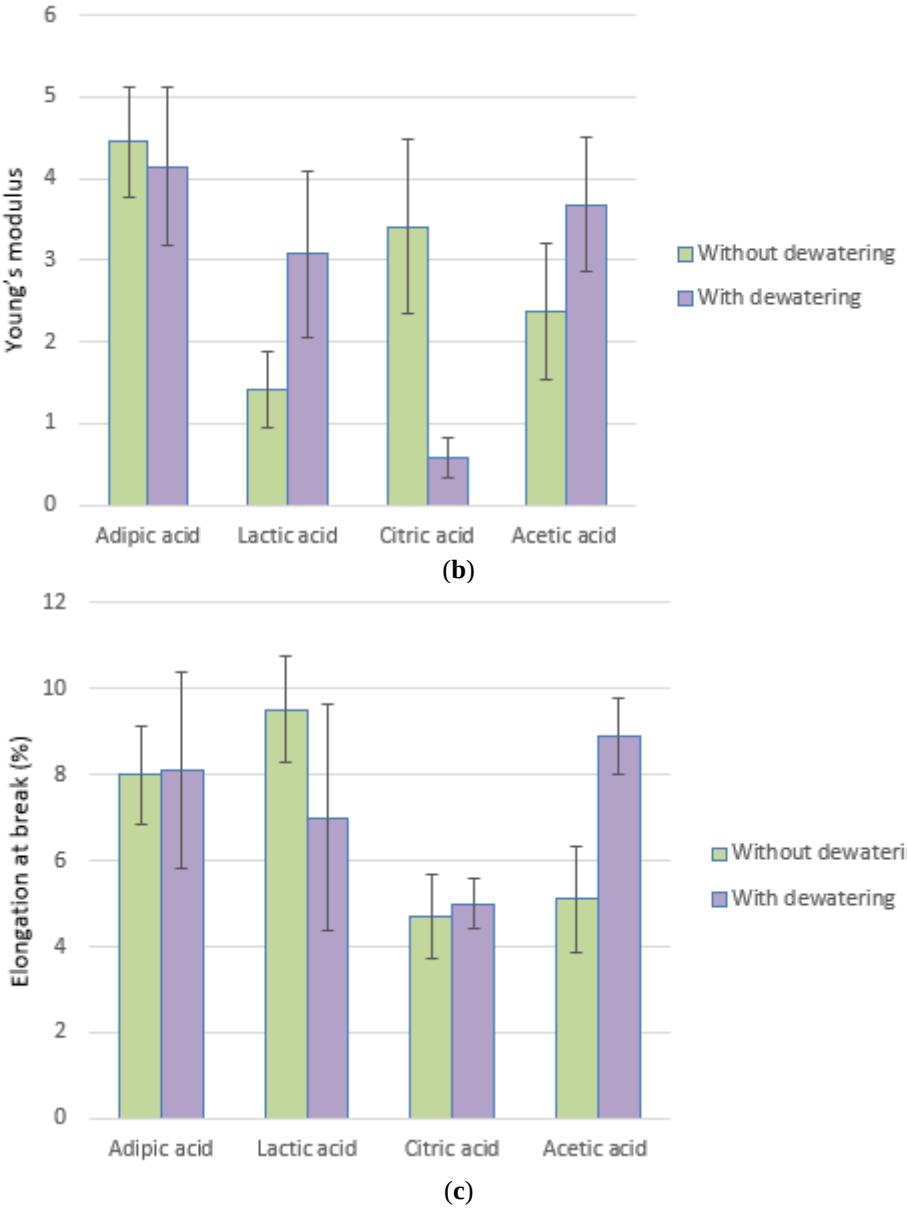

Figure 13. Mechanical properties of wet-spun fibers coagulated in (1:1) 10 % solution of NaOH and EtOH bath as the preeminent coagulation bath. (a) tensile strength, (b) Young's modulus, (c) Elongation at break.

Tensile strength of all monofilaments, which were dewatered with ethanol reduced, regardless of solvent types and coagulation agents. This may be attributed to the higher internal porosity of the fibers after dewatering in EtOH bath. The higher porosity may be caused by the lower surface tension and the lower polarity of ethanol compared to water, decreasing the capillary forces acting on chitosan chains during the drying. A similar phenomenon has been described for nanocellulose membranes, which were subjected to ethanol dewatering (Sehaqui et al., 2016; Henriksson et al., 2008). Moreover, elongation at break of most fibers was diminished after experiencing dewatering bath (c.f. Tables 9, 10, 11 and 12). Ethanol-dried monofilaments showed larger diameter in comparison to those directly collected after the washing process since the immediate removal of water with ethanol resulted in a more porous fiber and consequently a larger diameter, mainly due to the entrapment of the drying agent in the dehydrant molecules (Knaul et al., 1998a). Whereas, drying fibers at room temperature (without dewatering using EtOH), resulted in a more compact fiber. This is probably

explained by the longer time needed for the drying at room temperature, leading to the creation of stronger interaction between the chitosan chains.

4.1.3.1 Monofilaments obtained using adipic acid

Considering fibers prepared using adipic acid as the solvent in different coagulating agent, the diameter of obtained monofilaments were between 165 and 286 micrometer. Dehydration by ethanol enhanced the diameters remarkably. The tensile strength of the monofilaments obtained from AD was between 74.2-147.9 MPa and the fibers collected without dehydration demonstrated 18 % (for NaOH), 46 % (for NaOH-EtOH), and 91 % (for H_2SO_4-EtOH) higher tensile strength than those made with dewatering. Considering all the examined acids, when either NaOH- or H_2SO_4 -EtOH were used as the coagulation bath, by far the highest tensile strength and Young's modulus were attained using adipic acid as a solvent. For adipic acid samples, both NaOH and NaOH-EtOH baths generally contributed to achieving fibers with a better tensile strength in comparison to fibers obtained from other acids (LA, CI and AC). Thus, adipic acid performed as a proper solvent and the resulting fibers had in many cases even better mechanical strength compared to those made using conventional acids. From the mechanical strength point of view, the best monofilaments were acquired from [AD]-[NaOH-EtOH]-[N] (Table 9).

As reported earlier (Chen et al., 2008a), in porous chitosan membranes, adipic acid resulted in more flexible membranes based on the longer carbon backbone of adipic acid compared to other evaluated acids (acetic acid, oxalic acid, succinic acid, and malic acid). Additionally, chitosan and adipic acid displayed stronger interactions in the solution and in the fabricated membranes, leading to higher mechanical strengths. Therefore, adipic acid worked as a good solvent for chitosan, but it also caused further advantages like playing a role of a cross-linking reagent for chitosan (Chen et al., 2008b). In addition, Falamarzpour et al. (2017) reported that using adipic acid to produce chitosan films prevented loss of strength and modulus in comparison to production of chitosan films using acetic acid. This can result from hydrogen bonds and ionic interactions between chitosan and adipic acid, contributing to the physical cross-linking of chitosan by adipic acid. Such a cross-linking decreases the capability of chitosan chains for slippage, causing a remarkable increase in the Young's modulus. The range of elongation at break and Young's modulus for adipic acid fibers were between 1.23-4.45 GPa and 1.8 to 8.1%, respectively, due to the fabrication conditions.

Table 9. Mechanical properties of monofilaments made from adipic acid as the solvent using wet spinning

Sample	Diameter (mm)	Young's modulus (GPa)	Elongation at break (%)	Tensile Strength (MPa)
[AD]-[NaOH]-[N]	0.165 (±0.02)	4.11 (± 0.7)	6.5 (± 2.1)	137.5 (± 9.1)
[AD]-[NaOH]-[Y]	0.221 (±0.03)	1.23 (± 0.5)	5.2 (± 1.9)	116.8 (± 6.3)
[AD]-[NaOH-EtOH]-[N]	0.183 (±0.01)	4.45 (± 0.7)	8.0 (± 1.1)	147.9 (±6.9)
[AD]-[NaOH-EtOH]-[Y]	0.231 (±0.01)	4.15 (± 0.9)	8.1 (± 2.3)	101.4 (±6.7)
[AD]-[H_2SO_4 -EtOH]-[N]	0.197 (±0.03)	3.17 (± 0.3)	1.9 (± 0.8)	141.7 (± 4.9)
[AD]-[H_2SO_4 -EtOH]-[Y]	0.286 (±0.02)	2.13 (± 0.5)	1.8 (± 0.9)	74.2 (± 1.3)

4.1.3.2 Monofilaments made using lactic acid

Wet-spun monofilaments obtained from lactic acid as a solvent exhibited inferior tensile strength (except the sample [LA]-[NaOH-EtOH]-[N]) than wet-spun fiber made using adipic acid.

Among the series of wet-spun fibers from lactic acid, the NaOH-EtOH coagulation bath without dewatering (Table 10) contributed by far the the highest tensile strength, which was also comparable with monofilaments produced by using adipic acid. Similar to adipic acid fibers, dewatering decreased the tensile strength of the fibers. Besides, [LA]-[NaOH-EtOH]-[N] had the elongation at break 9.5%, which was the highest flexibility. The range of Young's modulus of lactic acid fibers was between 1.411 GPa to 3.62 GPa.

Table 10. Mechanical properties of fibers made from lactic acid as the solvent using wet spinning.

Sample	Diameter (mm)	Young's modulus (GPa)	Elongation at break (%)	Tensile Strength (MPa)
[LA]-[NaOH]-[N]	0.193 (±0.01)	3.62 (± 0.2)	3.3 (± 1.0)	89.5 (± 2.6)
[LA]-[NaOH]-[Y]	0.235 (±0.02)	2.49 (± 0.2)	2.9 (± 0.3)	58.8 (± 4.9)
[LA]-[NaOH-EtOH]-[N]	0.187 (±0.03)	1.41 (± 0.5)	9.5 (± 1.2)	151.7 (± 8.7)
[LA]-[NaOH-EtOH]-[Y]	0.226 (±0.01)	3.07 (± 1.0)	7.0 (± 2.6)	76.6 (± 4.6)
[LA]-[H2SO4 -EtOH]-[N]	0.217 (±0.02)	3.24 (± 0.2)	3.6 (± 0.6)	84.7 (± 2.5)
[LA]-[H_2SO_4 -EtOH]-[Y]	0.269 (±0.01)	1.22 (± 0.5)	3.3 (± 0.7)	58.7 (± 4.1)

4.1.3.3 Monofilaments made using citric acid

Regarding citric acid monofilaments, as for other discussed treatments, the coagulation bath NaOH-EtOH led to the highest strength (Table 11). [CI]-[NaOH-EtOH]-[N] and [CI]-[H_2SO_4-EtOH]-[N] resulted both in the highest tensile strength and elongation at break among the citric acid samples. However, the mechanical strength of these fibers was not comparable with that of adipic acid and lactic acid samples. Furthermore, the stoichiometric amount ($\frac{0.239}{3}$ mol/L) of citric acid did not dissolve chitosan, resulting in the application of more citric acid (0.239 mol/L). As a result, chitosan solution with citric acid had a lower pH than other spinning solutions (c.f. Table 7). Lower pH might have affected the properties, but further investigations are required in this regard. In addition, monofilaments' diameters were generally larger than the wet-spun fibers obtained using other acids. 2.1% to 4.7% and 0.58 to 3.41 GPa were the range of elongation at break and Young's modulus of wet-spun monofilaments made by citric acid, respectively.

Table 11. Mechanical properties of fibers made from citric acid as the solvent using wet spinning

Sample	Diameter (mm)	Young's modulus (GPa)	Elongation at break (%)	Tensile Strength (MPa)
[CI]-[NaOH]-[N]	0.186 (±0.01)	2.38 (± 0.31)	2.9 (± 0.4)	86.2 (± 4.1)
[CI]-[NaOH]-[Y]	0.218 (±0.02)	1.75 (± 0.91)	2.7 (± 0.9)	50.4 (± 4.2)
[CI]-[NaOH-EtOH]-[N]	0.264 (±0.01)	3.41 (± 1.06)	4.7 (± 1.0)	110.7 (± 2.4)
[CI]-[NaOH-EtOH]-[Y]	0.275 (±0.03)	0.58 (± 0.24)	5.0 (± 0.6)	54.4 (± 5.3)
[CI]-[H2SO4 -EtOH]-[N]	0.232 (±0.02)	1.75 (± 0.32)	4.5 (± 1.1)	106.3 (± 7.4)
[CI]-[H2SO4 -EtOH]-[Y]	0.293 (±0.01)	0.83 (± 0.22)	2.1 (± 0.8)	54.3 (± 4.2)

4.1.3.4 Monofilaments made using acetic acid

Comparing the wet-spun fibers obtained using acetic acid and adipic acid, mechanical properties of adipic acid samples were generally higher than acetic acid samples. Again, the highest tensile strength acquired was for the fibers coagulated in NaOH-EtOH (Table 12).

Consequently, the only fibers with comparably high tensile strength as the ones with adipic acid was [AC]-[NaOH-EtOH]-[N]. Besides, [AC]-[NaOH-EtOH]-[Y] had the second-highest elongation at break (8.9%) within all evaluated acids' samples. Elongation at break of acetic acid fibers were between 1.3% to 8.9% and Young's modulus was between 0.88-3 to 74 GPa.

Table 12. Mechanical properties of fibers made from acetic acid as the solvent using wet spinning

Sample	Diameter (mm)	Young's modulus (GPa)	Elongation at break (%)	Tensile Strength (MPa)
[AC]-[NaOH]-[N]	0.19 (±0.02)	3.74 (± 0.52)	7.3 (± 0.9)	92.1 (± 4.5)
[AC]-[NaOH]-[Y]	0.241 (±0.01)	1.09 (± 0.43)	1.3 (± 0.4)	33.2 (± 1.1)
[AC]-[NaOH-EtOH]-[N]	0.250 (±0.02)	2.37 (± 0.83)	5.1 (± 1.2)	150.1 (± 9.8)
[AC]-[NaOH-EtOH]-[Y]	0.185 (±0.03)	3.68 (± 0.82)	8.9 (± 0.9)	97.1 (± 8.9)
[AC]-[H_2SO_4 -EtOH]-[N]	0.203 (±0.03)	1.71 (± 0.16)	4.1 (± 0.4)	79.6 (± 5.6)
[AC]-[H_2SO_4 -EtOH]-[Y]	0.279 (±0.02)	0.88 (± 0.19)	3.2 (± 0.6)	70.8 (± 3.0)

In this research work, the highest tensile strength achieved was for the wet-spun monofilaments using adipic acid (147.9 MPa), which is higher than the strength (126 MPa) reported by Han et al. (2016) for the obtained chitosan fiber from formic acid as the solvent by wet spinning procedure. This is also higher than the tensile strength (72.3 MPa) of wet-spun fiber obtained from fungal hydrogel treated by lactic acid (Svensson et al., 2021). However, the strength was lower than that of wet-spun chitosan fibers produced by utilizing lactic acid as the solvent (261 MPa) (da Silva et al., 2019)). This difference may be explained by the presence of methanol in their coagulation bath, which was 70% aqueous solution of 1M NaOH and 30% methanol. As reported earlier by Knaul et al. (1998b) tensile strength of methanol-dried chitosan fibers were higher than the strength of fibers produced by using ethanol as coagulation bath. Methanol was not utilized in the study at hand because of the its high toxicity as well as being fossil-derived (Maoxia Ran, 2019). The highest Young's modulus (4.52 GPa) achieved here was related to adipic acid samples, which is not comparable to Young's modulus of chitosan fiber (25.2 GPa) produced by da Silva et al. (2019). However, this value is at the same range of Young's modulus (4.97 GPa) reported earlier by Svensson et al. (2021) for wet-spun fungal chitosan monofilaments. Elongation at break of 8.9% and 5.7% were reported for chitosan fibers produced by wet spinning by da Silva et al. (2019) and Toskas et al. (2013), respectively, which are lower than the highest elongation attained in this work (9.5%). Higher elongation at break of31.5%, 23.1%, and 11.3% for chitosan monofilaments produced by wet spinning were evaluated by Han et al. (2016), Fan et al. (2007) and Tamura et al. (2004), respectively. Hirano et al. (2000) and Yan et al. (2014) described that stretching of fibers in different baths and the draw ratio optimization can result in higher tensile strength and Young's modulus. As reported earlier by Dresvyanina et al. (2013) when stretching was not applied for wet-spun chitosan monofilaments, tensile strength and Young's modulus of fibers were about 168 MPa and 6.33 GPa, respectively. Considering the same condition of spinning procedure such as feed rate, shear rate and residence time in coagulation bath, in contrast, tensile strength and Young's modulus of monofilaments were altered to 219 MPa and 7.93 GPa, respectively for 100% degree of stretching (Dresvyanina et al., 2013). Therefore, the mechanical strength of chitosan monofilaments examined in this project can be improved by optimizing of other parameters.

4.1.4 Chemical structure of the produced monofilaments

To examine the chemical structure of pure chitosan powder and the obtained monofilaments, FTIR spectroscopy was performed. Figure 14 illustrates the vibrational spectra of the original chitosan powder and the wet-spun monofilaments, which were fabricated using adipic acid as a new solvent. The characteristic absorption bands of original chitosan powder exhibited at 3357 cm^{-1} and 2872 cm^{-1}, were attributed to the -OH group and CH_3 groups, respectively (Flores-Hernández et al., 2014). Furthermore, peaks displayed at 1647 cm^{-1}, 1589 cm^{-1}, and 1320 cm^{-1} corresponded to C=O stretching (amide I), N-H group bending vibration of the primary amine, and C-N stretching (amide III), respectively. Besides, the corresponding bands of -CH_2 bending and - CH_3 bending absorption appeared at 1419 cm^{-1}, and 1374 cm^{-1}, respectively (Li et al., 2016). The bands identified at 1149 cm^{-1} and 1023 cm^{-1} were attributed to the stretching of C-O groups (Toskas et al., 2013). Except two differences, for wet-spun fibers obtained utilizing adipic acid, the majority of the absorption bands occurred at the same regions compared with vibrational spectra of original chitosan powder. The first difference was that two absorption bands appeared at about 2870-2920 cm-^{1} for all adipic acid samples while only one absorption band was identified in the same region for original chitosan sample. Also, bands displayed at 2877 cm^{-1} and 2917 cm^{-1} corresponded to -CH_2 groups of adipic acid seeing the original adipic acid spectrum. As a consequence, the additional band can be caused by the existence of adipic acid as a crosslinker between chitosan chains (Falamarzpour et al., 2017). The second difference was that the hydroxyl group absorption band for [AD]-[H_2SO_4 -EtOH]-[N] and [AD]-[H_2SO_4 -EtOH]-[Y], which were identified at 3226 cm^{-1} at 3232 cm^{-1}, respectively, became significantly wider. As mentioned earlier, for the original chitosan, the hydroxyl group absorption band appeared at 3357 cm^{-1}. Moreover, the band as shown at 2950 cm^{-1} of adipic acid spectrum was related to the -OH of carboxyl group. Thus, this supports the function of adipic acid as a cross-linker, resulting in to the shift of the absorption band of hydroxyl group.

Figure 14b demonstrates the FTIR spectra of the monofilaments with the highest tensile strength produced from adipic acid, lactic acid, citric acid, and acetic acid. These monofilaments were coagulated in NaOH-EtOH without dewatering. When citric acid was used as the solvent, a reduction in transmittance (an increase in absorbance) around 1640 cm^{-1} was observed, which is mainly because citric acid has three carboxyl groups, contributing to an increase in the absorptions of C=O groups. Furthermore, a decrease in transmittance (an increase in absorbance) is observed around 3355 cm^{-1} for citric acid monofilaments, which may be attributed to increasing number of hydroxyl groups in citric acid compared to the other acids (Cruz et al., 2016).

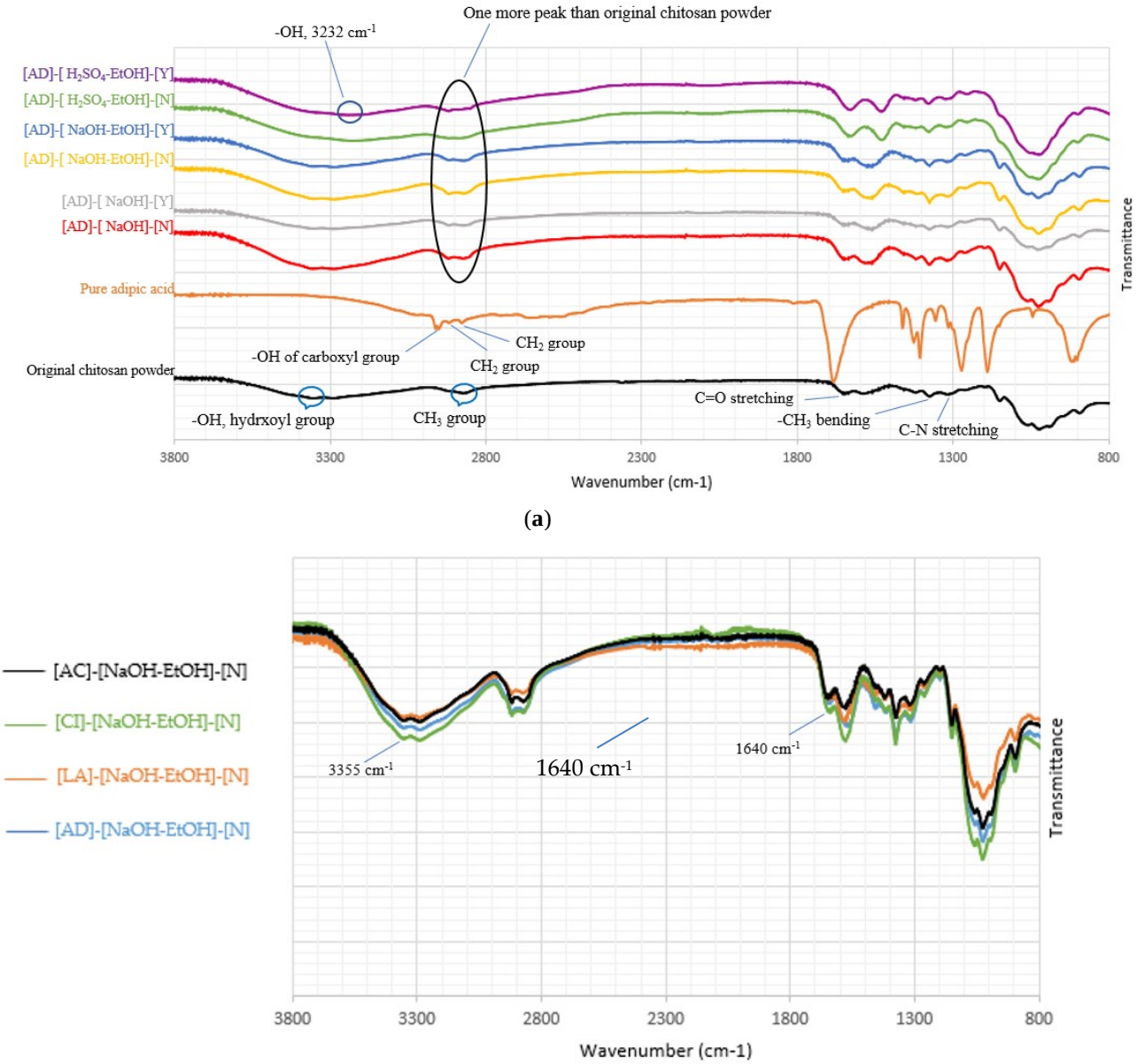

Figure 14. FTIR spectra of wet-spun fibers. (a) adipic acid monofilaments and pure chitosan, (b) comparison between the fibers with highest tensile strength produced from other conventional solvents and adipic acid.

4.1.5. Differential Scanning Calorimetry analysis

Thermograms of original chitosan powder and wet-spun chitosan fibers with the highest tensile strength is represented in Figure 15. Figure 15a illustrates the first heating run. This heating run demonstrates endothermic peaks, which can be caused by absorbed moisture (Dong et al., 2004). Peaks of pure chitosan, adipic acid and acetic acid monofilaments were appeared at around 105℃. However, the peak of lactic acid sample was seen at about 92 ℃. On the other hand, all four peaks disappeared as it is displayed in Figure 15b, which further supports the idea that water evaporation took place during the first DSC run. In order to eliminate the influence of moisture on glass transition temperature (Tg) measurement, the second heating run should be deliberated. Second heating run images showed a small changes of baseline inclination at about 105℃, which could possibly correspond to the Tg of chitosan

powder and chitosan fiber while this value is in contrast to the value of Tg reported by Dong et al. (2004). This means the different treatment using different acids did not contribute to remarkable changes in Tg of chitosan fibers in comparison to original chitosan powder. Another aspect to point out is that while Tg of the common polymers can be demonstrated by DSC, chitosan's Tg is still a controversial issue. The major cause may be rooted in the fact that chitosan is a natural polymer, subsequently some properties of chitosan (e.g. degree of crystallinity, molecular weight and degree of acetylation) can show wide variations because of the source and method of extraction, leading to influencing the Tg (Neto et al., 2005). To explain further, Ratto et al. (1995) determined the Tg of chitosan at 30 ℃ for water contents between 8 to 30%. However, Lazaridou and Biliaderis (2002) stated that the Tg of chitosan could be between -23 to 67℃. Sakurai et al. (2000) also observed the Tg of chitosan at higher temperature (203℃). As a result, the heterogenicity of some natural polymers like chitosan can set the stage for some difficulties in determining Tg.

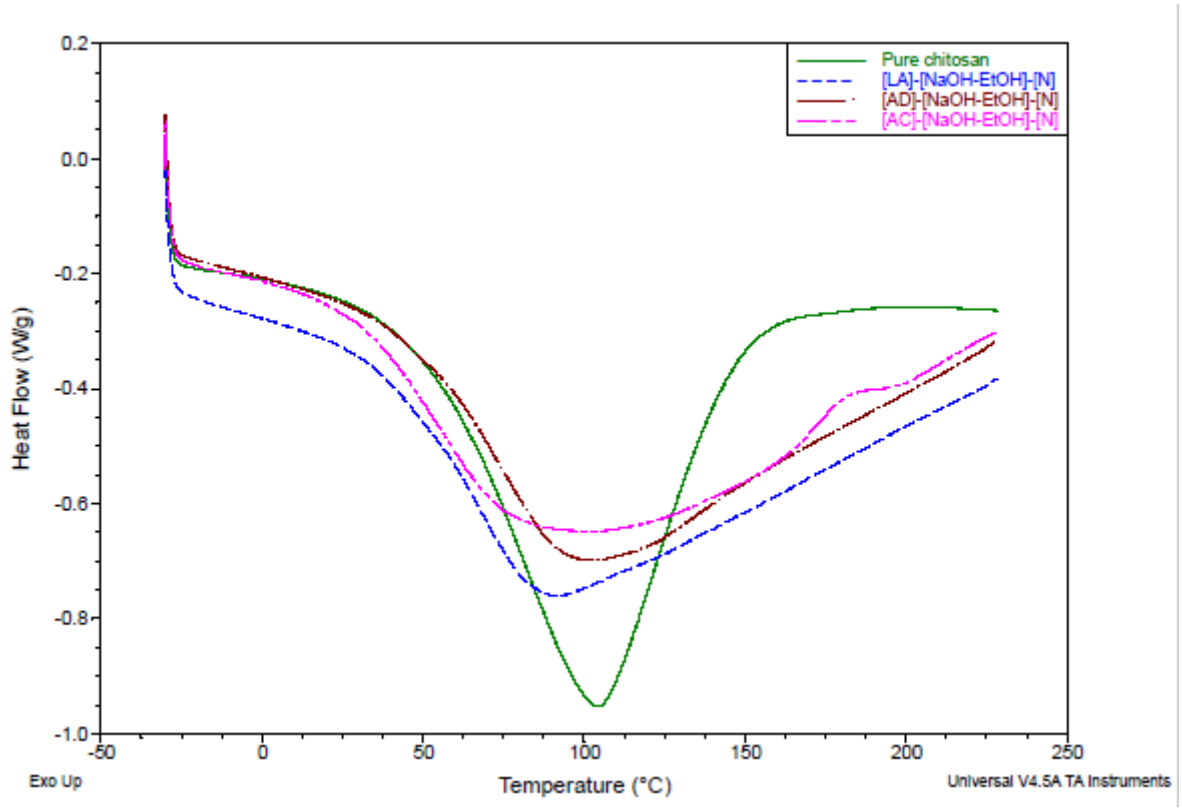

(**a**)

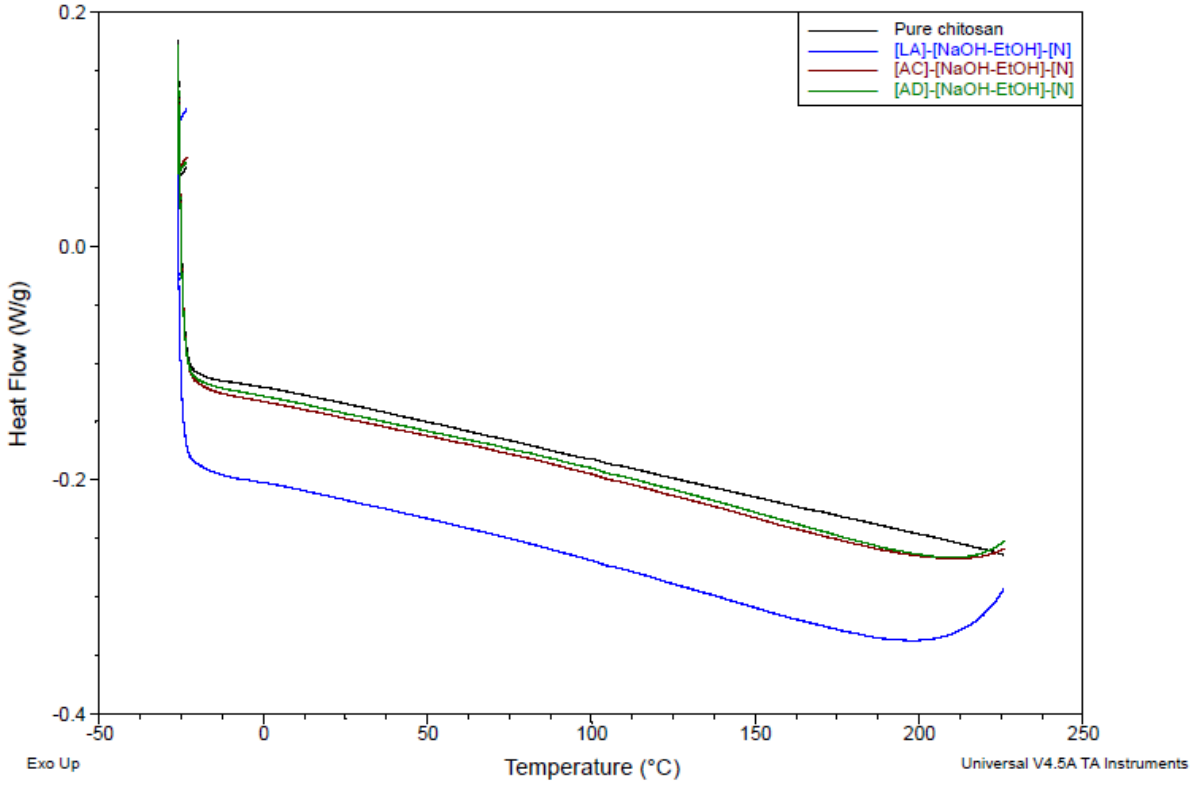

(**b**)

Figure 15. DSC thermograms of chitosan fibers and pure chitosan powder. (a) first heating run, (b) second heating run.

4.1.6 Water holding capacity

Table 13 represents the water retention of different chitosan fibers. The highest water retention (311.8%) was related to [AD]-[NaOH]-[N], which is in the same range of maximum water retention of chitosan fibers produced by Han et al. (2016) (333.4%). This is higher than the maximum water retention of chitosan film (189.7%) and chitosan nanocomposite (236.7%), which was reported by Riva et al. (2015). For sulfuric acid samples, we could not measure the dry weight since the wet sulfuric acid fibers were damaged by centrifugal forces and broken to small pieces, causing them to attach to the filter and centrifuge tube's wall. Consequently, it was impossible to collect and weigh them. Higher water retention property can be attributed to the matrix complexity of chitosan molecules in the fiber. Also, higher crystallinity of chitosan fiber may contribute to higher water absorption because of recovery of hydrogen bonding in chitosan molecules (Han et al., 2016). High water retention property of chitosan is interesting and the researchers explored the water holding capacity of chitosan-based composites. Researchers observed the influence of reinforcement on water retention (Riva et al., 2015). Increasing the water retention through novel adipic acid-based process will be interesting for the researchers working on composites with water holding capability.

Table 13. Water holding capacity of adipic acid samples and other acids with the highest tensile properties

Chitosan fibers	Water retention, %
[AD]-[NaOH]-[N]	311.8
[AD]-[NaOH]-[Y]	176.8
[AD]-[NaOH-EtOH]-[N]	230.2
[AD]-[NaOH-EtOH]-[Y]	200
[AD]-[H2SO4 -EtOH]-[N]	n/a

[AD]-[H2SO4 -EtOH]-[Y]	n/a
[LA]-[NaOH-EtOH]-[N]	233.9
[CI]-[NaOH-EtOH]-[N]	164.3
[AC]-[NaOH-EtOH]-[N]	192.6

4.2 Production of fungal fiber

4.2.1 Substrate preparation

Three different substrates (bread with different pre-treatments) were evaluated for fungal cultivation in order to find the optimal choice regarding hydrogel for wet spinning. Ground bread with a dry weight of 24.2% was considered as one of the substrates. The obtained biomass, AIM and hydrogels from the cultivation on ground bread contained small bread particles, which were problematic in wet spinning (Figure 16). This is why dried-milled bread was examined in order to eliminate the particles in the final hydrogel. Using the powder, the bread particles could still be observed in the biomass, AIM and hydrogels. The next trial was conducted on inner parts of bread. The idea was that since the problematic particles were very hard and rigid solid material, they might be related to the outer-burnt parts of bread rather than the inner parts. However, it did not make any difference, meaning similar particles again appeared in the final biomass.

As a consequence, white bread that did not contain fruits, custard or seed was chosen as the substrate for 1.3 m^3 bioreactor. Furthermore, different concentration of K_2HPO_4 as a part of the cultivation medium were used to evaluate the effect of K_2HPO_4 on the growth yield as well as chitosan content of biomass.

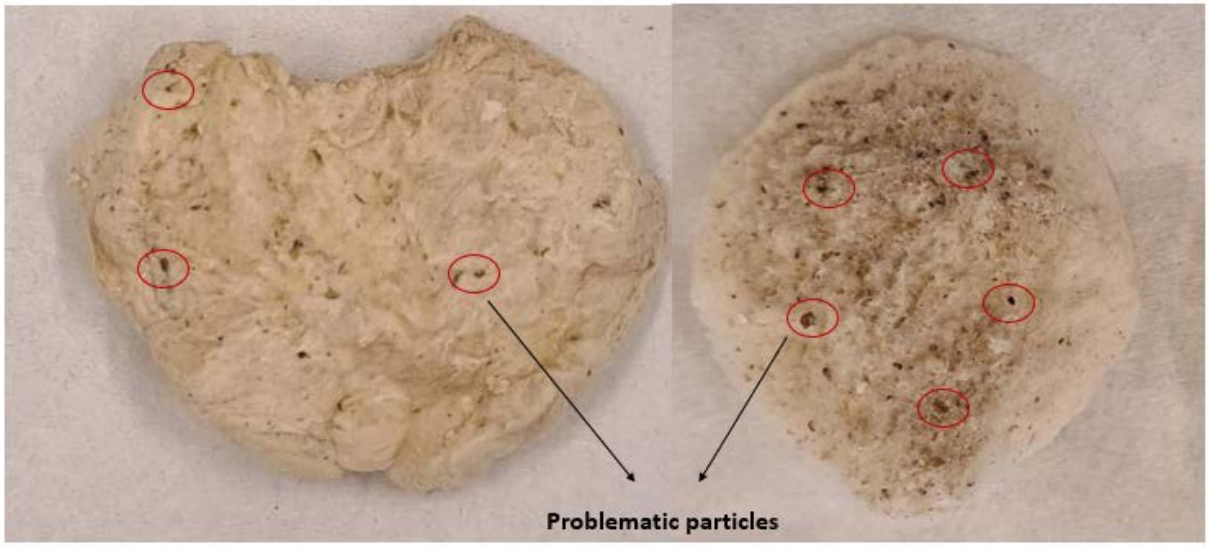

Figure 16. Bread particles in freeze-dried biomass and AIM obtained from cultivation on wet ground bread.

4.2.2 Shake flask cultivations

4.2.2.1 Biomass metabolites analysis

Table 14 shows the resulting metabolites of 48 h fungal cultivation on different substrates.

Table 14. Biomass metabolite concentration (g/L) (obtained from HPLC) after 48 hours of shake flask cultivation on different substrates (c.f. Table 5).

Sample	Glucose (g/L)	EtOH(g/L)	SugMix (g/L)	Acetic acid (g/L)
0-GB	0.044 ± 0.04	3.58 ± 0.11	0.17 ± 0.11	0

0.5-GB	0.032 ± 0.004	4.99 ± 0.72	0.13 ± 0.07	0.011 ± 0.004
1-GB	0.035 ± 0.05	4.22 ± 2.55	0.09 ± 0.04	0.017
2.5-IB	0.007 ± 0	4.86 ± 0.88	0.09 ± 0.03	0.01 ± 0.004
5-GB	0.01 ± 0.007	4.55 ± 0.1	0.1 ± 0.05	0
0-DB	0.2 ± 0.13	8.32 ± 0.55	0.21 ± 0.0	0
1-DB	0.07 ± 0.08	5.47 ± 0.66	0.20 ± 0	0
0-IB	0.8 ± 0	4.5 ± 0	0.12 ± 0.03	0

4.2.2.2 Yield of biomass and AIM (substrate: *ground bread).*

Biomass which was harvested after 48 hours, was freeze dried to measure the biomass yield (triplet samples). Table 15 represents the biomass yield (g biomass/g bread) and the final pH after harvesting. pH values changed for the samples containing phosphate compound (K_2HPO_4) in their cultivation medium. The biomass yield of all samples was in the same range. However, the sample without phosphate (0-GB) showed lower yield, which might be explained by the wider standard deviation of that sample. Therefore, from the biomass yield perspective, there was no priority between different substrates.

Table 15. Biomass yield, dry weight and final pH value from shake flask cultivation on 4% ground bread solution with different phosphate concentration.

Sample name	Final pH	Dry weight (%)	Biomass yield (g/g bread)
0-GB	3.4	1.3 ± 0.266	0.325 ± 0.266
0.5-GB	3.9	1.4 ± 0.035	0.354 ± 0.035
1-GB	3.9	1.4 ± 0.011	0.356 ± 0.011
2.5GB	4.0	1.3 ± 0.052	0.325 ± 0.052
5-GB	3.9	1.4 ± 0.039	0.348 ± 0.039

AIM was obtained through alkali treatment of biomass. The average weight of freeze-dried AIM from 0.5 g biomass is shown in Table 16. The highest AIM yield was achieved from 4% ground bread solution and 5 g/LK_2HPO_4 medium while 0.5 and 1 g/LK_2HPO_4 did not result in higher AIM yield compared to 0-GB sample. It seems 4% ground bread solution and 5 g/LK_2HPO_4 medium. As the result acquired were only from shake flasks, meaning that there were not enough materials to check the spinnability of the gel, phosphate supplement was not used in large-scale cultivations.

AIM dry weight was used to calculate the amount of acid for hydrogel preparation as follows;
Example: 5 g of 2.5-GB solution was taken to prepare 6% lactic acid solution with pH of 4.
$Dry\ weight = 13.4\%, \quad 13.4 \times 5 = 0.67\ g\ , 0.67/0.06 = 11.2$
$5g - 0.67 = 4.33\ g\ water\ content, 11.2 - 4.33 = 6.87\ g\ total\ water\ and\ acid$

Table 16. AIM yield of shake flask cultivation on ground bread.

Sample name	Freeze-dried AIM weight (g/0.5g biomass)	AIM yield (g AIM/g biomass)	AIM dry weight (%)
0-GB	0.088 ± 0.001	0.175 ± 0.001	16.8 ± 0.042
0.5-GB	0.085 ± 0.005	0.17 ± 0.005	13.5 ± 0.055
1-GB	0.085 ± 0.015	0.17 ± 0.015	13.5 ± 0.50
2.5-GB	0.105 ± 0.014	0.21 ± 0.014	13.4 ± 0.081
5-GB	0.107 ± 0.004	0.214 ± 0.004	11.5 ± 0.024

Freeze-drying was not done for dried-milled bread and bread inner parts. However, the dry weight of biomass was calculated as presented in Table 17.

Table 17. Biomass dry weight of shake flask cultivation on dried-milled bread and bread inner parts

Sample name	Final pH	Dry weight (%)
0-DB	3.2	15.3 ± 1.6
1-DB	3.6	11.8 ± 1.9
1-IB	2.8	8.1 ± 1.7

4.2.3 Cultivation in 1.3 m^3 bioreactor

For the large-scale fungal cultivation, the total volume of water and dry bread was 900 l and 36.17 kg (39.75 kg bread particles, dry weight 91%), respectively. This provides a bread concentration of 40 g/Lor 4% bread solution. *R. delemar* cultivation on white bread particles in a 1.3 m^3 bioreactor yielded around 36 kg wet biomass with an average of 14.88% dry weight (5.95 g biomass/L). As reported earlier by Bucuricova (2019), bread concentration of 75 g/Land 45 g/Lresulted in 12.27 g biomass/L and 7.92 g biomass/ L, respectively. The obtained dry biomass and the total dry bread used for the cultivation was 5356.8 g and 36172.5 g, respectively, leading to the biomass yield of 0.15 g dry biomass/g dry bread which is greater than the dry biomass yield (0.095 g/g bread) reported by Köhnlein (2020). Figure 17 demonstrates the glucose concentration in the course of time in cultivation medium, which was similar to the enzymatic hydrolysis of starch taking place in parallel with the fungal growth. Glucose concentration was 0.136 g/Lat 0 h and increased rapidly after 5 h, showing the start of exponential phase of growth. After 48 hours of cultivation the concentration of glucose was 11.41 g/L, which further supports that a healthy and good cultivation was performed. The glucose concertation reached a maximum of 18.357 g/L31 h after onset of the cultivation. The ethanol and acetic acid concentration was 0.943 g/L(Figure 18) and 0 g/L48 hours after inoculation, respectively, which indicates the cultivation was done without any contamination.

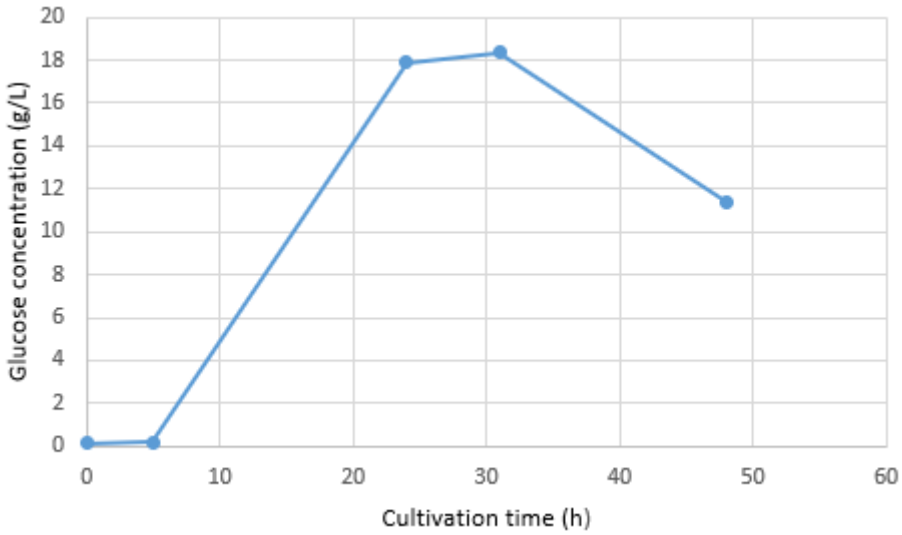

Figure 17. Glucose concentration over time in 1.3m^3 cultivation

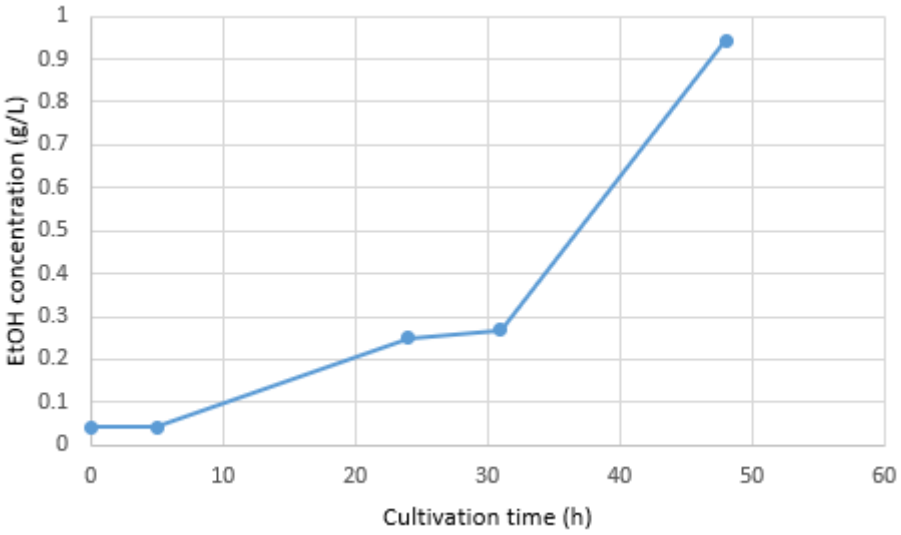

Figure 18. Ethanol concentration over time in 1.3 m^3 cultivation

4.2.3.1 Wet spinning

Different groups of hydrogel preparation considered are listed in Table 18.

Table 18. Different combinations of hydrogel preparation using the AIM obtained from cultivation in 1M^3 bioreactor

Group	Samples name	pH value	Viscosity (mPa.s)	Concentrated via centrifugation	Rotary mixing	Concentrated via vacuum funnel
1	[LA]-[MKE]-[1P]	4.72	$10.8 * 10^3$	No	No	No
	[LA]-[MKE]-[3N]	4.79	$7.5 * 10^3$	No	No	No
	[LA]-[MKE]-[6N]	4.80	$7.2 * 10^3$	No	No	No
2	[LA]-[MKE]-[1P]	4.6	Not measured	Yes	No	No
	[LA]-[MKE]-[1N]	4.65	Not measured	Yes	No	No
	[LA]-[MKE]-[3N]	4.7	Not measured	Yes	No	No
	[LA]-[MKE]-[6N]	4.9	Not measured	Yes	No	Yes
3	[AD]-[MKE]-[1P]	4.8	23.5	No	Yes	No
	[AD]-[MKE-[1N]	4.8	11.6	No	Yes	No
	[AD]-[MKE-[3N]	4.8	13.8	No	Yes	No
	[AD]-[MKE-[6N]	4.8	12.5	No	Yes	No
	[AD]-[MKE-[10N]	4.8	14.4	Yes	Yes	Yes
4	[LA]-[[MKE]-[1P]	3.8	$1.24 * 10^3$	No	Yes	No
	[LA]-[MKE]-[1N	3.8	$1.3 * 10^3$	No	Yes	No
	[LA]-[MKE]-[3N]	3.8	$1.1 * 10^3$	No	Yes	No
	[LA]-[MKE]-[6N]	3.8	993	No	Yes	No
	[LA]-[MKE]-[10N]	3.8	406	No	Yes	Yes
5	[LA]-[MKG]-[1P]	3.8	$1.3 * 10^3$	No	Yes	No
	[LA]-[MKG]-[1N]	3.8	$1.2 * 10^3$	No	Yes	No
	[LA]-[MKG]-[3N]	3.8	$1.0 * 10^3$	No	Yes	No
	[LA]-[MKG]-[6N]	3.8	687.6	No	Yes	No
	[LA]-[MKG]-[10N]	3.8	570	No	Yes	Yes

As reported earlier by Ifuku (2014), by passing purified materials with chitin through the grinder, the resultant mixture is a gel-like substance containing nanofibrils. Moreover, similar to chitin behavior, viscosity values of cellulosic materials usually increase by passing through the grinder, contributing to a high viscous, transparent and gel-like material (Iwamoto et al., 2011). However, in general, viscosity of the ground materials decreased by increasing the

number of grinding cycles. Although, it was expected to obtain gel-like material with higher viscosity by increasing the number of grinding cycles regardless of gap size or the type of grindstone, grinding treatment did not result in nanofibrils formation. In following paragraphs, each group will be discussed separately.

Group one (c.f. Table 18) had the highest viscosity among all groups since AIM-water suspension had greater concentration (2%) than the other groups (1.35%). Moreover, the gap size for negative cycles was – 70 µ for this group. Whereas it was -100 µ for all other four groups. Centrifugation was not done for this group in order to evaluate the possibility of acquiring spinnable gel using grinding treatment without any further treatment. However, such a hydrogel was not good at all for wet spinning, mainly due to low concentration, which led to coagulation ofmonofilaments in the bath. The pH values for this group changed slightly.

The second group (c.f. Table 18) is related to preparing hydrogels from AIM-water suspension (1.35%). Since the suspension was more diluted compared to group one, AIM-water suspension did not remain in the grinder. The pH value again has been changed marginally, stemming from manual mixing. The highest concentration achieved via centrifugation was 3.2% and hydrogel with that concentration was utilized for wet spinning. However, it did not contribute to continuous fiber formation. To explain further, fibers were broken immediately after injection into the coagulation bath, mostly due to the fact that hydrogel was not uniform enough. Moreover, it seemed that the hydrogel should have been more concentrated to be able to produce continuous fibers after injection. Therefore, if the hydrogel is not uniform and concentrated enough, getting continuous fiber is not possible. As a consequence, the sample [LA]-[MKE]-[6N] was passed through the vacuum funnel filtration, resulting in around 5% hydrogel (average dry weight).
As previously mentioned, samples with pH values of 2.5, 3, 3.5 and 4 were prepared from [LA]-[MKE]-[6N] (pH 4.9) by using lactic acid. All samples were utilized for wet spinning. Monofilaments were formed from all hydrogels (5% dry weight, different pH values). Considering fibers' uniformity, hydrogels with lower pH (2.5, 3 and 3.5) produced better fibers compared to others. However, fibers were very brittle, causing in breakage during collection process. Considering ease of handling, obtained fibers from hydrogel with pH 5 were collected much easier compared to other obtained fibers. Fibers achieved from hydrogel with pH 4, were not uniform and could not be handled easily. As explained earlier, all hydrogels were sonicated prior to wet spinning. It should be noted that sonication did not make any difference in regard to the quality of obtained fibers. The aging influence on [LA]-[MKE]-[6N] (pH 4.9, group 2) was examined as well. As a result, the gelling was reduced after 1 month (kept at 4℃) since the hydrogel lost some of its water content. Conversely, the same aging period did not affect 6N hydrogels with the pH value of 2.5 and 3, meaning that [LA]-[MKE]-[6N] (pH 2.5 and 3, group 2) could contribute to continuous fiber formation and it was possible to collect fibers.

Group 3 (c.f. Table 18) corresponded to hydrogel treated by adipic acid. Since it was concluded that mixing the suspension manually might not result in an AIM-water suspension with uniform pH value throughout the suspension, rotary evaporator (Heidolph instruments, Germany) was used for this hydrogel. As a result, the obtained pH value of 4.8 did not change for different grinding cycles, which means that rotary mixing was effective. Hydrogels'

viscosity of group 3 were significantly lower than the other groups, which is probably because the hydrogel was not homogenous at all and the liquid fraction was separated from the AIM, causing two separated phases. Furthermore, based on the oCelloScope images of lactic acid hydrogel (Figure 19), it seemed while size of fibrils had been reduced from AIM to 6N sample, 6 times grinding cycles did not contribute to nanofibrils. That is why 10 negative cycles of grinding was planned to be examined as well. Therefore, for the adipic acid hydrogel, 10 times grinding cycles were studied. In order to obtain a more uniform hydrogel, [AD]-[MKE]-[10N] was centrifuged. However, the spinning was not performed since the centrifuged hydrogel looked like aggregated non-uniform materials, which was definitely not spinnable. [AD]-[MKE]-[10N] sample was also vacuum funnel filtred, but similar result was obtained. As previously mentioned, unlike lactic acid hydrogels, there was no need to dilute the AIM-water suspension before adding that into the funnel. It is a further support showing that adipic acid hydrogels were two separated phases. The dry weight was measured to be 6.9%. Getting 6.9% dry hydrogel in the same time compared to the lactic acid hydrogel filtration, might not be rooted in vacuum funnel filtration. It seemed that the liquid fraction of the suspension passed through the filter easily since it was a separate phase.

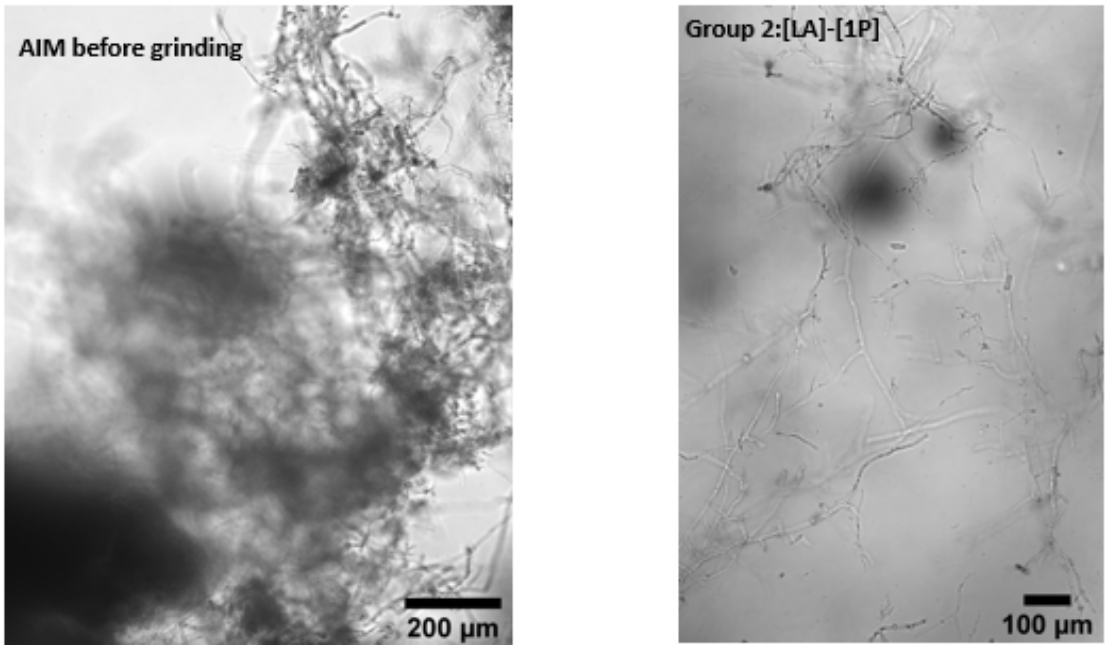

(**a**)

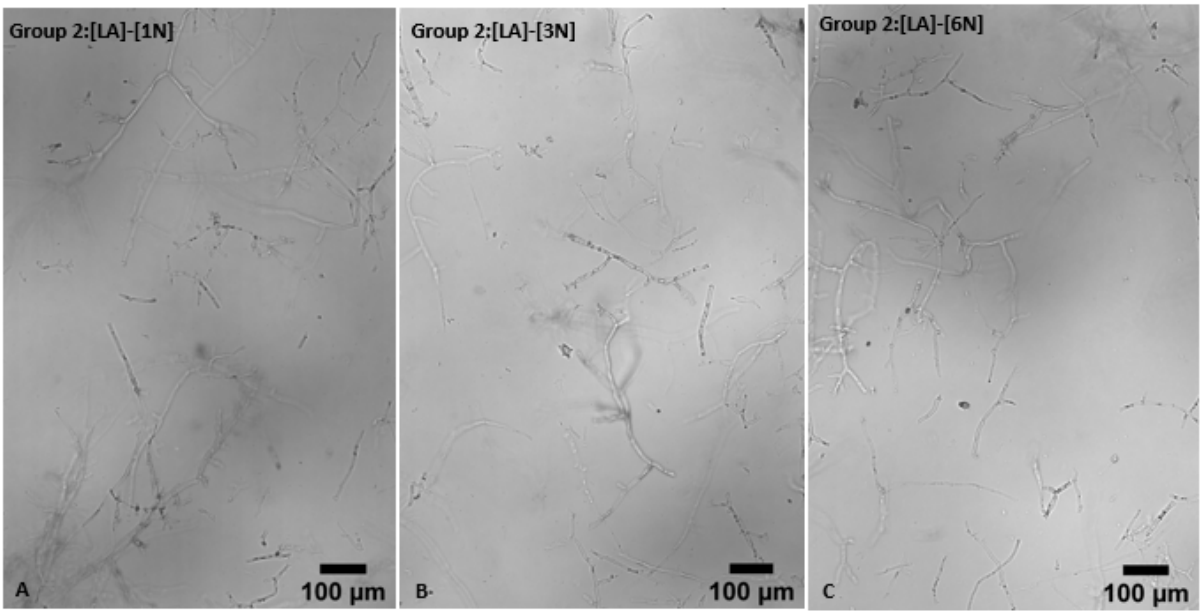

(**b**)

Figure 19. Microscope images (from oCelloScope) representing fungal fibers in AIM with and without treatment. (a) AIM without any treatment (left) and group2 [LA]-[MKE]-[1P] (right), (b) A is related to group2 [LA]-[MKE]-[1N], B is corresponded to group2 [LA]-[MKE]-[3N] and C is related to group2 [LA]-[MKE]-[6N].

Group 4 and 5 (c.f. Table 18) represent other grinding treatments, which were done to evaluate lactic acid treatment for 10 N cycles. The pH value for both groups' hydrogel was 3.8 due to the homogenizing with rotary mixing step. None of the hydrogels were centrifuged and samples of 10 N cycles passed through the vacuum funnel filtration. The viscosity value of different hydrogels belonging to either group 4 or 5 were in the same range, meaning that different grindstone had the same influence on hydrogels, from the viscosity value point of view. In general, viscosity has been reduced by increasing the number of cycles. The dry weight of [LA]-[MKE]-[10N] and [LA]-[MKG]-[10N] was 4.5% and 6.8% respectively. The difference in dry weight could be caused by different time of applying vacuum funnel filtration. Regarding wet spinning, it was impossible to form continuous fiber using [LA]-[MKE]-[10N] (group 4, 4.5%) sample, probably due to the low concentration of hydrogel. However, the same sample with the concentration of 5.2% contributed to forming fibers, but fibers were not uniform. Comparing this sample ([LA]-[MKE]-[10N], group 5, 4.5%, pH 3.8) with [LA]-[MKE]-[6N] (group 2, 5%, pH around 5), the second one resulted in more uniform, stable and easily-handle fibers, which might result from different grinding cycles. Therefore, performing 6N cycles lead to better result than 10N cycles.

Using the other hydrogel, [LA]-[MKG]-[10N] (group 5, 6.8%) for wet spinning led to forming continuous fibers; however, it was not possible to collect and fix fibers on whiteboard. Considering previous trials, about 5% concentration of hydrogel resulted in better spinnability. Therefore, [LA]-[MKG]-[10N] (group 5, 6.8%) was diluted to obtain 5% sample, which was used for wet spinning. The fibers were formed in very small pieces, but they were somehow thin and not attached to each other to be able to hold the fiber. It was impossible to collect such fibers. Another experiment was diluting [LA]-[MKG]-[10N] (group 5, 6.8%) to 6%, contributing to almost the same as 5% concentration. It formed a bit more stable fibers; however, impossible to take out any piece from the bath. As described in section 3.3.5 the needle used for all wet spinning had the diameter of 1.2 mm. For [LA]-[MKG]-

[10N] (group 5) hydrogel, the needle with the diameter of 2.1 mm was also evaluated, which was not helpful.
In brief, the optimum grinding cycle and the optimum concentration may be 6N and 5% to 5.5%. pH value may have remarkable effects on the quality of fibers in terms of uniformity and obtaining continuous fibers and lower pH values (2.5 to 3) led to high quality fibers.

4.2.4 Measuring GlcN and GlcNAc content of both cultivations

The content of GlcN and GlcNAc from cell wall analysis is represented in Table 19. Alkali treatment for all samples contributed to a higher GlcN content than the GlcNAc content, indicating that chitosan was more predominant than chitin, which could be caused by occurring the significant deacetylation during NaOH treatment at 121°C for 20 minutes. The results for the 1.3 M3 bioreactor are close to the results reported by (Svensson et al., 2021). It is crystal clear presence of phosphate compound (K_2HPo_4) in the cultivation medium has led to lower chitin and chitosan in the fungal cell wall. The lowest amount of GlcN and GlcNAc resulted from the sample 5-GB, which had 5% K_2HPo_4 in the cultivation medium.

Table 19. GlcN and GlcNAc content in fungal cell wall for shake flask cultivations and cultivation in 1.3 M^3 bioreactor

Sample	GlcN (g/g AIM)	GlcNAc (g/g AIM)
0-GB	0.377 ± 0.002	0.122 ± 0.0
0.5-GB	0.348 ± 0.001	0.107 ± 0.0
1-GB	0.355± 0.019	0.115 ± 0.0
2.5-GB	0.348 ± 0.029	0.114 ± 0.0
5-GB	0.307 ± 0.003	0.104 ± 0.0
AIM (1.3 M^3 bioreactor)	0.359 ± 0.013	0.196 ± 0.0

4.2.5 Scanning Electron Microscopy (SEM) of AIM and hydrogels

SEM images illustrates that hydrogels had interconnected porous structure while AIM did not show such an interconnected structure, which might be rooted in the protonated NH_3^+-groups of chitosan created by the addition of lactic and adipic acids. Comparing the effect of lactic and adipic acid, adipic acid did not result in the same interconnected structure, which agrees with the previous observations. As explained earlier, hydrogels treated by adipic acid was not that homogenous and they showed two separated phases.

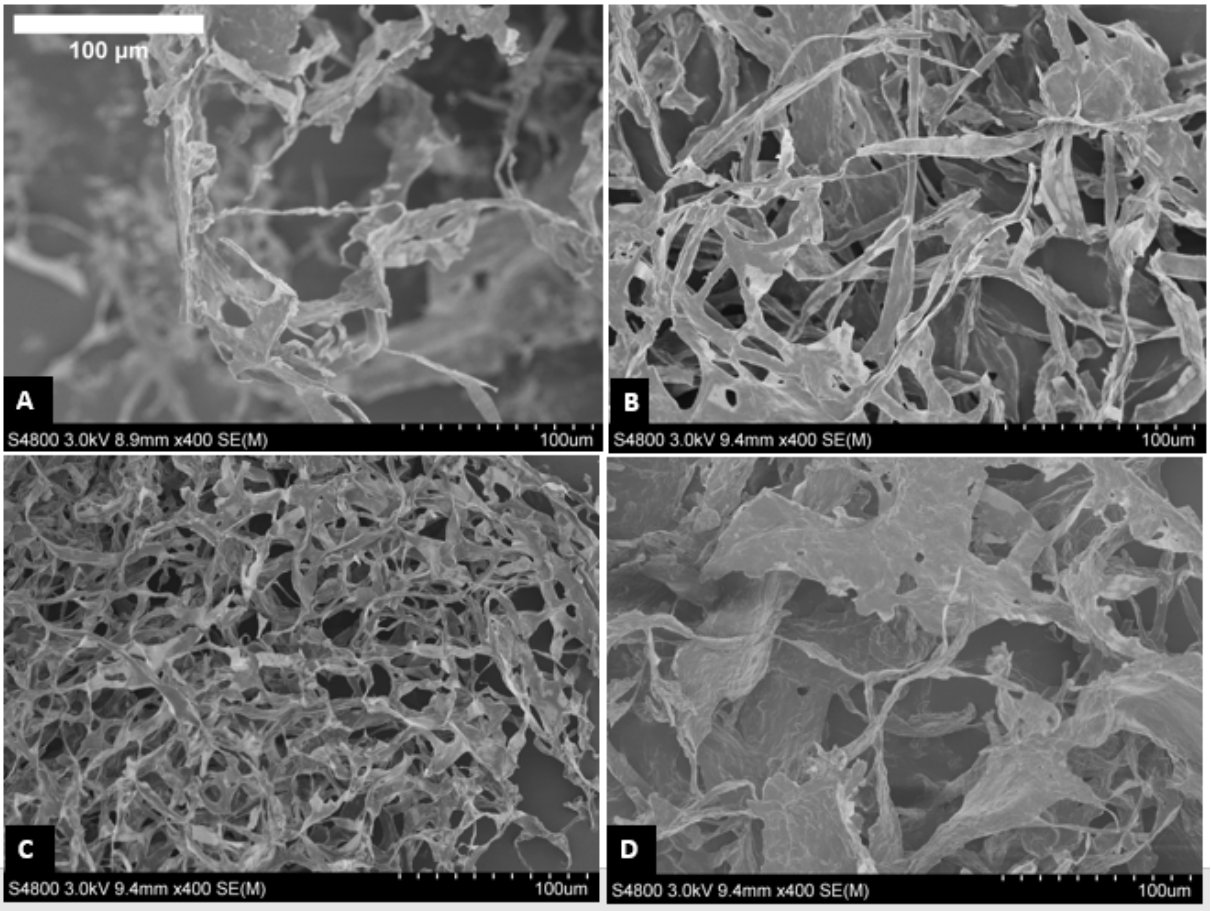

Figure 20. SEM pictures of A) AIM before adding acid, B) [LA]-[MKE]-[10N], C) [LA]-[MKG]-[10N], D) [AD]-[MKE]-[10N].

4.2.6 Mechanical properties of fungal fibers

As previously explained (section 4.2.3.1, group 2), monofilaments were produced using hydrogels with pH values of 2.5, 3, 3.5 and 4, which were prepared from [LA]-[MKE]-[6N] (pH 4.9). By utilizing lactic acid to adjust the pH value. Fibers with pH 2.5 showed higher tensile strength compared to other fibers as it is represented in Figure 21. The results are in line with the observation during wet spinning since fibers from hydrogel with pH 2.5 were more stable, uniform and smoother in coagulation bath. Tensile strength of the fiber (pH, 2.5) was around 82, which is higher than the tensile strength (72.3 MPa) of fungal fiber reported by Svensson et al. (2021).

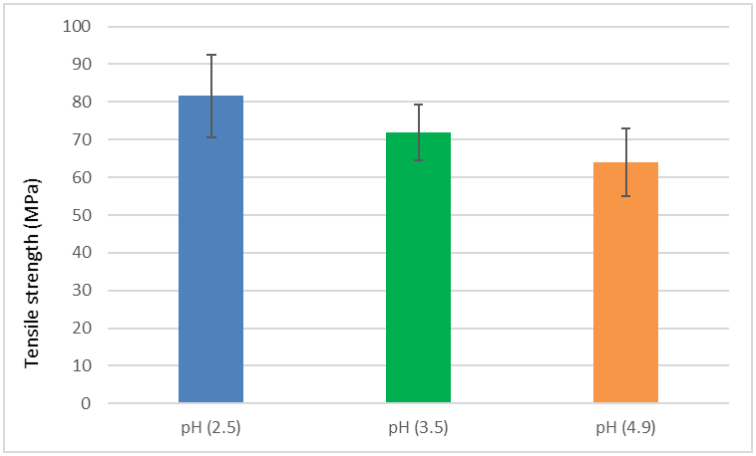

Figure 21 Tensile strength of fungal fibers obtained from hydrogels with different pH values, which were prepared from group 2 [LA]-[MKE]-[6N].

4.2.7 Antimicrobial properties of fungal fibers

In order to examine the possibility of using the fungal fiber for sutures applications, antibacterial test against the *Escherichia coli* was evaluated. The sample [LA]-[MKE]-[6N] belonging to group 2 of hydrogels (c.f. table 18) with the pH of 4.9, 2.5 and 3.5 were tested. As it is shown in the Figure 22 that the wet-spun monofilaments with pH 2.5 hinder the growth of *E coli*. However, *E coli* was grown in the presence of two other samples, which means they don't have antibacterial properties. It seems protonation of chitosan is necessary to have antimicrobial properties. In the sample with lowest pH, most probably a large number of chitosan amino groups still stay protonated upon coagulation in ethanol bath and therefore, they exhibit antimicrobial properties. However, in other fibers, the number of protonated chitosan groups are probably not high enough to make the fiber antimicrobial.

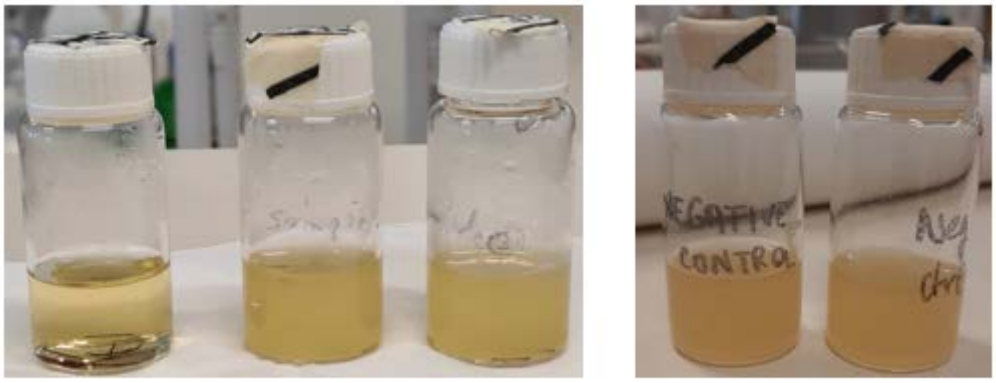

Figure 22. Antibacterial properties of a) fibers obtained from [LA]-[MKE]-[6N] belonging to group 2 of hydrogels (c.f. table 18). Left (pH 2.5), middle (pH 3.5) and right (pH 4.9), and b) blank samples.

5 conclusions

Wet spun chitosan fibers were produced successfully using lactic acid, citric acid or acetic acid as a solvent. Our results demonstrated that adipic acid has a great potential as a solvent

for the production of chitosan monofilaments. Obtained fibers from adipic acid generally showed higher tensile strength (147.9 MPa) than the ones produced using commonly used acid solvents under the same conditions. This could be caused by the adipic acid potential to create physical crosslinks between chitosan chains. Moreover, the properties of the monofilaments were affected by different coagulation baths. Considering higher mechanical strength, the best coagulation bath was NaOH-EtOH. Regarding second phase of the project, scaling up the process in 1.3 m^3 bioreactor was performed successfully. Comparing hydrogels treated with adipic and lactic acids, lactic acid resulted in hydrogels with better spinnability. In particular, 6 negative cycles contributed to more spinnable fibers than that of suspensions were passed through the grinder 10 times. To optimize the grinding treatment and produce continuous fungal fiber, further research is needed. The tensile strength of wet-spun fiber, obtained from fungal hydrogels is around 82 MPa and can be improved by optimizing the grinding treatment. Fungal cell wall analysis showed that GlcN and GlcNAc content in the fungal cell wall attained from $1.3M^3$ bioreactor (0.359 and 0.196 (g/g AIM), respectively) were significantly higher than the GlcN and GlcNAc content acquired from shake flasks cultivations containing K_2HPo_4 in their medium. Fungal fibers with pH 2.5, which were wet spun from 6 negative cycles of grinding treatment and lactic acid treatment was antibacterial against *Escherichia coli*, making them as a good alternative for suture applications. However, additional *in vitro* and *in vivo* trials are crucial to examine the fungal fiber for such applications.

6 Future research

- Increase and test the number of grinding cycles treatments to check whether is it possible to obtain nanofibrils or not.

- Evaluating the problematic brown bread particles and find a way to remove them during the process, contributing to not being limited to very sorted substrate.

- Produce fibers to be tested (biocompatibility, blood compatibility) for sutures applications in *in vivo* trails. Evaluation of drug delivery capabilities of the obtained sutures (*in vitro* and *in vivo*).

REFERENCES

AFZAL, A., ZUBAIR, U., SAEED, M., AFZAL, M. & AZEEM, A. 2020. Fibres for Medical Textiles. *In:* AHMAD, S., RASHEED, A. & NAWAB, Y. (eds.) *Fibers for Technical Textiles.* Springer.

AKRAM, Z. & MOHAMMAD, T. 2010. Production of low molecular weight chitosan by hot dilute sulfuric acid. *BioResources,* 5**,** 1554-1564.

AUGUSTINA EGBUTA, M., MWANZA, M. & OLURANTI BABALOLA, O. 2016. A Review of the Ubiquity of Ascomycetes Filamentous Fungi in Relation to Their Economic and Medical Importance. *Advances in Microbiology,* 06**,** 1140-1158.

BERGLUND, L., NOËL, M., AITOMÄKI, Y., ÖMAN, T. & OKSMAN, K. 2016. Production potential of cellulose nanofibers from industrial residues: Efficiency and nanofiber characteristics. *Industrial Crops and Products,* 92**,** 84-92.

BRANCOLI, P., ROUSTA, K. & BOLTON, K. 2017. Life cycle assessment of supermarket food waste. *Resources, Conservation and Recycling,* 118**,** 39-46.

BUCURICOVA, L. 2019. *Production of Edible Fungi Using Bread Waste.* Master of Science, University of Borås

CHEN, H.-L. & BURNS, L. D. 2006. Environmental Analysis of Textile Products. *Clothing and Textiles Research Journal,* 24**,** 248-261.

CHEN, P.-H., KUO, T.-Y., LIU, F.-H., HWANG, Y.-H., HO, M.-H., WANG, D.-M., LAI, J.-Y. & HSIEH, H.-J. 2008a. Use of Dicarboxylic Acids To Improve and Diversify the Material Properties of Porous Chitosan Membranes. *Journal of Agricultural and Food Chemistry,* 56**,** 9015-9021.

CHEN, P.-H., KUO, T.-Y., LIU, F.-H., HWANG, Y.-H., HO, M.-H., WANG, D.-M., LAI, J.-Y. & HSIEH, H.-J. 2008b. Use of Dicarboxylic Acids To Improve and Diversify the Material Properties of Porous Chitosan Membranes. *J. Agric. Food Chem.,* 56**,** 9015-9021.

COSTA DA SILVA, M., SILVA, H. N. D., HOLANDA, S. A., SILVA, A. R. O. & FOOK, M. V. L. 2020. Biodegradable polymeric wires: monofilament and multifilament. *Materials Research Innovations,* 24**,** 166-170.

CRUZ, R. D. C. A. L., DINIZ, L. G. M., LISBOA, H. M. & FOOK, M. V. L. 2016. Effect of different carboxylic acids as solvent on chitosan fibers production by wet spinning. *Matéria (Rio de Janeiro),* 21**,** 525-531.

CUI, Z., XIANG, Y., SI, J., YANG, M., ZHANG, Q. & ZHANG, T. 2008. Ionic interactions between sulfuric acid and chitosan membranes. *Carbohydr. Polym.,* 73**,** 111-116.

DA SILVA, M. C., DA SILVA, H. N., ALVES LEAL CRUZ, R. D. C., SAGOE AMOAH, S. K., DE LIMA SILVA, S. M. & LIA FOOK, M. V. 2019. N-Acetyl-D-Glucosamine-Loaded Chitosan Filaments Biodegradable and Biocompatible for Use as Absorbable Surgical Suture Materials. *Materials,* 12**,** 1807.

DAS, P., HEUSER, T., WOLF, A., ZHU, B., DEMCO, D. E., IFUKU, S. & WALTHER, A. 2012. Tough and Catalytically Active Hybrid Biofibers Wet-Spun From Nanochitin Hydrogels. *Biomacromolecules,* 13**,** 4205-4212.

DAVID, L., ENACHE, A. & PUAUX, J.-P. 2018. An experimental study of chitosan wet spinning process. *UPB Scientific Bulletin,* Series B.

DESORME, M., MONTEMBAULT, A., TAMET, T., MALEYSSON, P., BOUET, T. & DAVID, L. 2018. Spinning of hydroalcoholic chitosan solutions: Mechanical behavior and multiscale microstructure of resulting fibers. *Journal of Applied Polymer Science***,** 47130.

DONG, Y., RUAN, Y., WANG, H., ZHAO, Y. & BI, D. 2004. Studies on glass transition temperature of chitosan with four techniques. *J. Appl. Polym. Sci.,* 93**,** 1553-1558.
DRESVYANINA, E. N., DOBROVOL'SKAYA, I. P., POPRYADUKHIN, P. V., YUDIN, V. E., IVAN'KOVA, E. M., ELOKHOVSKII, V. Y. & KHOMENKO, A. Y. 2013. Influence of spinning conditions on properties of chitosan fibers. *Fibre Chemistry,* 44**,** 280-283.
EAST, G. C. & QIN, Y. 1993. Wet spinning of chitosan and the acetylation of chitosan fibers. *Journal of Applied Polymer Science,* 50**,** 1773-1779.
EME, L., SPANG, A., LOMBARD, J., STAIRS, C. W. & ETTEMA, T. J. G. 2018. Archaea and the origin of eukaryotes. *Nat Rev Microbiol,* 16**,** 120.
ENACHE, A. A. 2018. *Mathematical modelling of the chitosan fiber formation by wet-spinning.* PhD PhD, Université de Lyon; Universitatea politehnica.
FALAMARZPOUR, P., BEHZAD, T. & ZAMANI, A. 2017. Preparation of Nanocellulose Reinforced Chitosan Films, Cross-Linked by Adipic Acid. *International Journal of Molecular Sciences,* 18**,** 396.
FAN, L., ZHENG, H., XU, Y., HUANG, J. & ZHANG, C. 2007. Preparation and Properties of Chitosan/Konjac Glucomannan Blend Fibers. *Journal of Macromolecular Science, Part A,* 44**,** 439-443.
FERREIRA, A., ROCHA, F., MOTA, A. & TEIXEIRA, J. A. 2017. Nonmechanically Agitated Bioreactors. Elsevier.
FLORES-HERNÁNDEZ, C., COLÍN-CRUZ, A., VELASCO-SANTOS, C., CASTAÑO, V., RIVERA-ARMENTA, J., ALMENDAREZ-CAMARILLO, A., GARCÍA-CASILLAS, P. & MARTÍNEZ-HERNÁNDEZ, A. 2014. All Green Composites from Fully Renewable Biopolymers: Chitosan-Starch Reinforced with Keratin from Feathers. *Polymers,* 6**,** 686-705.
FOROUGHI, J., MIRABEDINI, A. & WARREN, H. 2018. Hydrogels Fibers. *In:* HAIDER, S. & HAIDER, A. (eds.) *Hydrogels* London, United kingdom: InTech.
GARCIA-RUBIO, R., DE OLIVEIRA, H. C., RIVERA, J. & TREVIJANO-CONTADOR, N. 2020. The Fungal Cell Wall: Candida, Cryptococcus, and Aspergillus Species. *Frontiers in Microbiology,* 10.
GEOGHEGAN, I., STEINBERG, G. & GURR, S. 2017. The Role of the Fungal Cell Wall in the Infection of Plants. *Trends in Microbiology,* 25**,** 957-967.
GOLNIT. 2017. *Surgical suture characteristics* [Online]. Available: https://www.golnit.com/suture-characteristics/ [Accessed].
HAMDINE, M., HEUZEY, M.-C. & BÉGIN, A. 2005. Effect of organic and inorganic acids on concentrated chitosan solutions and gels. *International Journal of Biological Macromolecules,* 37**,** 134-142.
HAN, T., NWE, N., WIN, P. P. & TAMURA, H. 2016. Spinning Process of Chitosan Fiber with Low Concentration of Formic Acid Solution and its Characteristics. *Journal of Modern Materials,* 1**,** 24-34.
HANEEF, M., CESERACCIU, L., CANALE, C., BAYER, I. S., HEREDIA-GUERRERO, J. A. & ATHANASSIOU, A. 2017. Advanced Materials From Fungal Mycelium: Fabrication and Tuning of Physical Properties. *Scientific Reports,* 7**,** 41292.
HAVERFORD. 2017. *Global Impacts of Infectious Disease* [Online]. Available: https://haverfordglobalimpacts2017.wordpress.com/2017/04/26/fungi/ [Accessed].
HENRIKSSON, M., BERGLUND, L. A., ISAKSSON, P., LINDSTRÖM, T. & NISHINO, T. 2008. Cellulose Nanopaper Structures of High Toughness. *Biomacromolecules,* 9**,** 1579-1585.

HIRANO, S., ZHANG, M., NAKAGAWA, M. & MIYATA, T. 2000. Wet spun chitosan–collagen fibers, their chemical N-modifications, and blood compatibility. *Biomaterials,* 21**,** 997-1003.
HYNNINEN, V., MOHAMMADI, P., WAGERMAIER, W., HIETALA, S., LINDER, M. B., IKKALA, O. & NONAPPA 2019. Methyl cellulose/cellulose nanocrystal nanocomposite fibers with high ductility. *European Polymer Journal,* 112**,** 334-345.
IFUKU, S. 2014. Chitin and chitosan nanofibers: preparation and chemical modifications. *Molecules (Basel, Switzerland),* 19**,** 18367-18380.
IFUKU, S., NOGI, M., ABE, K., YOSHIOKA, M., MORIMOTO, M., SAIMOTO, H. & YANO, H. 2009. Preparation of Chitin Nanofibers with a Uniform Width as α-Chitin from Crab Shells. *Biomacromolecules,* 10**,** 1584-1588.
IFUKU, S., NOMURA, R., MORIMOTO, M. & SAIMOTO, H. 2011. Preparation of Chitin Nanofibers from Mushrooms. *Materials,* 4**,** 1417-1425.
ISLAM, S., BHUIYAN, M. A. R. & ISLAM, M. N. 2016. Chitin and Chitosan: Structure, Properties and Applications in Biomedical Engineering. *Journal of Polymers and the Environment,* 25**,** 854-866.
IWAMOTO, S., ISOGAI, A. & IWATA, T. 2011. Structure and Mechanical Properties of Wet-Spun Fibers Made from Natural Cellulose Nanofibers. *Biomacromolecules,* 12**,** 831-836.
JONES, M., KUJUNDZIC, M., JOHN, S. & BISMARCK, A. 2020. Crab vs. Mushroom: A Review of Crustacean and Fungal Chitin in Wound Treatment. *Marine Drugs,* 18**,** 64.
KARIMI, K. & ZAMANI, A. 2013. Mucor indicus: Biology and industrial application perspectives: A review. *Biotechnology Advances,* 31**,** 466-481.
KHOR, E. & LIM, L. Y. 2003. Implantable applications of chitin and chitosan. *Biomaterials,* 24**,** 2339-2349.
KNAUL, J., HOOPER, M., CHANYI, C. & CREBER, K. A. M. 1998a. Improvements in the drying process for wet-spun chitosan fibers. *J. Appl. Polym. Sci.,* 69**,** 1435-1444.
KNAUL, J. Z. & CREBER, K. A. M. 1999. Erratum: Coagulation rate studies of spinnable chitosan solutions. 73**,** 2299-2299.
KNAUL, J. Z., HUDSON, S. M. & CREBER, K. A. M. 1999. Improved mechanical properties of chitosan fibers. *Journal of Applied Polymer Science,* 72**,** 1721-1732.
KNAUL, J. Z., MIKE HOOPER, CHRIS CHANYI & CREBER, K. A. M. 1998b. Improvements in the Drying Process for Wet-Spun Chitosan Fibers. *applied polymer science,* 69 (7)**,** 1435–1444.
KÖHNLEIN, M. B. M. 2020. *Preparation of films and nonwo-ven composites from fungal mi-crofibers grown in bread waste.* Master of Science University of Borås.
KUMAR, M. N. V. R. 2000. A review of chitin and chitosan applications.pdf. *Reactive & Functional polymers,* 46**,** 1-27.
LAZARIDOU, A. & BILIADERIS, C. G. 2002. Thermophysical properties of chitosan, chitosan–starch and chitosan–pullulan films near the glass transition. *Carbohydrate Polymers,* 48**,** 179-190.
LI, J., LIU, D., HU, C., SUN, F., GUSTAVE, W., TIAN, H. & YANG, S. 2016. Flexible fibers wet-spun from formic acid modified chitosan. *Carbohydrate Polymers,* 136**,** 1137-1143.
MAOXIA RAN, Y. L., LILING ZHANG, WEIHUA WU, JIARU LIN, QI LIU, SANTAO OU 2019. Clinical features, treatment, and prognosis of acute methanol poisoning: experiences in an outbreak. *Int J Clin Exp Med,* 12**,** 5938-5950.
MEYER, V., ANDERSEN, M. R., BRAKHAGE, A. A., BRAUS, G. H., CADDICK, M. X., CAIRNS, T. C., DE VRIES, R. P., HAARMANN, T., HANSEN, K., HERTZ-FOWLER, C., KRAPPMANN, S., MORTENSEN, U. H., PEÑALVA, M. A., RAM,

A. F. J. & HEAD, R. M. 2016. Current challenges of research on filamentous fungi in relation to human welfare and a sustainable bio-economy: a white paper. *Fungal Biology and Biotechnology,* 3.
MIRABEDINI, A., AZIZ, S., SPINKS, G. M. & FOROUGHI, J. 2017. Wet-Spun Biofiber for Torsional Artificial Muscles. *Soft Robotics,* 4**,** 421-430.
MOHAMMADI, M., ZAMANI, A. & KARIMI, K. 2012. Determination of glucosamine in fungal cell walls by high-performance liquid chromatography (HPLC). *J Agric Food Chem,* 60**,** 10511-5.
MONEY, N. 2016. Fungi and Biotechnology, . *The Fungi.* Third ed. San Diego, UNITED KINGDOM: Elsevier
NARANJO‐ORTIZ, M. A. & GABALDÓN, T. 2019. Fungal evolution: diversity, taxonomy and phylogeny of the Fungi. *Biological Reviews,* 94**,** 2101-2137.
NATIONS, U. 2021. *World population projected to reach 9.6 billion by 2050* [Online]. Available: https://www.un.org/en/development/desa/news/population/un-report-world-population-projected-to-reach-9-6-billion-by-2050.html [Accessed 21 May 2021].
NETO, C. G. T., GIACOMETTI, J. A., JOB, A. E., FERREIRA, F. C., FONSECA, J. L. C. & PEREIRA, M. R. 2005. Thermal Analysis of Chitosan Based Networks. *Carbohydrate Polymers,* 62**,** 97-103.
NIU, W., WILLETT, H., MUELLER, J., HE, X., KRAMER, L., MA, B. & GUO, J. 2020. Direct biosynthesis of adipic acid from lignin-derived aromatics using engineered Pseudomonas putida KT2440. *Metabolic Engineering,* 59**,** 151-161.
PILLAI, C. K. S., PAUL, W. & SHARMA, C. P. 2009. Chitin and chitosan polymers: Chemistry, solubility and fiber formation. *Progress in Polymer Science,* 34**,** 641-678.
PILLAI, C. K. S. & SHARMA, C. P. 2010. Review Paper: Absorbable Polymeric Surgical Sutures: Chemistry, Production, Properties, Biodegradability, and Performance. *Journal of Biomaterials Applications,* 25**,** 291-366.
POCHANAVANICH, P. & SUNTORNSUK, W. 2002. Fungal chitosan production and its characterization. *Letters in Applied Microbiology,* 35**,** 17-21.
POKHREL, S. & YADAV, P. N. 2019. Functionalization of chitosan polymer and their applications. *Journal of Macromolecular Science, Part A,* 56**,** 450-475.
POLEN, T., SPELBERG, M. & BOTT, M. 2013. Toward biotechnological production of adipic acid and precursors from biorenewables. *Journal of Biotechnology,* 167**,** 75-84.
POWERS-FLETCHER, M. V., KENDALL, B. A., GRIFFIN, A. T. & HANSON, K. E. 2016. Filamentous Fungi. *Microbiology Spectrum,* 4.
QIN, Y. 2015. A brief description of textile fibers *Medical Textile Materials.* Cambridge, UNITED KINGDOM: Elsevier Science & Technology.
QIN, Y. 2016. Surgical sutures. *Medical Textile Materials.*
QU, L.-J., GUO, X.-Q., TIAN, M.-W. & LU, A. 2014. Antimicrobial fibers based on chitosan and polyvinyl-alcohol. *Fibers and Polymers,* 15**,** 1357-1363.
RAAFAT, D. & SAHL, H.-G. 2009. Chitosan and its antimicrobial potential - a critical literature survey. *Microbial Biotechnology,* 2**,** 186-201.
RATTO, J., HATAKEYAMA, T. & BLUMSTEIN, R. B. 1995. Differential scanning calorimetry investigation of phase transitions in water/ chitosan systems. *Polymer,* 36**,** 2915-2919.
REBELO, R., FERNANDES, M. & FANGUEIRO, R. 2017. Biopolymers in Medical Implants: A Brief Review. *Procedia Engineering,* 200**,** 236-243.
RIVA, G. H., GARCÍA-ESTRADA, J., VEGA, B., LÓPEZ-DELLAMARY, F., HÉRNANDEZ, M. E. & SILVA, J. A. 2015. Cellulose - Chitosan Nanocomposites - Evaluation of Physical, Mechanical and Biological Properties. InTech.

ROY, J., SALAÜN, F., GIRAUD, S., FERRI, A. & GUAN, J. 2017. Chitosan-Based Sustainable Textile Technology:Process, Mechanism, Innovation, and Safety. *Biological Activities and Application of Marine Polysaccharides.*

SAHOO, D., SAHOO, S., MOHANTY, P., SASMAL, S. & NAYAK, P. L. 2009. Chitosan: a New Versatile Bio-polymer for Various Applications. *Designed Monomers and Polymers,* 12**,** 377-404.

SAKURAI, K., MAEGAWA, T. & TAKAHASHI, T. 2000. Glass transition temperature of chitosan and miscibility of chitosan/poly(N-vinyl pyrrolidone) blends. *Polymer,* 41**,** 7051-7056.

SALEHINIK, F., BEHZAD, T., ZAMANI, A. & BAHRAMI, B. 2021. Extraction and characterization of fungal chitin nanofibers from Mucor indicus cultured in optimized medium conditions. *International Journal of Biological Macromolecules,* 167**,** 1126-1134.

SCHMITZ, AUZA, KOBERIDZE, RASCHE, FISCHER & BORTESI 2019. Conversion of Chitin to Defined Chitosan Oligomers: Current Status and Future Prospects. *Marine Drugs,* 17**,** 452.

SEHAQUI, H., MICHEN, B., MARTY, E., SCHAUFELBERGER, L. & ZIMMERMANN, T. 2016. Functional Cellulose Nanofiber Filters with Enhanced Flux for the Removal of Humic Acid by Adsorption. *ACS Sustain. Chem. Eng.,* 4**,** 4582-4590.

SILVIA HÜTTNER, R. N., ANTON JOHANSSON, PAULO TEIXEIRA, PUCK ACHTERBERG 2020. Recent Advances in the Intellectual Property Landscape of Filamentous Fungi. *Mycorena, Whitepaper*.

SINGH, D. K. & RAY, A. R. 2000. Biomedical Applications of Chitin, Chitosan, and Their Derivatives. *Journal of Macromolecular Science, Part C*

Polymer Reviews, 40**,** 69-83.

STATISTA. 2020. *Annual per capita household food waste of selected countries worldwide as of 2020* [Online]. Available: https://www.statista.com/statistics/933059/per-capita-food-waste-of-selected-countries/ [Accessed 21 May 2021].

SU, C.-H., SUN, C.-S., JUAN, S.-W., HU, C.-H., KE, W.-T. & SHEU, M.-T. 1997. Fungal mycelia as the source of chitin and polysaccharides and their applications as skin substitutes. *Biomaterials,* 18**,** 1169-1174.

SVENSSON, S. E., FERREIRA, J. A., HAKKARAINEN, M., ADOLFSSON, K. H. & ZAMANI, A. 2021. Fungal textiles: Wet spinning of fungal microfibers to produce monofilament yarns. *Sustainable Materials and Technologies,* 28**,** e00256.

SYNOWIECKI, J. & AL-KHATEEB, N. A. 2003. Production, Properties, and Some New Applications of Chitin and Its Derivatives. *Critical Reviews in Food Science and Nutrition,* 43**,** 145-171.

TAMURA, H., TSURUTA, Y., ITOYAMA, K., WORAKITKANCHANAKUL, W., RUJIRAVANIT, R. & TOKURA, S. 2004. Preparation of chitosan filament applying new coagulation system. 56**,** 205-211.

TAN, S. C., TAN, T. K., WONG, S. M. & KHOR, E. 1996. The chitosan yield of zygomycetes at their optimum harvesting time. *Carbohydrate Polymers,* 30**,** 239-242.

TOSKAS, G., BRÜNLER, R., HUND, H., HUND, R.-D., HILD, M., AIBIBU, D. & CHERIF, C. 2013. Pure chitosan microfibres for biomedical applications. *AUTEX Research Journal,* 13.

WIKIPEDIA. 2020. *Surgical suture* [Online]. Available: https://en.wikipedia.org/wiki/Surgical_suture [Accessed].

YAN, W., SHEN, L., JI, Y., YANG, Q. & SHEN, X. 2014. Chitin nanocrystal reinforced wet-spun chitosan fibers. *Journal of Applied Polymer Science* 131.

YILMAZ ATAY, H. 2019. Antibacterial Activity of Chitosan-Based Systems. Springer Singapore.
YUDIN, V. E., DOBROVOLSKAYA, I. P., NEELOV, I. M., DRESVYANINA, E. N., POPRYADUKHIN, P. V., IVAN'KOVA, E. M., ELOKHOVSKII, V. Y., KASATKIN, I. A., OKRUGIN, B. M. & MORGANTI, P. 2014. Wet spinning of fibers made of chitosan and chitin nanofibrils. *Carbohydrate Polymers,* 108**,** 176-182.
ZAMANI, A. 2010. *Superabsorbent polymers from the cell wall of zygomycetes fungi.* PhD, Chalmers University of Technology.
ZARGAR, V., ASGHARI, M. & DASHTI, A. 2015. A Review on Chitin and Chitosan Polymers: Structure, Chemistry, Solubility, Derivatives, and Applications. *ChemBioEng Reviews,* 2**,** 204-226.